Miniaturization of Multiplexed sensor for continuous health monitoring systems

by

Mohammad Soltani

A thesis
presented to the University of Waterloo
in fulfillment of the
thesis requirement for the degree of
Doctor of Philosophy
in
Electrical and Computer Engineering

Waterloo, Ontario, Canada, 2022

Examining Committee Membership

The following served on the Examining Committee for this thesis. The decision of the Examining Committee is by majority vote.

Supervisor: Bo Cui
Professor, Dept. of Electrical and Computer Engineering,
University of Waterloo

Internal Member: Guo-Xing Miao
Associate Professor, Dept. of Electrical and Computer Engineering,
University of Waterloo

Internal Member: Siva Sivoththaman
Professor, Dept. of Electrical and Computer Engineering,
University of Waterloo

Internal-External Member: Michael Pope
Associate Professor, Dept. of Chemical Engineering,
University of Waterloo

External Member: Bo Tan
Professor, School of Aerospace Engineering,
Ryerson University

Author's Declaration

I hereby declare that I am the sole author of this thesis. This is a true copy of the thesis, including any required final revisions, as accepted by my examiners.

I understand that my thesis may be made electronically available to the public.

Abstract

Continuous health monitoring systems are an essential part of current and future life. Monitoring biological signals helps us detect health issues in the early stages. Besides the early-stage disease diagnosis, some patients also need a continuous system to monitor their physical condition continuously.

In this research, we focused on two types of monitoring systems. The first type of sensor has been used to detect and prevent complications in surgical operations and then determine the need for post-operational treatments. Abdominal surgery, generally done for removing some part of the digestive system, is one of the most common of surgical operations. One common complication after this type of surgery is the anastomotic leak. This complication is among the most dreadened problems that happen to the patients, typically one or two weeks after the surgery. This dreadened issue can be readily prevented using a continuous monitoring system that detects abnormal pH variations in the abdominal fluid. This research shows a possible approach to monitoring point-of-care (POC) and preventive action toward this complication using an electrochemical on-chip pH sensing system.

The second part of this research focused on a continuous glucose monitoring system to monitor interstitial fluid glucose concentration. Continuously monitoring blood glucose levels attracts considerable attention due to high complications in diabetic patients. The vast increase in people with diabetes due to the current human lifestyle makes it essential to fabricate a lower-cost monitoring system that can detect glucose and other biological parameters. To efficiently monitor glucose levels and detect other parameters that affect glucose monitoring, we proposed a platform that can simultaneously be used with several bio-signals, such as glucose concentration and pH level. An electrochemical multiplexed

sensing platform has been developed to detect these biological signals from interstitial fluid (ISF).

To improve the capabilities of this device, the fabrication has been done on a flexible substrate. Using self-assembly nanostructure processing methods and materials synthesis, some novel forms of self-assembled nanostructure have been investigated that can improve the sensing capabilities of the fabricated flexible electrodes. New materials such as semiconducting oxides and their effect on sensing capabilities have been discussed, and possible future directions have been proposed. Also, to extract ISF efficiently, polymeric microneedle arrays have been implemented with the device to extract and bring the ISF to the surface of the electrodes for detection.

Acknowledgements

I want to thank all the people who helped me through this research, especially Prof.Bo Cui, for his outstanding supervision. Also, I want to thank Dr. Mahla Poudineh, which this research can not be done whiteout her support and all the committee members for their excellent suggestions and comments.

I want to also thank CMC microsystems for their financial and technical help for this research. Also, University of Waterloo administration and specifically quantum nano center.

Dedication

I dedicate my dissertation work to my family and many friends. A special feeling of gratitude to my loving parents, whose words of encouragement and push for tenacity ring in my ears. My brother Soheil, and my sisters Sima, have never left my side and are very special. I also dedicate this dissertation to my many friends who have supported me throughout the process. I will always appreciate all they have done.

Table of Contents

List of Tables

List of Figures

Chapter 1

Introduction to wearable sensors for health monitoring

This chapter provides introductory information about wearable sensors and biosensors.

1.1 Background and motivation

The term "biosensor" was first introduced in the 1960s by Clark and Lyons. Nowadays, biosensors play a vital role in our everyday life. Biosensors are analytical devices that transform biological responses to electronic or optical signals [48]. Various biosensor-contained equipment has been commercialized, which helps patients, specialists, and scientists better understand what happens inside the human body.

Various types of biosensors have been developed. Some of these different classifications of biosensors are enzyme-based, tissue-based, immunosensors, DNA type, thermal, piezoelectric, optical, magnetic, and electrochemical biosensors. This grouping of

biosensing devices might be based on sensing methods or technological phenomenological perspective. The novel scientific approach improves the biosensors and their possible application conditions such as smaller sizes, efficient energy consumption, and higher sensitivity.

The improvement in science and technology of micro- and nanofabrication play a vital role in developing new and efficient biosensors by miniaturizing and improving the efficiency. Some of these recent fabricated devices and their applications have been reported recently, such as Quantum dot bio-sensors for ultrasensitive multiplexed diagnosis (cancer treatment)[49], Combination of Surface Plasmon Resonance (SPR) and isothermal titration calorimetry (ITC) bio-sensors[50], Optically based biological detection for defence or the femtosecond phenomena and non-linear optics applied sensors. Google's smart contact lenses for detecting blood sugar by analyzing the tears[51], are based on novel nanofabrication technology. From a historical perspective, improvement in sensors technology has been at its fastest pace in recent years (Fig1.1).

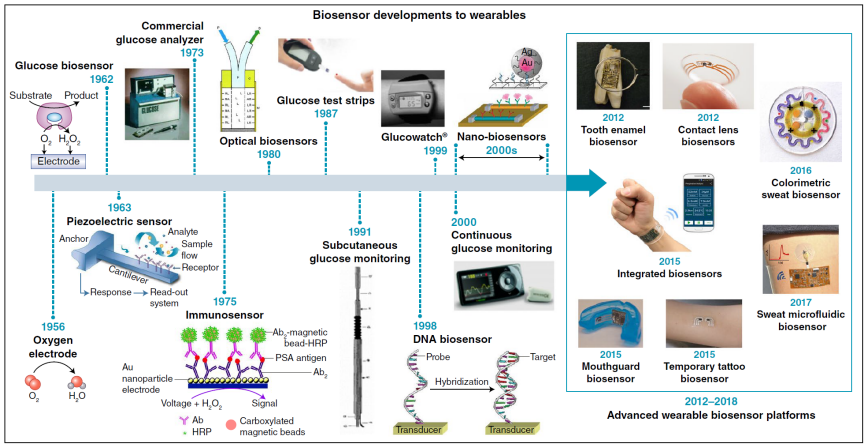

Figure 1.1: Biosensors historical technology improvements (Reprint with permission from [3]

Biosensors have been used for different types of health monitoring systems, from analyzing general biosignals to helping users define their health conditions to detecting and analyzing extreme health conditions that practitioners can use to immediately detect complications in the first stages and prevent the death of the patients. In this research, we focus on developing a sensor platform that can be helpful to the surgeons to avoid post-operative complications after colorectal surgery and another platform that can be used for analyzing glucose and pH level in ISF of diabetic patients as a part of a continuous health monitoring system.

The development of an electrochemical sensing system, as one of the most essential and reliable biosensor platforms, has been studied for these applications. The field of electrochemical biosensing is still developing. Therefore, based on the critical condition, there is still a need to have smaller, more reliable, and more reproducible sensor design and fabrication.

1.2 Colorectal surgery and its' post-operational complications

Biosensors have been used for different health monitoring systems. Novel improvement in the implantable and biocompatible sensors makes these monitoring devices one of the prominent candidates for future safe surgeries. Colorectal surgery is a type of operation that deals with digestive system disorders such as colon cancer(Fig 1.2). Every year, many patients encounter complications after these operations, which leads to the loss of their lives. As one of the most critical operations in the health care system, colorectal surgery needs biological monitoring during and after the operation.

A high probability of anastomotic leakage or infection causes a high mortality rate under colorectal surgery. However, few studies have focused on this issue. Design and fabrication of reliable devices that can monitor the patients' health a few weeks after the operation are still of significant interest. Conventional methods for monitoring these complications, such as CT-Scan systems, are expensive and do not have continuous monitoring features. On the other hand, one of the easiest ways to observe potential leakages or infections is to monitor the pH changes[52] as shown in Fig.1.3. Therefore, the need for a suitable bio-implantable or bio-compatible pH monitoring system with high precision is indisputable.

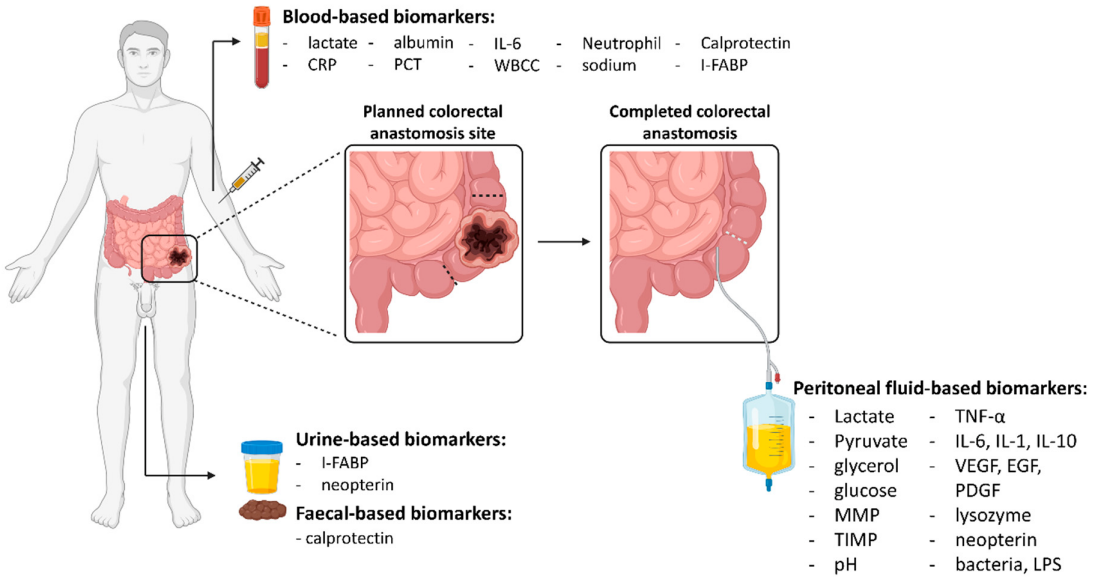

Figure 1.2: Colorectal cancer and some of its' conventional detection and monitoring [4]

Continuous monitoring of pH can be done with electrochemical or optical techniques. These two main techniques have been used for the fabrication of several types of pH sensor equipment for other applications (Fig1.3). This research will discuss fabrication

methods to modify electrochemical pH biosensors for this specific application. Also, the possible approaches to improving the sensor's sensitivity and reliability using various nanofabrication methods will be presented.

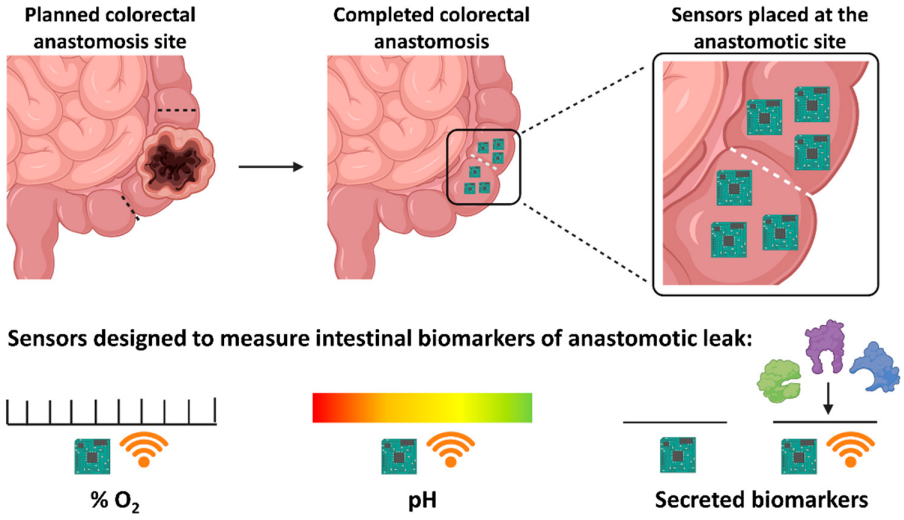

Figure 1.3: Cancer, leakage, or infection detection possible sensing mechanisms[4]

1.3 Glucose monitoring

The increasing number of health problems as a result of changes in nutrition and lifestyle is the biggest challenge for human life. The high demand for continuous and wearable health monitoring systems is inevitable. Diabetes, as one of these health issues, is and will be one of the most complicated issues for this century. This problem is strongly correlated to the glucose level in human blood as one of the most essential and crucial parameters that show humans' health condition. The high glucose level might show some worrisome health conditions and problems of our health system.

The increasing number of people with diabetes causes a high cost of medication and treatment for governments and public health systems. Therefore, controlling glucose in diabetic patients is the key to controlling the symptoms and preventing severe symptoms for patients. Based on the World Health Organization (WHO), the number of people worldwide diagnosed with diabetes increased from 108 million in 1980 to 422 million in 2014 [53]. Based on the estimation done by the Canadian Diabetes Association, the cost of diabetes for the Canadian health system was about $3.1 billion in 2020, and it is estimated to be $15.36 billion in cost of the health system in 2021[54]

Date back to 1971, when the first glucose monitoring system was introduced, several equipment and methodologies of blood sugar characterization have been developed and introduced. Characterization of blood sugar can be done in discrete or continuous ways. Based on the time frame factor, the characterization of the blood sugar can be categorized as continuous monitoring or discrete (one-time) characterization method. The discreet characterization method in blood sugar monitoring is the most common way used in the past decades. For this purpose, ordinarily, a Finger-prick glucometer has been used. In this system, the glucose will be measured using a needle prick on the fingertip to get a tiny droplet of blood to pour on a test strip for a glucometer (Fig 1.4).

Figure 1.4: Fingerprick Glucometer[5]

1.3.1 Monitoring multiple biological signals

Some of the biological signals interfere with each other's detection capability. For example, parameters like pH, cortisol concentration and temperature affect our ability to detect glucose levels in interstitial fluid. Besides, these biological parameters, as well as other parameters are essential to monitoring different health situations in patients. Therefore, there is a need to develop a multi-sensor platform that can detect several biomarkers simultaneously.

1.3.2 A painless glucose monitoring

The Invasive ways of monitoring systems for biosensing are generally harmful and not favourable compared to minimally -invasive and non-invasive methods. As shown in Fig 1.5 for one of the commercially available sensor systems, the needle inserted under the skin can cause bleeding and harm patients. Even though the accuracy of invasive methods is generally higher and easier to analyze, their effectiveness as a result of using them for a more extended period makes it the least favourable way of sensing compared to the other two categories.

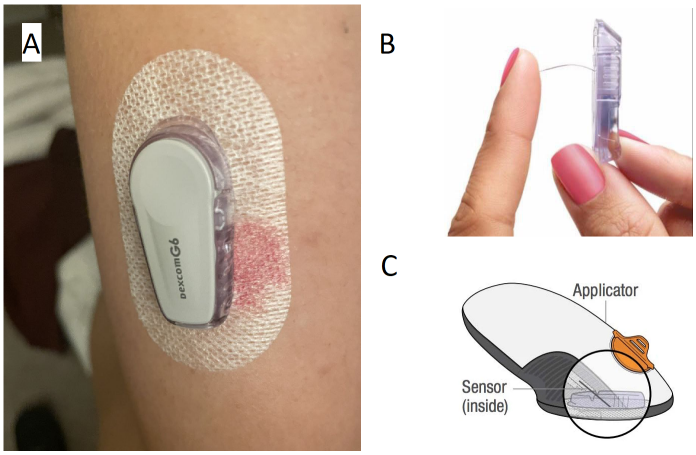

Figure 1.5: Different types of Glucose sensing methods and technologies. A) bleeding as a result of an invasive method of glucose sensing, B)The needle used in this system, and C) the method of inserting needle under the patients' skin (B and C are Dexcom G6 Sensor adapted from www.dexcom.com

One of the improvements in wearable devices is applying a microneedles-based system as a minimally invasive method for sensing and drug delivery. Researchers have introduced well-established materials and processes for the fabrication of microneedles, such as rigid silicon (Fig1.6-a) or flexible polymer (Fig1.6-b).

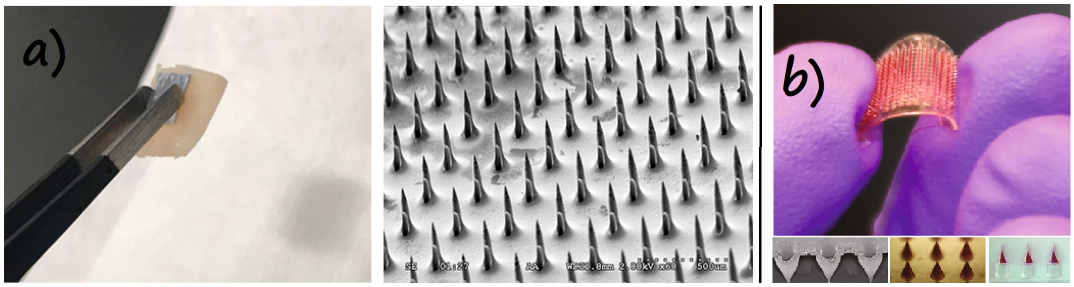

Figure 1.6: Different types of microneedles were fabricated using. a) silicon (rigid) (adapted with permission from [6]) , b) polymeric materials (flexible) (adapted with permission from[7])

These platforms generate an excellent opportunity for miniaturizing sensors and reducing harmfulness for the patients.

1.4 Research objectives and thesis outline

This study aims to develop two sensor platforms. First, the pH sensor POC monitoring device helps practitioners prevent dreadened post-operative complications in patients with colorectal surgery in the earliest stages. Second, this research aims to develop a sensing platform that can detect glucose and pH level (and other bio-signals in future) from interstitial fluid (ISF). In this research, our focus is on minimally invasive monitoring systems with the possibility to use them for a wearable device. The improvement in sensing mechanisms and new materials, and methods of multi-analyte sensing, will be introduced and discussed. In the first part of this thesis, a background about the nanofabrication and principles of desired sensors based on literature review were discussed. In the next section, Chapter 3, the fabrication processes for both rigid

and flexible devices were outlined. The designs, preparation and POC application based on anastomotic leak detection for colorectal surgery post-operation treatment were elaborated, and the final device design was shown.

In the second part, Chapter 4, the similar approach for glucose sensing mechanisms was clearly described, and the required fabrication and characterization were defined and presented. In the last part of the research, Chapter 5, our approach to enhance the sensitivity and build a platform that can be used for both pH and glucose sensing in a multiplexed system was described. This platform can be used for several biomarker detections. However, in this research, we focused on pH and glucose. The sensor platform (which was designed for potential future detection of several biomarkers) was also used with the implementation of microneedles to extract and practically analyze the ISF. At the end of Chapter 6, the conclusion and future directions were presented.

Chapter 2

Biosensing platforms, materials, methods and fabrication

2.1 pH measurement: background review, fabrication and characterization

pH sensing devices have been developed for a long period of time, from 1934 that Arnold Beckman introduced first and most popular pH analyzer using glass electrode to the novel potentiometric pH sensing to the surface plasmon resonance (SPR). The design of the sensors highly depends on their applications, availability and cost of fabrication. In-vivo and in-vitro bio pH sensors, among all the other types of sensors, attract considerable attention. The basic idea of monitoring health using a quick and reliable mechanism makes these sensors one of the most attractive devices in this field. As a system that can monitor health complications and symptoms, a pH sensor can be named as one of the most crucial types of equipment among other biomedical devices.

This chapter will introduce a brief theory and mechanisms of pH sensing and the desired biocompatible pH sensing fabrication advancements. At the end of the chapter, we will discuss characterization methods as well.

2.1.1 The definition of pH

The pH value represents the activity of hydrogen-ions in the solution. The pH scale was first introduced by Danish biochemist Sorensen in 1909. This term was named Pondus Hydrogenii or Potential Hydrogenii and was represented as $\mathrm{P_H} = -\log(\mathrm{C_H}/\mathrm{mole} \cdot \mathrm{dm}^{-3})$. However, according to the manual of symbols and terminology for physicochemical quantities and units by the International Union of Pure and Applied Chemistry (IUPAC), the activity of hydrogen ions in the solution or pH can be defined, using the molarity term, as:

$$pH = -loga_H = -log\frac{m_H\gamma_H}{m_0}$$

where m_H is molarity of hydrogen ion, γ_H the molar activity coefficient of hydrogen ion, and m_0 is 1 $mole \cdot kg^{-1}$[55, 56, 57].

2.1.2 pH measurement methods

Several pH measurement methods have been introduced and fabricated based on different applications. In this section, essential methods of pH sensing will be discussed, such as potentiometric (like glass electrode), amperometric, and optical.

2.1.2.1 Potentiometric pH measurement methods

Measuring pH values in different conditions is a critical factor determining the possibility of using it in specific environments. Potentiometric pH measurement is the most common type of pH monitoring. Various kinds of potentiometric pH measurement devices have been invented and introduced. In this section, some of the most important ones will be discussed.

Glass electrode

Glass electrodes are the most widely used method of measuring pH values in aqueous media. This pH probe measures the potential difference between the glass electrode membrane and the reference electrode. These two electrodes are generally combined into a single probe, also referred to as a combination electrode.

In this case of glass electrodes, the reaction of the glass electrode in the solution leads to a pH-dependant potential of the glass membrane due to the ion exchange between hydrogen ions in the solution and the equivalent cation in the glass membrane. Since the potential difference of the glass membrane is small by the change in the pH, there is a need for a suitable reference electrode and a high impedance meter[8].

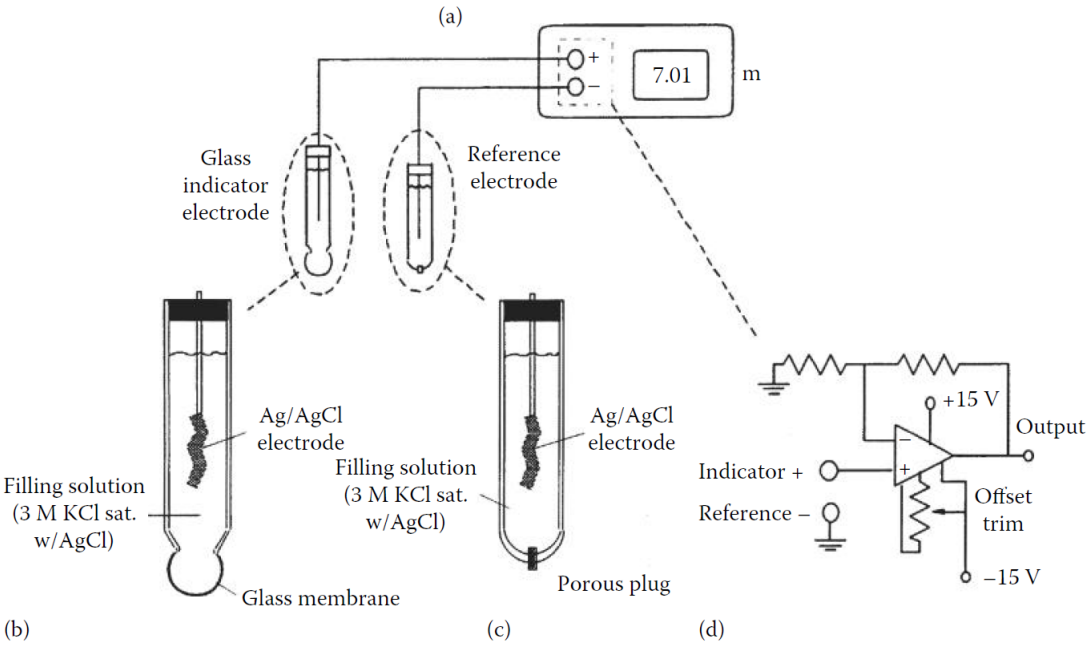

Figure 2.1: Glass membrane electrode (Reprint with permission from [8])

The thickness of the glass membrane is usually around 0.1mm. The membrane is between two mediums, the filling solution of the electrode with defined composition and pH, and the surrounding solution for which the pH is measured. There is a reference element immersed in the filling solution. This reference element (typically AgCl coated silver wire) makes an electrical connection with the inner side of the glass membrane. The other reference electrode illustrated in Fig.2.1 makes the connection with the outer side of the glass membrane. The electrical potential between the electrode immersed in the filling solution inside the glass electrode and the reference electrode in the testing solution provides the pH measurement [57].

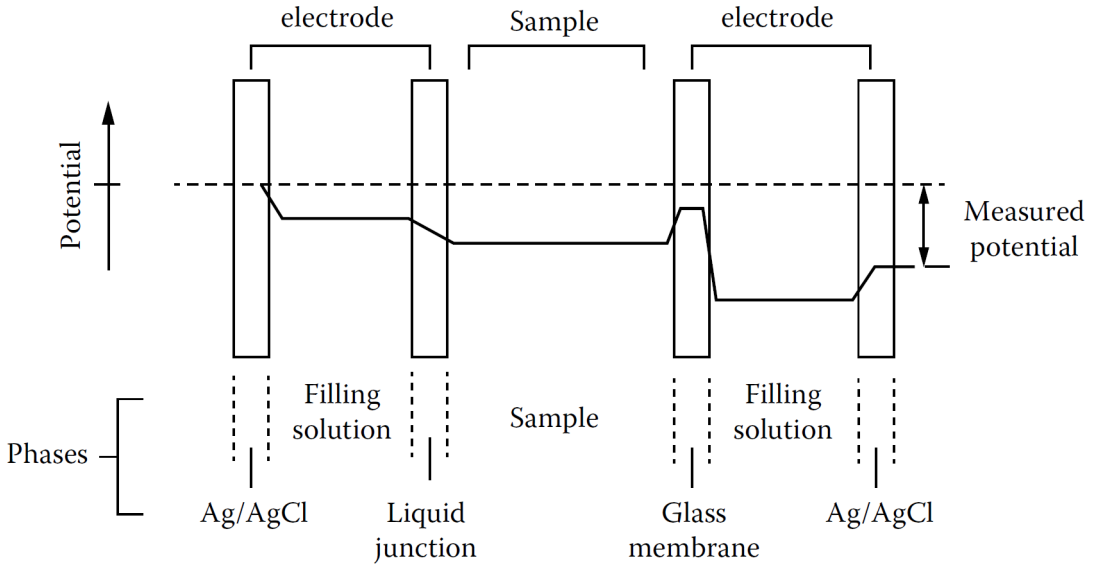

Figure 2.2: Schematic potential differences across interfaces for a glass electrode (Reprint with permission from[8])

Glass electrode membranes are mainly made of silica, alkali metal oxides, and alkali oxides. The alkali metal oxides provide the ions with mobility like Na and Li, acting as a charge carrier and exchanging protons in the glass layer. Some components, such as calcium oxide, are also added to increase the chemical stability of the glass membranes[8].

pH measurement ions sensetive filed effect transistor (ISFETs)

One of the most crucial developments in pH sensing is applying the Ion-Sensitive Field Effect Transistor (ISFET). Piet Bergveld first introduced ISFET in 1970s[58]. This sensing device is derived from the metal-oxide-semiconductor field-effect transistor (MOSFET) as one of the most common building blocks for integrated circuits. These silicon chips consist of pH-sensitive membranes, like the one in glass electrodes, with the ability of amplification using the field-effect transistor[59]. Compared to the glass electrodes, this type of pH

measurement device has an integrated amplification system, and also it has a smaller size and lowers energy consumption[60]. Another significant advantage of these electrodes is the ability to be used in different industries (like food industries) where the glass electrodes become unacceptable safety hazards.

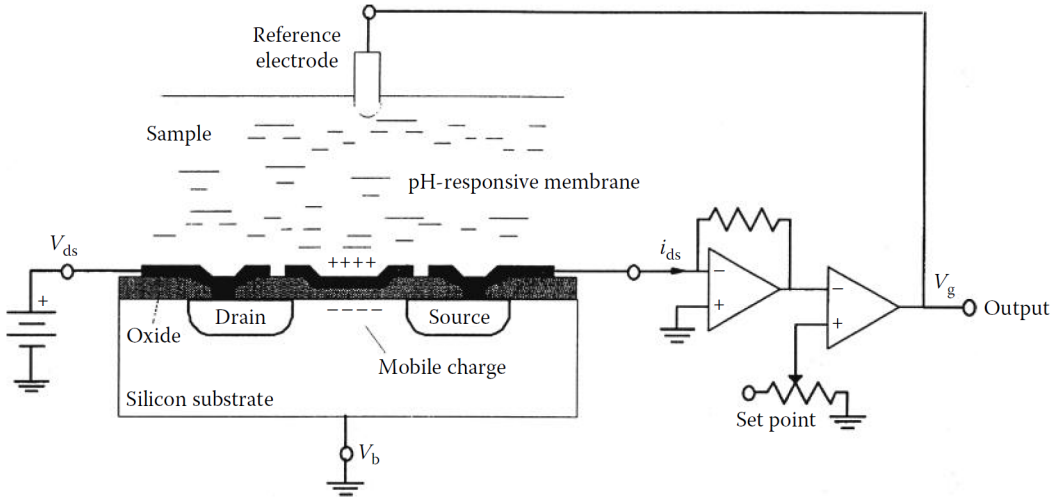

Figure 2.3: Schematic of ISFET based pH sensor (pH-FET) (Reprint with permission from [8])

The main difference between ISFET and MOSFET is that the metal gate material in the MOSFET is replaced by a pH-sensitive membrane material like silicon nitride[61], aluminum oxide[62], zeolite [63] or tantalum oxide[64] in contact directly with the testing solution[59]. Fig. 2.3 shows the schematic circuit and structure of the pH-sensitive ISFET. The electrical connection through the RE is applied. The specific voltage applied to the RE will charge the capacitor in the solution, insulating layer and silicon substrate. This phenomenon creates a mobile charge through the channel, and therefore, the applied voltage between the drain, and the source makes the current flow through the channel[65]. The drain current based on the "Charge imaging" model [57], can be

calculated as follows:

$$i_{ds} = Av_{ds}Q_{ds} = AV_{ds}C_2(v_g - V_T - \frac{Vds}{2})$$

Where i_{ds} is the drain current, A is a constant geometrical factor, V_{ds} is the applied voltage on the drain and Q_c is the mobile charge in the channel.

The mobile charge depends on the applied voltage to the RE (V_g), the threshold voltage used to introduce mobile charge V_T, and the capacitance of the gate region C_2. The threshold voltage also depends on the phase-boundary potential across the interface between the sample and the pH-sensitive insulating layer. The proton adsorption on this surface leads to Nenrstian dependence of the potential on the activity of the H^+ ions. Therefore the change in pH modulates the drain current of the device[57].

$$i_{ds} = Av_{ds}C_2(v_g - V_T + 2.3\frac{RT}{F}pH - \frac{Vds}{2})$$

The drain current in this system is typically on the order of nano-ampere or even lower. Therefore this regime is not suitable for high-frequency applications. However, it is ideal for potentiometric sensing, which leads to ultra-low-power instrumentation[66].

2.1.2.2 Amperometric pH measurement methods

Most of the reported pH sensing devices are potentiometric types. Few amperometric pH sensors have been reported[67]. In standard amperometric pH sensing devices, the potential is a constant value, and the concentration of electroactive species is determined by Faradaic current[68]. This process leads to voltammograms or amperometric curves, which reflect the pH change of the solution. Unlike the potentiometric measurement methods, which are

based on the shift in the potential of the redox species, the amperometric type regularly uses the pH-switchable permselectivity of self-assembled monolayer[69] or redox-sensitive polymer on the surface of the electrode[70]. Despite the high sensitivity of potentiometric or amperometric pH measurement devices due to their controlled potential techniques, amperometric pH sensing devices are rarely reported in the field of pH sensors.

On the other hand, some researchers use materials such as PANI or iridium oxide (which is well known for potentiometric devices) in an amperometric device and emphasize the ability of these materials to act as a novel amperometric pH sensing[71, 15].

2.1.2.3 Optical pH measurement methods

Optical measurement methods can also be used for the detection of pH. This goal can be achieved by several optical methods conducted by spectrophotometric, spectrofluorimetric or other related methods[72]. For the case of in vivo pH measurements, various techniques have been utilized for pH measurement using optical science. Fluorescence ratio imaging microscopy is an example of optical science for monitoring the intracellular pH in tumour cells. Furthermore, other processes such as NMR have been reported for monitoring temperature-induced changes in pH. This method was used to study the role of intracellular pH in the protein maintenance function in fishes[73]. Furthermore, surface plasmon resonance (SPR) based sensors attracted considerable attention during the previous decade. Mishra and Gupta[74] fabricated an SPR fibre optic pH sensor using layers of Ag/ITO/Al/hydrogel films over an unclad core of an optical fibre. Due to the change in the refractive index of the hydrogel layer as a result of swelling or shrinkage, the resonant wavelength shifts toward blue in transmitted spectra. Semwal and Gupta[75] use the same phenomenon using reduced graphene oxide (rGO) and PANI nanocomposites coating on a silver-coated

unclad optical fibre. The shift in plasmon resonance in this sensor is due to the change in the refractive index of the pH-sensitive rGO-PANI film. Another exciting research in the field of optical pH sensors was done by Zhou et al.[9]. In this optical pH sensor, 400nm hole arrays were fabricated in a grafted Poly(2-dimethylaminoethyl methacrylate) on flat silicon substrates, and immobilization gold nanoparticles were used to make a metamaterial absorber. The change in hole dimensions resulting from pH variations leads to an SPR shift in metamaterial absorber. This change was used for the detection of pH changes in the surrounding media. The schematic of this process is illustrated in Fig.2.4.

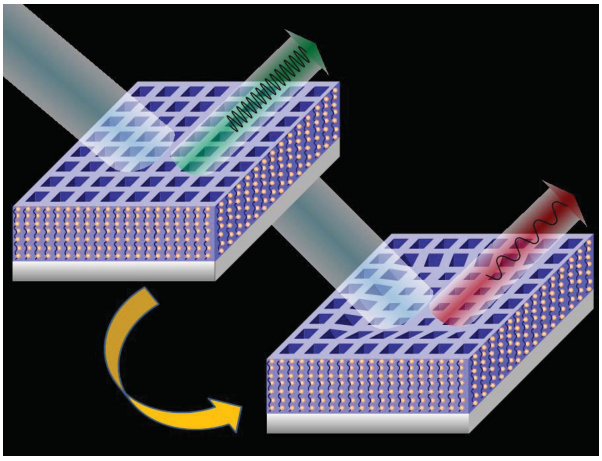

Figure 2.4: Schematic of pH-sensitive metamaterial absorber (Reprint with permission from [9]

2.1.2.4 Miniaturizing pH sensor

Miniaturizing pH monitoring systems play a vital role in pH monitoring because of their advantages over other techniques. The main advantage of these methods is that it only needs a small amount of sample volume[76]. These microelectrode systems can be amperometric or potentiometric. The potentiometric types typically have a simpler design

and a more straightforward measurement method than the other pH sensing devices.

2.1.3 Fabrication methods toward miniaturization

Miniaturization capability is critical for minimizing energy consumption, increasing sensitivity and decreasing the required amount of sampling solution. Micro- and nanofabrication are the primary science behind miniaturization[77]. There have been several methods of fabricating smaller devices toward ultra-micro- or nanoscale devices, from lithographic techniques that go back to 1822 when Nicphore Nipce placed an oiled paper over a glass plate which was coated with bitumen (asphalt) dissolved in lavender oil to copy an etched print on the paper [78], up to the novel techniques such as extreme ultraviolet lithography (EUV) or self-assembled nanopatterning methods.

One of the first miniaturized electrochemical sensors reported for in vivo applications was used for glucose monitoring and pH sensing[79]. This device used potentiometric pH measurement and was fabricated using a carrier membrane on a conductive polymer[80]. Some researchers focused on the improvement in the sensitivity of microscale devices using micro and nanopatterning methods. The aid of simulation software is also undeniable, such as COMSOL®multiphysics[81, 10], ANSYS®[66], open-source or user-code software packages. Applying these software packages helps scientists improve and understand the phenomena happening in the micro or nanoscale sensors when they are exposed to the actual environment. For example, Yoon et al.[10] reported that the zigzag and interdigitated structures of a microdevice improve its sensitivity due to the electrolyte current density distribution at the tip of sharp edges (Fig 2.5).

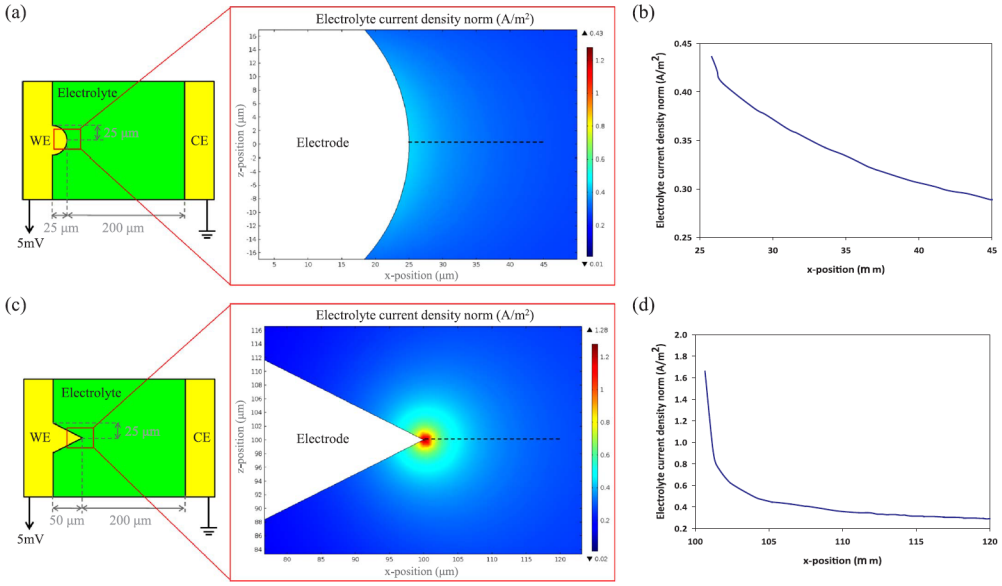

Figure 2.5: Effect of sharp edges on the sensitivity of electrochemical sensor based on the simulation (Reprint with permission from [10])

One of the goals for miniaturization is to increase the sensing ability per unit area of the device. Obtaining that sensitivity can be done with the help of micro and nanofabrication techniques via expanding the surface area. Based on this point of view, some researchers fabricate micro and nanostructures such as nanopillars (based on substrate patterning) on the working electrode area of pH sensors to improve the sensitivity[11]. However, as illustrated in Fig2.6, the size of the pillars is larger than what should be classified as a nanoscale device. Improvement in the surface area of microchip devices, besides the improvement in the fabrication science and technology, gives researchers the ability to enhance the efficiency of sensors.

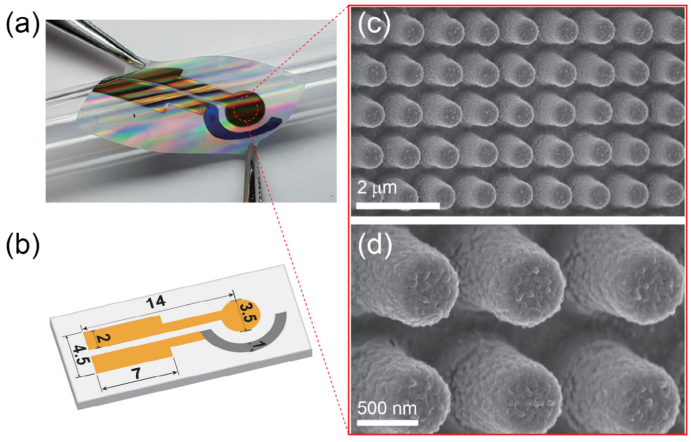

Figure 2.6: fabricated nanostructures on the working electrode area (Reprint with permission from [11])

For the ISFET type of sensor, generally, the pH sensors' reported sensitivity, including ISFETs or miniature pH sensors, are in the order of Nernstian pH sensitivity($\sim$ 58mV/pH at RT)[82] or slightly super-Nernstain sensitivity (Maximum $\sim$ 70-80mV/pH)[83, 64]. However, it was emphasized that change in the sensors' surface area by fabricating nanopillars on the gate leads to improvements. Pan et al[83]. analyze the effect of surface morphology of the gate material (in this case, CeT_xO_y film fabricated by magnetron sputtering) on the pH sensitivity. They reported an improvement in the sensitivity up to 89.81 mV/pH. Also, Hajmirzaheydarali et al.[12, 84] used the same approach by making polysilicon nanopillars with sequential deep reactive ion etching process on the gate area for pHFETs (Fig.2.9). They claimed to achieve extremely high sensitivity (400mV/pH).

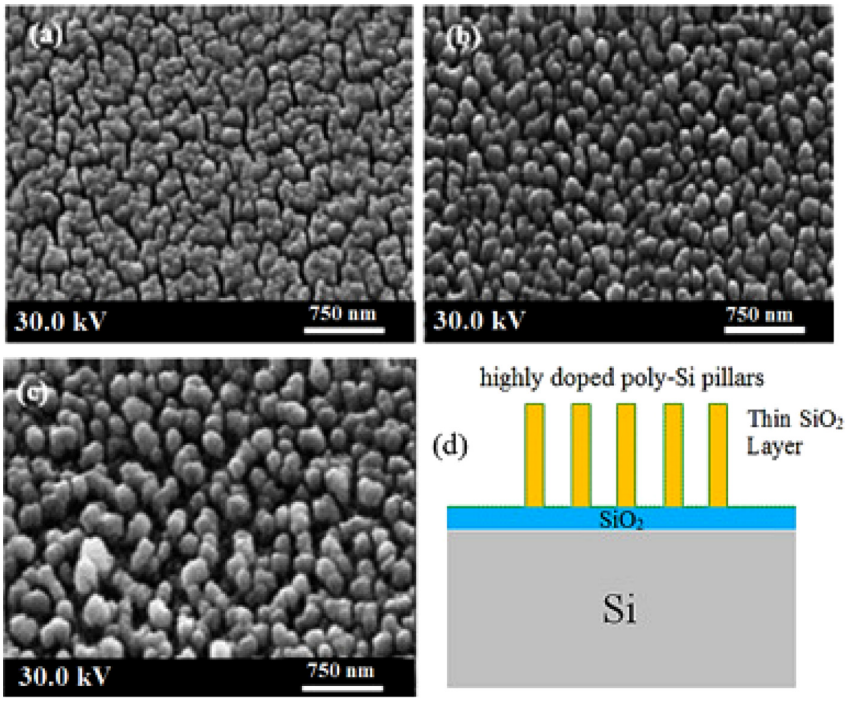

Figure 2.7: Nanopatterning of ISFET sensors' gate material [12]

High aspect ratio nanostructures on the electrode area can be achieved using various techniques. For instance, making nanopatterned metal as mask material for deep silicon reactive ion etching (DRIE) on silicon-based substrates or oxygen plasma on flexible substrates, as well as some wet chemical etching methods.

Another way to improve the sensitivity of the sensors, beyond using etching and lithography methods, is to apply prefabricated nanostructures on the electrode surface. Some researchers have reported sensitivity improvements using these methods. For example, Linghao He et al. [85] fabricated a core-shell nanostructure coated with needle-like Polyaniline (PAni) and used that for the rapid detection of malathion. In addition to integrated nanostructures in sensors, some other high precision methods of

the bottom-up approach of nanofabrication such as two-photon lithography of high-molecular-weight poly(ethylene glycol) diacrylates as a pH-sensitive hydrogel were reported[86]. 3D structure pH-sensitive polymerized hydrogel was fabricated in the specific area of the surface using this method (Fig.2.8). However, the application of this fabrication method is restricted, and it is not suitable for industrial or commercial production.

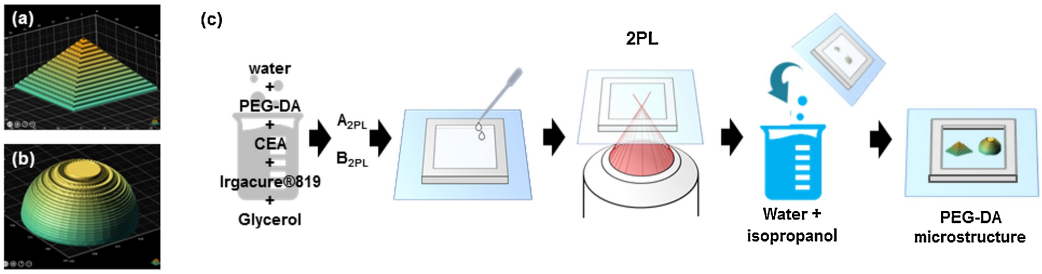

Figure 2.8: 3D structure of pH-sensitive hydrogel fabricated using two-photon lithography (2PL) [11]

2.1.3.1 Effect of nanostructures on sensitivity; theoretical perspective

The effect of nanostructures on the sensitivity of the electrodes for pH sensors and ISFETs is not fully understood. Several theories have been developed, each of which partially explains the behaviour of modified sensors with nanostructures. Some of the theoretical benefits for nanostructures in electrochemical sensors are[68]:

- Nanoelectrodes reduce the Ohmic (iR) drop distortion due to the change in surface area and therefore can be used to detect chemical reactions in poorly conducting media.

- Proportionality of double-layer capacitance to the surface area is more diminutive for nanoelectrodes and reduces the RC time constants (R is the resistance and C is the capacitance). Smaller RC value enables high-speed voltammetric experiments as a result of fast electron transfer.

- The increase in mass transport from or to the electrodes by decreasing electrode size. This higher mass transfer rates can be explained due to radial (nonplanar) diffusion. This nonplanar diffusion lead to ultrafast electrochemical measurements compare to normal flat electrodes.

- As a result of the increase in mass transport rates and reduced charging current, nanoelectrodes show exceptional signal to noise ratio (S/N)

These phenomena lead to ultrafast electrochemical measurements. Some other researchers elaborate on the effect of design on the sensitivity of electrodes, such as Kuo et al.[10] (as mentioned in the previous section). They showed that the sharp edges affect the current distribution and lead to a higher sensitivity (Fig.2.5) in pH. COMSOL simulations approved this phenomenon. For the ISFETs, the effect of the nanostructures in the gate area was discussed by Hajmirzaheydarali et al.[12]. He suggested that the nanostructures on the gate area affect the electrical double layer (EDL). As illustrated in Fig. 2.9, the nanostructures' spacing and morphology affect the EDL based on his proposed theory.2.9 They mentioned that the distances between the nanostructures concerning the Debye-length (λ) affect the electrode's capacitance as shown mathematically in the equation below, and therefore, it affects the sensitivity.

$$C_{DL} = C^0_{DL}(\frac{sinh(\frac{D}{2\sqrt{2}\lambda})}{cosh(\frac{D}{2\sqrt{2}\lambda})})$$

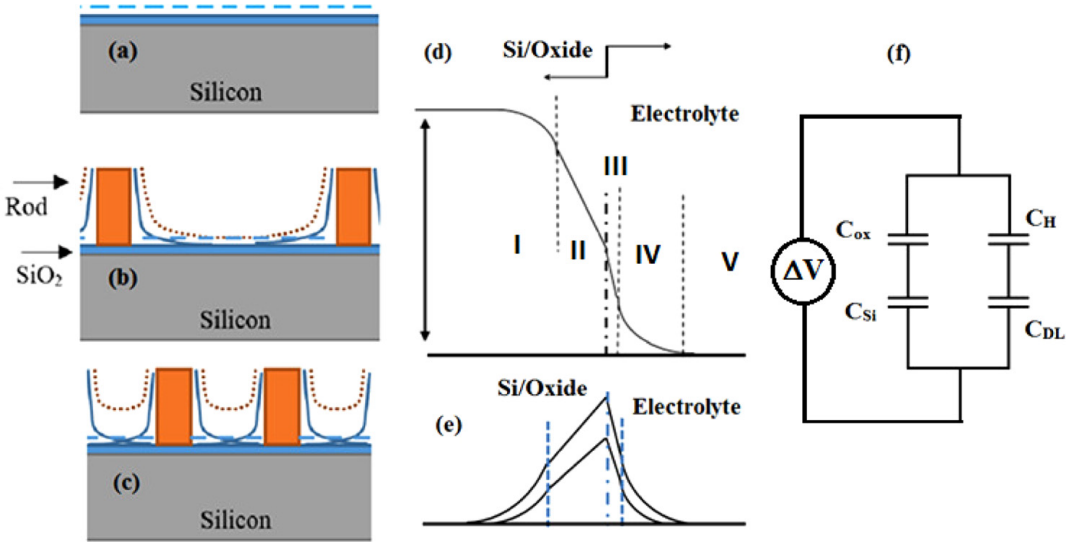

Figure 2.9: Electrical double layer and the effect of nanostructures on it. a) Extension of the diffuse layer close to the surface b)Nanostructures with large distances and negligible overlapping c)When the nanostructures are close to each other. d)The energy diagram of the device concerning the electrolyte solution e) The dashed-dotted line points at the electrolyte-oxide interface where the site-binding charges are accumulated without considering the effect of the reference electrode.)The equivalent circuit proposed representing EDL characteristics[12]

2.1.4 pH-sensitive materials

Depending on the measurement technique and the type of device being fabricated, various materials were proposed.

Based on the definition mentioned in the literature, any material that changes its properties, dimensions, colour, etc., as a result of exposure to different pH media, can be classified as pH-sensitive materials[87]. The materials which change their electrical or

optical properties are generally better candidates for sensor application.

In this project, we are interested in solid state pH sensitive materials. Several types of pH sensitive materials have been reported including metal oxides[16, 88] (e.g. IrO_2, RuO_2, SnO_2, PtO_2, $ZrO-2$, Ta_2O_5, TiO_2, C_2O_3, WO_3, Pb_O2, Bi_2O_3, Nb_2O_5), carbon materials[62] (e.g. carbon nanotubes, Graphene), and polymers[89] (e.g. acidic, basic or neutral).

According to Fog and Buck [88], metal oxides with electronic conductivity (due to oxygen deficiency) can be classified as pH-sensitive metal oxides. However, they concluded that modifying these materials is a prerequisite for highly acidic or basic media. This was confirmed by other researchers as well. Manjakka[16] conducted this modification by making some composites with binary metal oxide (e.g. by adding Cu_2O, SnO_2, TiO_2 or Ta_2O_5 to RuO_2). These combinations have been used for supercapacitors as well.

On the other hand, a wide range of polymeric materials that can be used to fabricate pH sensing devices has been reported. These pH-sensitive polymers can be classified as follows[89]:

- Polymers with acidic groups (accepting protons in low pH values and release protons at neutral or high pH values) such as poly(methacrylic acid) (PMAAc)
- Polymers with basic groups (accepting protons in low pH values and form a positively charged polymer chain like poly(2-(dimethylamino)ethyl methacrylate) (PDMA)
- Neutral pH-sensitive polymers

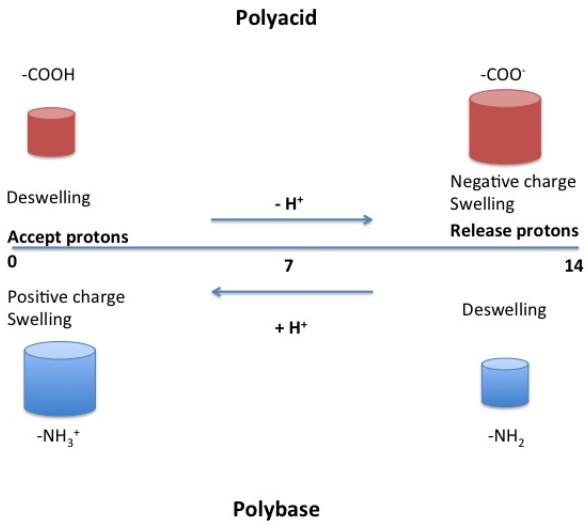

Figure 2.10: Schematic of how different types of polymers respond to pH changes.

Another classification based on the polymer structures is

- Linear homopolymer
- Amphiphilic block copolymer
- Double hydrophilic block copolymer in forms of micelles, vesicles, star, branched, hyperbranched, polymer brushes, dendrimers, nanogels, microgels, and hydrogels (macrogels).

These polymers change their shape or dimensions as a result of pH changes (Fig.2.10). Therefore, despite their importance for drug delivery or other applications, these classifications are unsuitable for electronic pH sensitivity measurement. Some other polymers, such as polyaniline (PANI), well-known for their optical and electronic

properties, respond to pH variations by changing their structure and, therefore, their electrical or optical properties[13]. The schematic representation of how pH changes affect the structure of PANI is illustrated in Fig 2.11

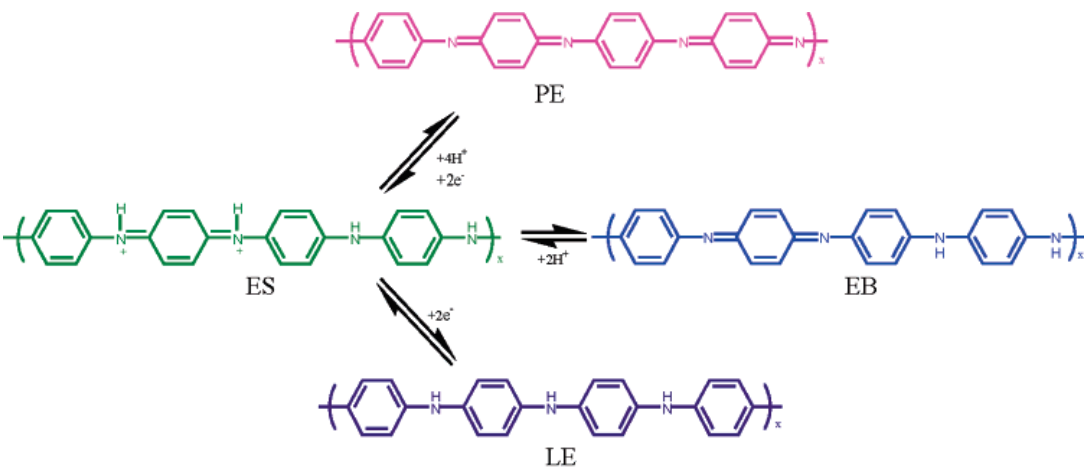

Figure 2.11: Structure response in PANI as a result of pH changes[13].

The material's performance, also for the ISFET sensors, has a significant effect on the sensor's sensitivity. Abdolkader and Alahdal [14] uncover the difference between the pH-sensitive materials used for ISFET sensors and their impact on pH sensitivity based on numerical simulations (Fig2.12). As illustrated in this figure, there is an enormous variation in pH sensitivity based on selecting pH-sensitive materials.

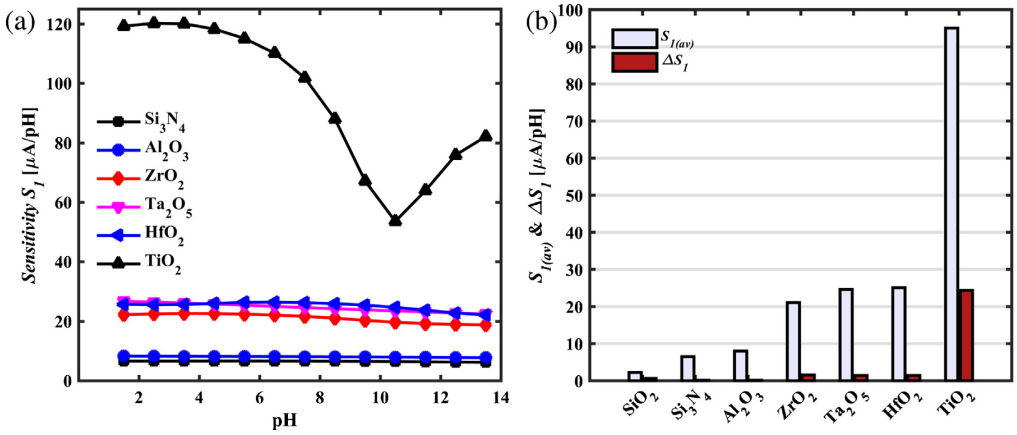

Figure 2.12: Effect of high high dielectric constant (κ) materials on the ISFET pH sensitivity (Based on signal to noise ratio)- The numerical results[14]

2.1.5 Characterization

The researchers have used various techniques for the characterization of pH sensors and their materials. Regarding the pH sensitivity of potentiometric sensors, most research suggests the change in potential vs the pH values as the best way to characterize the sensors. The resulted slope of the potential variations vs. pH graph demonstrates the pH sensitivity values (Fig 2.13).

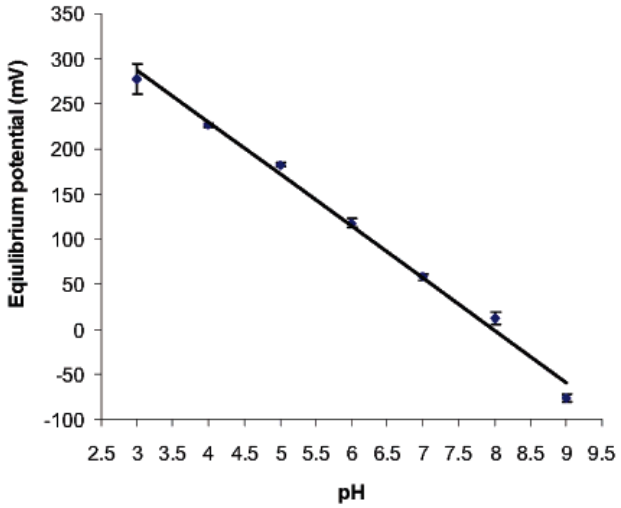

Figure 2.13: Potential vs. pH[13].

For the amperometric type of pH sensor, as shown in Fig2.14, Cyclic Voltammetry (CV) test is a generally acceptable method of characterization of different pH values in solutions. Also, Ge et al. reported the application of the CV test [13] to figure out the electroactivity of the films and substrate in the surrounding medium.

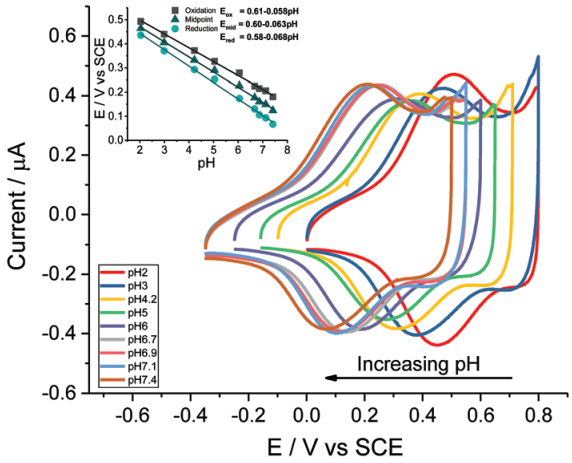

Figure 2.14: Cyclic voltammetry method of sensing characterization [15]

Some optical characterization methods have also been used, including attenuated total reflection (ATR), X-ray photoelectron spectroscopy (XPS) to find out the effect of pH on the bonds or chemical state and surface hydroxylation of the sensing layer[16] and FTIR, UV-Vis[90], and Raman Spectroscopy[91] for the sensing material characterization.

Furthermore, many researchers use the electrochemical impedance spectroscopy (EIS) technique as a non-destructive characterization method for pH sensor evaluation[92]. For example, Manjakkal[16, 91, 93] stated that in low frequencies, the capacitance, absolute value of impedance, and phase angle of pH achieved from EIS depend on pH for metal oxide films (Fig.2.15).

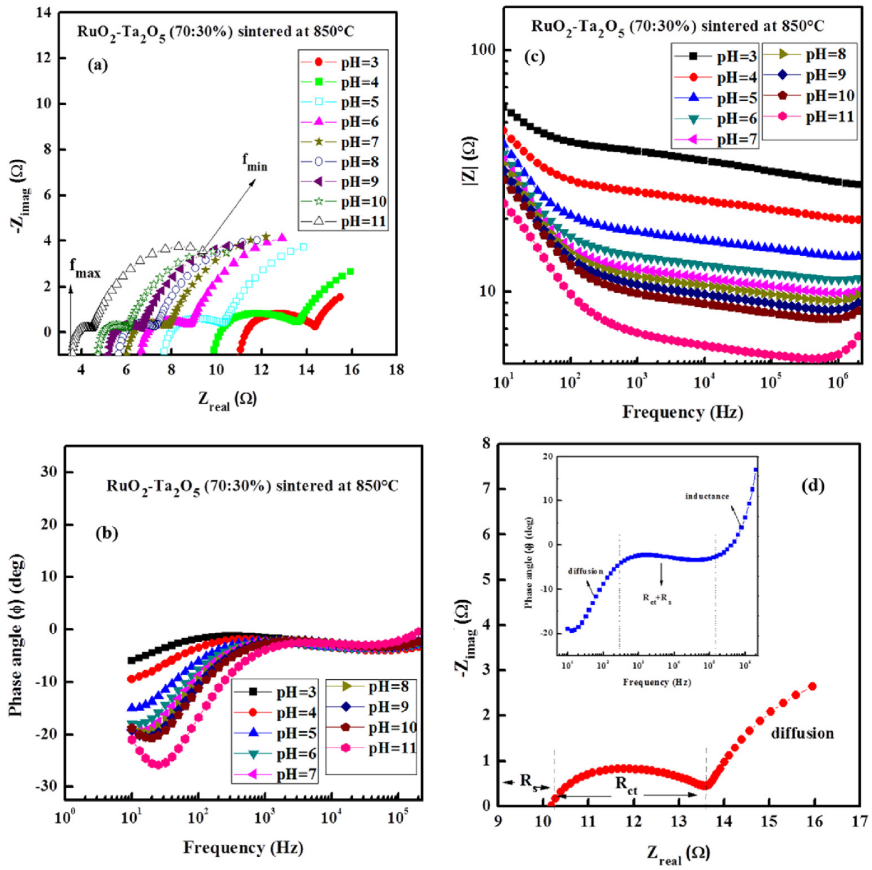

Figure 2.15: a)Nyquist plot b) Bode phase plot, c) Bode plot, and d) schematic representation of Nyquist plot and Bode plot as a result of pH changes[16]

2.2 Glucose sensing

Access to a glucose monitoring system is critical for diabetic patients. As mentioned before, one of the crucial points toward preventing hospitalization for diabetes is the monitoring of blood sugar levels in patients. This sugar type is called glucose which causes the problem for patients. The first commercially available glucose monitoring

system days back in 1971. An American company, named Anton Clemens, made this equipment. The glucose monitoring in this equipment was done by measuring the reflectance of the blood using some enzyme-based strips. Before this testing method, the colour of blood was estimated based on the chart of colour changes. However, this equipment was only used by the clinics, physicians and hospitals [20].

2.2.1 Types of Diabetes

Various types of diabetes have been named and distinguished, which are mostly related to glucose levels. However, the reasons for these types of diabetes disease can be different. Diabetes-related glucose level has two main types called Type 1 and Type 2. However, some other glucose level health issues can be categorized as diabetes disease. For example, Gestational diabetes and Prediabetes can be considered temporary and-or transformable types that can cause problems in patients if not treated well. The conditions of these forms as named are briefly described here [54]:

- Type 1- This class of diabetes happened as a result of an autoimmune problem. This disease is also named insulin-dependent diabetes. The body of patients in this category is diagnosed with the lack of ability to produce its insulin. Therefore, their body can not moderate their blood sugar level. Statistically, around 10 percent of diabetics are diagnosed as type 1.

- Type 2- This category includes most of the patients generally called diabetes. In this type, the patient's body might not sufficiently use the insulin produced by the body or provide enough insulin. This disease can usually be moderated by eating healthy and sports activities to control the blood sugar level.

- Gestational diabetes- This group of diseases is a temporary kind that arises within the pregnancy period for women. Depending on the risk factors, the probability to diagnosed with this type for women with pregnancy is about 3 to 20 percent. Even though considered a temporary category of disease, these patients and their future children might have a higher risk of type 2 diabetes in the future.

- Prediabetes- In this group of patients, the blood sugar levels are high, but they might not be high enough to be considered type 2. It has an increased risk of developing type 2. However, this does not mean all of the cases will develop to type 2 in future.

- Diabetes insipidus - This rare category is not generally considered a type of diabetes and is unrelated to blood sugar. However, the patients with diabetes insipidus might have similar symptoms as diabetes patients. Some hormone problems cause this group of diseases. These hormones, which are produced by special nerve cells in the hypothalamus (some part of the brain), are called vasopressin (AVP) and antidiuretic hormone (ADH) [94].

2.2.2 Glucose monitoring

The Finger-Prick type of sensors usually uses an enzyme-based electrochemical glucose monitoring system which will be comprehensively described in the following subsection. The detailed layer-by-layer structure of commercial test strips for these types of glucometer is shown in Fig2.16.

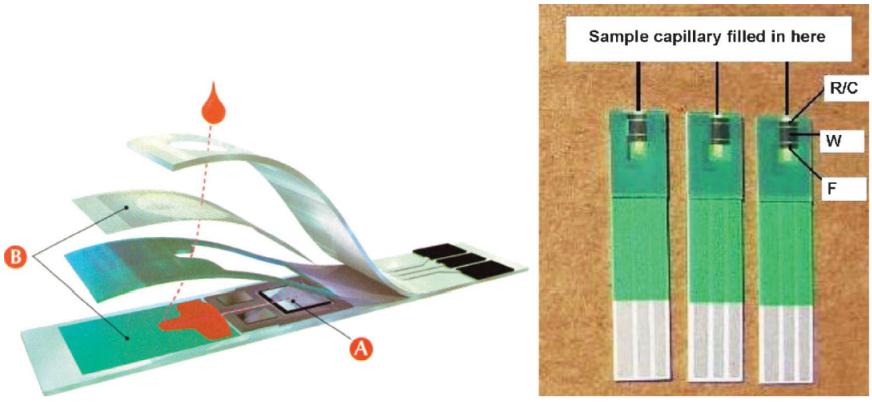

Figure 2.16: Left: layer by layer structure of a commercial test strip for glucometer (A) Electrode system, and (B) Hydrophobic Layer [17] Right: three different commercial glucometer test strips R/C, W and F correspond to Reference/Counter, working, and fill electrode respectively [18]

Another conventional way to measure glucose in body fluid is by using urine as a sample. In this method, the effect of sample fluid on the colour change of strips can define the range of glucose and other parameters (such as pH, protein, ketones, etc.) based on the visual comparative chart (check Fig2.17).

Figure 2.17: Commercial urine glucose test strips[19]

Another way to arrange different types of blood sugar measurement methods is to consider their condition of being invasive or not invasive. Therefore, three groups of characterization methods can be named non-invasive, minimally invasive, and invasive. For a non-continuous way of measurement as described above, we can consider finger-prick glucometer as an invasive quantitative method. However, the urine dipstick is the non-invasive qualitative way to analyze body sugar.

Discrete glucose monitoring systems are time-consuming and might not be practical, as they should be, to control blood sugar levels all the time. Another and more efficient way to control glucose levels in the body is by continuously characterizing the blood glucose level. During the past decade, contentious glucose monitoring systems have attracted considerable attention among scientists and industries researchers. Various monitoring techniques have been developed and tested, as shown in Fig2.18.

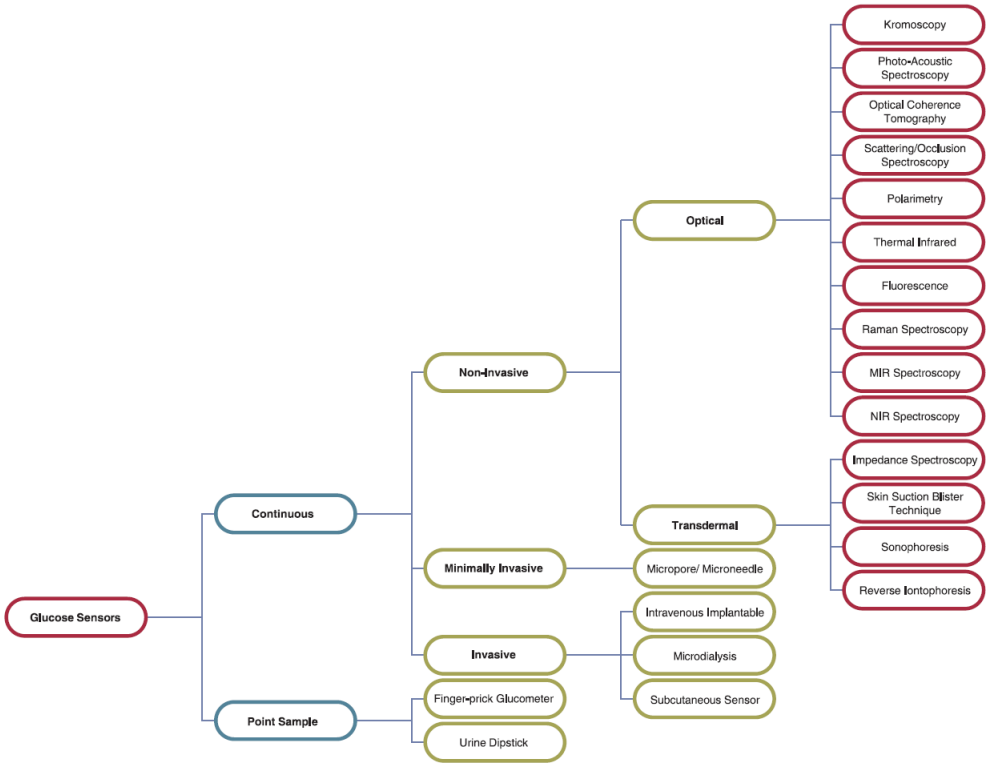

Figure 2.18: Different types of Glucose sensing methods and technologies[20]

2.2.3 Continuous glucose monitoring systems

Problematic use of discrete and one-time glucose monitoring systems makes it hard to keep glucose level stable for patients. These fluctuations in blood sugar levels result in a high amount of complications for diabetic patients. This condition leads to need of a monitoring system that can continuously monitor the glucose level in various states for a longer time.

Advances in battery development and miniaturization of electrochemical and optical methods lead to improved continuous monitoring systems. As mentioned in the previous

section, most of these developed systems still use invasive techniques. These systems can analyze the blood [15], interstitial fluid (ISF) [21, 95, 96, 97], tear [98], saliva [99, 100], sweat [101, 22] or other body fluids or even breath to determine the amount of sugar in blood Fig 2.19.

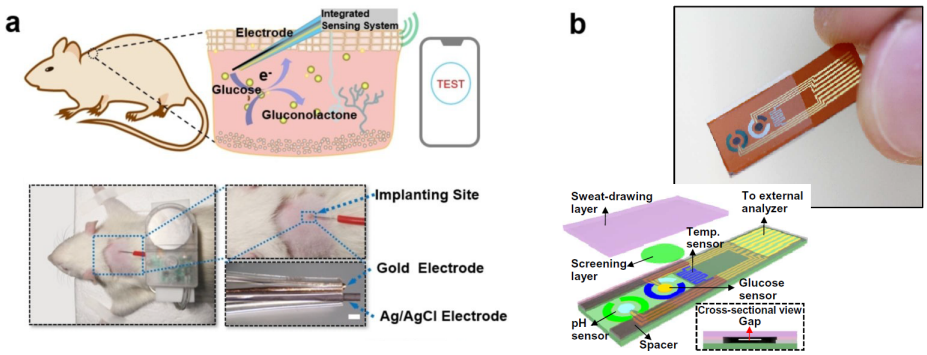

Figure 2.19: two different continuous glucose monitoring systems A)Non-enzymatic glucose sensing based on interstitial fluid [21] B)Electrochemical pH and glucose sensor based on sweat[22]

Most of the novel continuous glucose monitoring methods are non-invasive based on optics, photonics or RF sensing. These methods can be found on acetone level in-breath, intrinsic properties of glucose, such as absorption coefficient, specific optical rotation, or Raman spectroscopic shift, or based on properties of tissue or blood, like refractive index, scattering coefficient, permittivity and conductivity [102].

Despite improvements in the sensing technology, continuous glucose monitoring (CGM) systems are generally developed for type 1 diabetics since their blood glucose level change is more critical than type 2 diabetics. This lack of development in glucose monitoring for type 2 is also related to the cost of these monitoring devices. The cost of a smart glucose monitoring system is generally around $3000 to $6000 per year [54].

The primary system of any biosensing device is to convert the biological or chemical signal to an electronic signal. The equipment that can do this conversion is called a transducer. The transduction mechanism can be electrochemical, optical or photonics, piezoelectric, mechanical, or thermal-based. However, one of the most important and widely used methods of this conversion has been electrochemical transduction[103].

2.2.4 Electrochemical glucose sensing

Electrochemical sensors are among the most favourable types of transduction methods to detect biological signals due to their simplicity, reproducibility, and low fabrication cost.

These electrochemical biosensors have been widely used for glucose sensing for a long time. They normally used blood sugar or sugar content in interstitial fluid as a sample for glucose measurement. The first glucose sensor using enzymes for electrode surface was developed in 1962 by Clark and Lyons. Clark uses the enzyme-based electrode system to convert an electroactive surface to an electroactive material. Based on this system, two electrode systems were demonstrated. The first electrode contains at least one enzyme in a sandwich-type layer between the substrate electrode and a membrane. It converts the substrate to electroactive material using some interfering species(Fig 2.20. The other electrode system analyses the interfering species in the solution. Using two measured currents (subtraction), Clark was able to monitor the glucose in the solution [23].

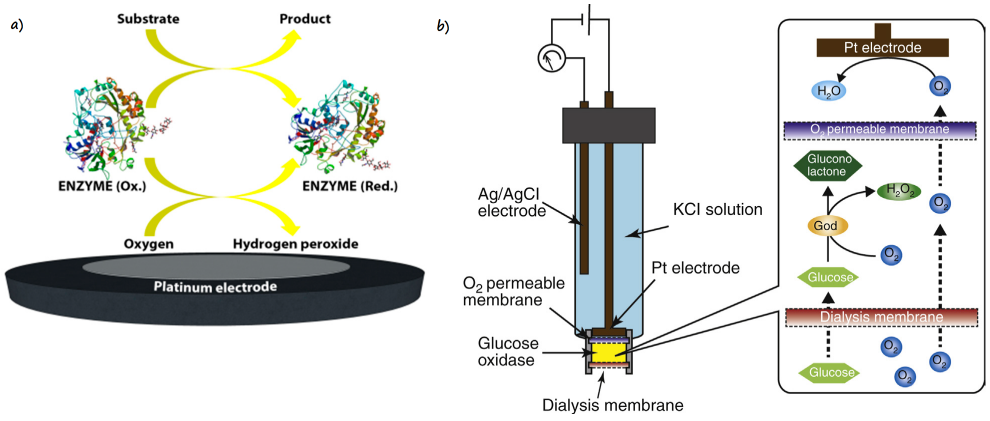

Figure 2.20: Clark Glucose sensor simple mechanisms on a) electrode surface [23] and b) The complete electrodes system measurement methodology[24]

The principal method used for the Clark electrode is based on amperometric measurement. Based on this method, the potential is applied between the electrodes (reference and working electrodes). In this case, since the current passes through the reference electrode to alter the measurement, it usually consists of a third electrode (or electrode system) to carry the current.

2.2.4.1 enzymatic glucose sensors

The most common way of sensing glucose in the electrochemical devices developed commercially is based on enzymes. The regular enzymes used for sensing contain a redox group which changes during the process of sensing. These types of glucose enzymes are:

- Glucose oxidase (GOx)
- Glucose dehydrogenases (GDH)

In the natural system, the enzymes oxidize their substrate by accepting electrons and changing to an inactive reduced state. These enzymes give their electron to oxygen and produce hydrogen peroxide (H_2O_2) [103].

Three generations of enzymatic glucose sensing systems have been developed based on different mechanisms. In the first generation of glucose sensors from the first sensor designed by Clark and Lyson, the GOx enzyme has been used, and the oxygen is used as an electron acceptor. In this system, the oxygen in the solution has been detected by an oxygen sensor to define glucose concentration using oxygen consumption and generation of hydrogen peroxide [104].

There is an artificial acceptor in the second generation instead of oxygen in the first generation of sensors. The reaction of these artificial electron acceptors was analyzed colorimetrically or electrochemically. The employment of artificial electron acceptors instead of oxygen help to avoid any other redox species getting involved.

The last sensing mechanisms of an enzymatic glucose sensor, third generation, eliminates the artificial electron mediators (which can be toxic) and avoids interference in the systems with oxygen monitoring and oxygen reduction in the blood by directly transferring electrons to the electrode[25]. These three types of enzymatic glucose sensor generations are also briefly shown in Fig 2.21

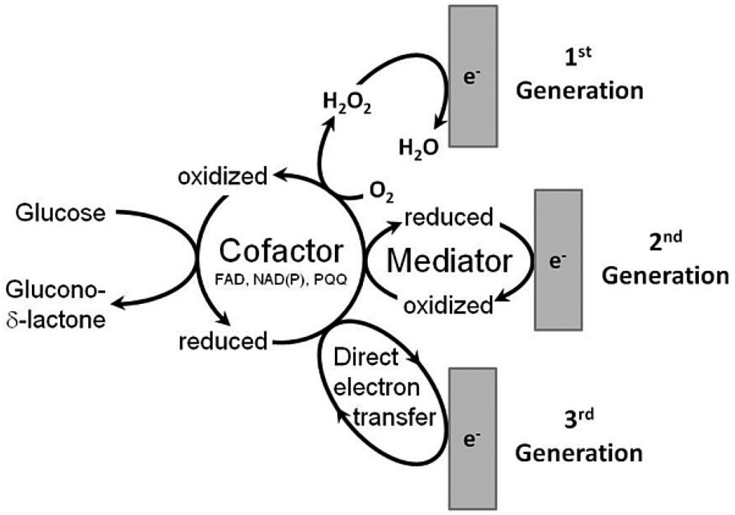

Figure 2.21: Generations of enzymatic glucose sensing [25]

Based on the enzyme commission (EC) number system, the oxidoreductase (an enzyme that acts as a catalyze to transfer electrons from one molecule) with the CH-OH group is classified as EC 1.1. group. Various types of oxidoreductase are in this group, which can be used for glucose monitoring and act as the reducing tail of glucose (O-H). Here are the brief itemized group of these oxidoreductases[25, 105] :

- EC 1.1: Acting on the CH-OH group of donors

  EC 1.1.1: With NAD+ or NADP+ as acceptor

  EC 1.1.2: With a cytochrome as acceptor

  EC 1.1.3: With oxygen as acceptor

  EC 1.1.4: With a disulfide as acceptor

  EC 1.1.5: With a quinone or similar compound as acceptor

EC 1.1.7: With an iron-sulfur protein as acceptor

EC 1.1.9: With a copper protein as acceptor

EC 1.1.98: With other, known, physiological acceptors

EC 1.1.99: With unknown physiological acceptors

As mentioned earlier in this section, these groups are classified as glucose oxidase (GOx) and glucose dehydrogenases (GDH). This classification is based on the ability to react with external electron acceptors. Glucose oxidase (GOx) is the group of oxidoreductase that can use oxygen as an external electron acceptor, generating H_2O_2 and are classified under the group number EC 1.1.3. On the other hand, glucose dehydrogenases (GDH) do not use oxygen as an electron acceptor. This group uses different types of artificial and natural electron acceptors. The GDH group is subdivided based on redox co-factors (non-protein components that act as electron acceptors). As shown in Fig. 2.22 these co-factors are nicotine adenine dinucleotide (NAD) or nicotine adenine dinucleotide phosphate (NADP) and are mentioned as group EC 1.1.1. The GDHs that use the pyrroloquinoline quinone (PQQ) is categorized as EC 1.1.5, and the GDHs that use other types of acceptors, including flavin adenine dinucleotide (FAD) are based on EC 1.1.99. Some of these subgroups are also presented in different types themselves [25].

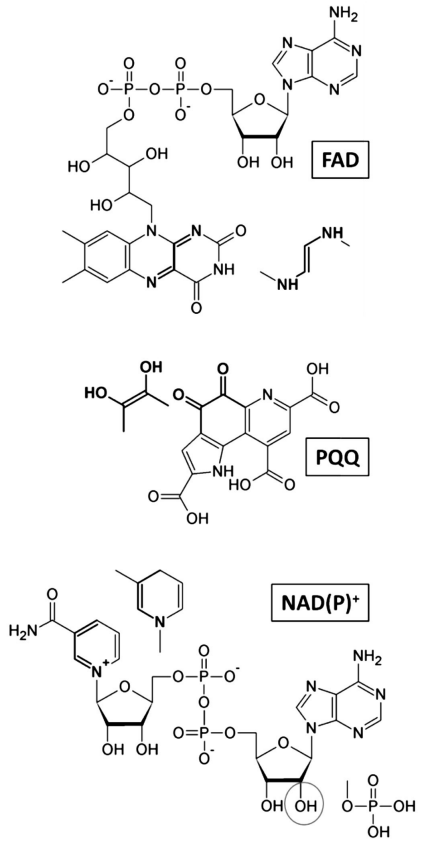

Figure 2.22: glucose dehydrogenases (GDH) co-factors types [25]

Some of the benefits and drawbacks of these enzymes can be considered as [103]:

- GOx is not expensive. However, the need for oxygen in this system is inevitable. With depletion of oxygen, the performance which is typically based on oxygen depletion or production of H_2O_2 decreases.
- NAD^+ GDHs' subgroup is independent of oxygen and has attracted incredible attention recently. However, the cost of these enzymes makes it hard to use them as glucose sensors.

- PQQ-GDHs are also one of the most efficient enzyme systems and have a rapid electron transferability. But this system is also expensive for application in sensors.

However, the main problem with the enzymatic sensing mechanism is the immobilization and reproducibility. Since the activity of the immobilized enzyme highly affect the sensitivity of glucose sensors so that reproducibility remains an important issue for this type of sensor[28].

Immobilization of enzymes and enzyme loss

As we discussed, non-enzymatic glucose sensing is the most commonly applied method of sensing in commercial glucose monitoring systems, and the drawbacks of this system make it reasonable to develop other forms of sensing. The catalytic activity of enzymatic glucose sensors is generally decreased due to the immobilization process (Fig.2.23). This issue reduced the performance. There have been several methods proposed to make sure the enzyme immobilization will not lead to enzyme loss. However, this issue is still one of the main problems with the fabrication of enzymatic glucose sensors[106].

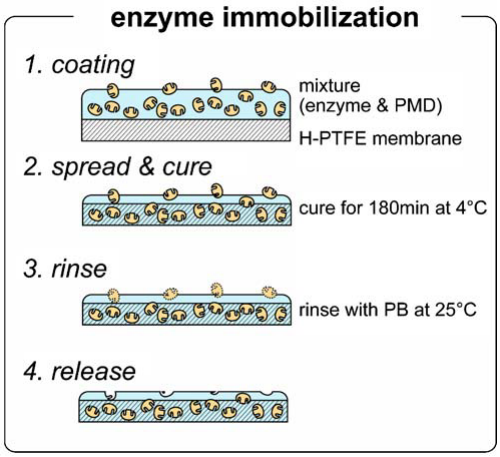

Figure 2.23: Enzymes immobilization general schematic process flow [26]

Despite improvement in fabrication and theory of glucose sensors, their dependency on the ambient conditions is one of their most significant issues. The GOx, as the most promising enzyme material, is highly affected by pH ranges (in the 2-8 range), temperatures (below 44°C) and humidity [1].

2.2.4.2 Non-enzymatic glucose sensor

The non-enzymatic glucose sensing platform was developed due to drawbacks and instabilities in enzymatic sensing. All types of enzyme-based sensors requires complicated enzyme immobilization.The high oxygen dependency of these sensors makes them unproficient and unreliable for sensing applications. Non-enzymatic doesn't have oxygen limitation as we have for most enzyme electrodes, in which, abnormal oxygen concentrations cause a deviation in received sensor signals compared to normal oxygen concentrations.[28]. Moreover, the other electroactive species in the solution can easily manipulate these types of glucose analyzers. These problems are still not completely resolved in new generations of enzymatic glucose sensors[1], which makes a non-enzymatic type a suitable approach for simple, lower cost and more reliable sensor production.

The elimination of enzymes and the electro-oxidation of glucose on the surface generates another possibility for sensing systems to detect glucose. This type of glucose sensor is commonly named the fourth generation of glucose sensors. The general comparison between the familiar generations of the glucose sensor is illustrated schematically in Fig 2.24

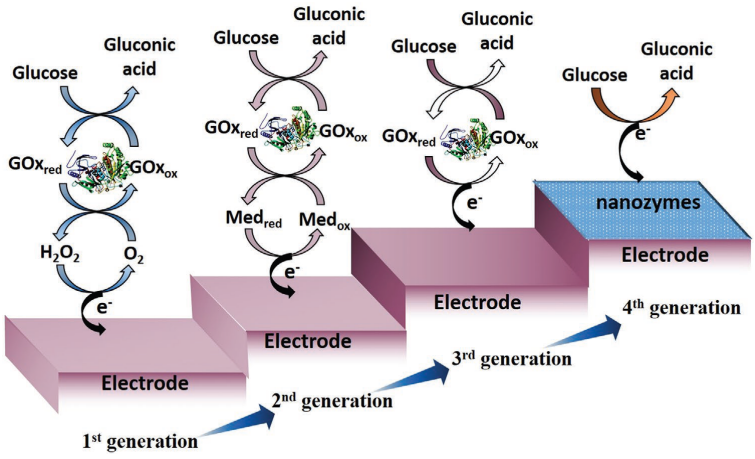

Figure 2.24: Generations of Glucose sensors, including non-enzymatic sensing [27]

The natural D-glucose are known based on five different isomers (see Fig. 2.25). In aqueous solutions, the g-glucose, cyclize rapidly and results in a furanose, a five-membered ring, or , pyranose, a six-membered ring. Based on the arrangement of of the hydroxyl group attached to C-1, the two cyclic glucoses can be distinguished into α and β anomers. The α and β anomers, equilibrate by acid-catalyzed hydrolysis through an open-chain structured g-glucose intermediate. This process is known as mutarotation which is normally slow and takes up to 2 hours to reach equilibrium. This equilibrium and isomeric ratio are highly dependson the physico-chemical environment, such as pH, temperature, and the presence of other ions [28, 1, 107].

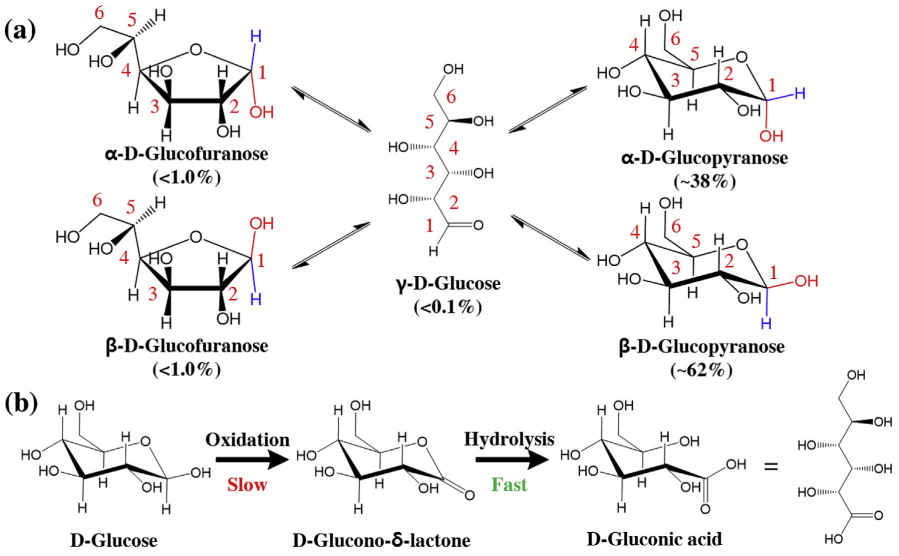

Figure 2.25: (a) Molecular structures of various D-glucose isomers and their composition ratio in aqueous glucose solution at standard condition. (b) General process of glucose oxidation. [28]

The ideal system in which the glucose is directly oxidized on the surface of the electrodeis first developed by Walter Leob in 1909, a long time before the first glucose sensor was proposed by Clark. He showed the possibility of oxidizing glucose on a lead anode's surface[1]. Various types of these types of sensors have been developed and tested for glucose sensing for over a decade.

In this type of glucose sensor electrodes, most electrocatalytic processes happened through adsorption where reactant molecules adsorb onto active sites of the electrode. Different factors such as electronic states, empty d-orbitals, or defects affect the adsorption process [28]. The dependency on such factors shows the importance of surface condition and morphology in these types of sensors.

In non-enzymatic glucose sensors, after the adsorption of the reactant, breaking bonds

and formation of intermediates occur. When the oxidation state of the redox center is changed, it results in weakened interaction between the product and electrode, which lead to desorption of the reaction product from the electrode surface. This process are commonly named as the chemisorption model[28] which is shown in Fig.2.26-a.

Despite the incredible attention toward non-enzymatic glucose sensors over a decade, this type of sensor typically had problems that make them unsuitable for practical sensors. The sensitivity of these devices varies based on the surface morphology and catalysts used.

Non-enzymatic glucose sensors have been typically used in two different regimes. The first is the fixed potential, chronoamperometric method for electrochemical determination, shown in the Table 2.1. Another possible way to use these sensors is through flow injection analysis (FIA) and liquid chromatography (LC). The sensitivity will be high in these cases, but not always as high as enzymatic glucose sensor, and the sensors will last for a long lifetime due to elimination of enzymes[1].

Table 2.1: Non-enzymatic sensors based on fixed potential, chronoamperometric for electrochemical analyzes[1]

Material(s)	*Sensitivity (mA $mM^{-}1cm-2$)*	*Linear range (mM)*	*LOD (μM)*	*Year*	*Ref**
Porous Layers					
Ni-Au	5.1	1e-3 to 10	-	2009	108
Pt	0.642	0.1 to 1.5	-	2008	53
Pt	0.291	1 to 10	-	2008	69
Pt-Ir	0.0937	1 to 10	-	2008	76

Au	0.0466	5e-3 to 10	3.2	2008	81
Pt	0.0375	0.05 to 30	50	2008	71
Au	0.032	2 to 20	2	2007	83
Pt-hollow	0.0313	1e-3 to 10	0.1	2005	68
Au	0.0118	2 to 10	5	2007	82
C-ordered	0.0108	2.5 to 5	20	2007	186
PtPb on Ti	0.0108	1 to 16	-	2008	77
Pt	0.0017	1 to 10	97	2007	72
Pt	0.00083	-	-	2008	70
Nanotubes, Nanoparticles, and Nanostructures					
Pt-CNT	0.28	2e-4 to 12	0.2	2009	55
Cu-CNT-GC	0.256	5e-4 to 0.5	0.3	2004	59
SWCNT	0.2486	0.01 to 2.16	10	2007	158
Pd-SWCNT	0.16	0.5 to 17	0.2	2009	244
Ni-MWCNT	0.0369	5e-3 to 2.8	1	2009	60
CuS-CNT	0.035	1e-3 to 12	1	2009	55
MnO2-MWCNT	0.03319	0.01 to 28	-	2008	160
PtRu-MWCNT	0.02826	1 to 15	25	2008	56
PtPb-MWCNT	0.0178	up to 11	1.8	2007	57
Cu-CNT-GC	0.01776	7e-4 to 3.5	0.2	2007	163
Pt-MWCNT	0.01183	1 to 9 & 9 to 23	50	2008	54
PtRu-MWCNT-GC	0.0107	0.2 to 15	50	2009	128
SnO2-CNT	0.0099	3e-3 to 12	3	2009	55

CuS	0.00784	0.05 to 5	-	2008	245
Cu2O-MWCNT	0.00653	5e-5 to 5e-3	0.1	2009	
C-MWCNT	0.00436	2e-3 to 11	1	2004	157
Au	0.00113	1 to 42.5	10	2009	92
Pt	0.0001	2 to 14	1	2005	75
Pt-MWCNT	-	1 to 26.5	-	2007	166
CoOx-MWCNT-GC	-	0.15 to 5	70	2008	167
Ni	1.04	0.01 to 10	2.7	2010	106
Ni-C	0.4202	2e-3 to 2.5	1	2009	107
Cu-SWNT-GC	0.256	5e-4 to 0.5	0.3	2004	59
Ni-C(liquid)	0.202	0.05 to 23	6	2009	112
Au-ITO	0.1835	4e-3 to 0.5	5	2009	86
Au-Silicate	0.179	7.5e-5 to 7.5e-4	0.1	2006	87
Pt	0.1377	0.2 to 3.2	5	2007	73
Pt	0.0615	up to 20	1	2008	74
CuS2-CNT	0.035	1e-3 to 12	0	2009	55
PtPb-MWCNT	0.0178	up to 11	1.8	2007	57
Ni-GC-Pt	0.00144	up to 8	15	2007	192 & 246
Ni-Ti	7.32	0.05 to 0.6	1.2	2008	3
Ni(NW)	1.043	5e4 to 7	0.1	2009	247
CuO-NFs-GC	0.4313	6e-3 to 2.5	0.8	2009	248

Cu(NSphere)-Nafion	0.40453	up to 2.55	1	2008	249
Cu(Nanobelt)	0.0798	0.01 to 1.13	10	2009	250
Pt	0.0121	1 to 20	1.2	2008	251
PtPb (NWire)	0.01125	1 to 11	8	2008	78
C	0.0081	up to 7	0.2	2009	153
Pt	0.00052	2 to 20	-	2010	159
CuO(NWires)	0.00049	4e-4 to 2	0.049	2008	252
Cu(NRod)	0.00045	0.01 to 0.1	1.2	2008	168
***Original article reference numbers**					

One of the main concerns with those developed sensors is their selectivity (the ability of the sensor to respond to a particular analyte without interference from others). However, the durability and sensitivity show a promising approach toward a better future of this type of glucose sensor.

Chemisorption and effect of surface condition and morphology Direct glucose oxidation on the surface of the electrode is the primary process for non-enzymatic sensors. This process is called chemisorption on the surface or electrocatalysis of glucose. This process consists of the attachment of molecules to the surface of the electrode. These attachments are highly dependent on the d-electron or d-orbitals of the electrode material[28, 1].

The chemisorption process includes some forming and breaking the bonds between molecules and the surface of the electrode (Fig 2.26 a). Therefore the medium strength of this bond will be ideal for glucose sensing using a non-enzymatic mechanism. [1]. It was proposed that the presence of some mediators, like hydrous oxide, on the surface of the electrode enhance the electro-oxidation of glucose (Fig 2.26 b) [28].

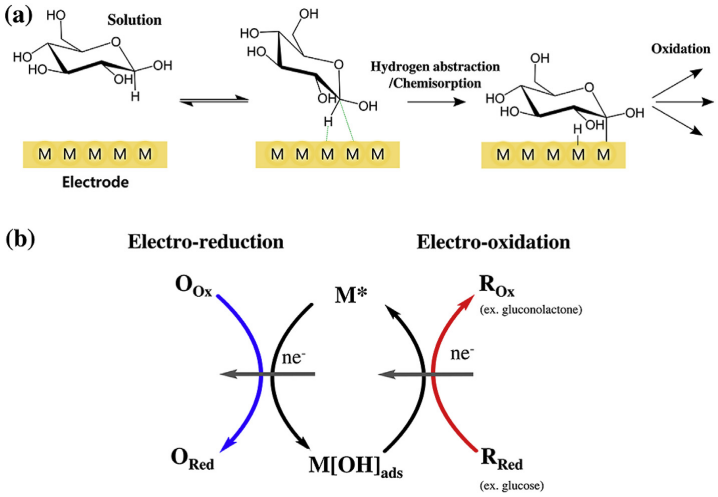

Figure 2.26: a) Chemisorption of Glucose on the surface of the electrode and b)hydrous oxide (OH_{ads})/atom mediator model [28]

The glucose-sensing mechanism is also highly dependent on the orientation and surface morphology of electrodes [1]. Adzic [29] showed that the orientation of single-crystalline gold film affects the chemisorption and detection of glucose sensors (Fig2.27 a). In another work, Kokkinidis [30] showed the effect of crystal orientation on the chemisorption process and sensing for platinum electrodes(Fig2.27 b).

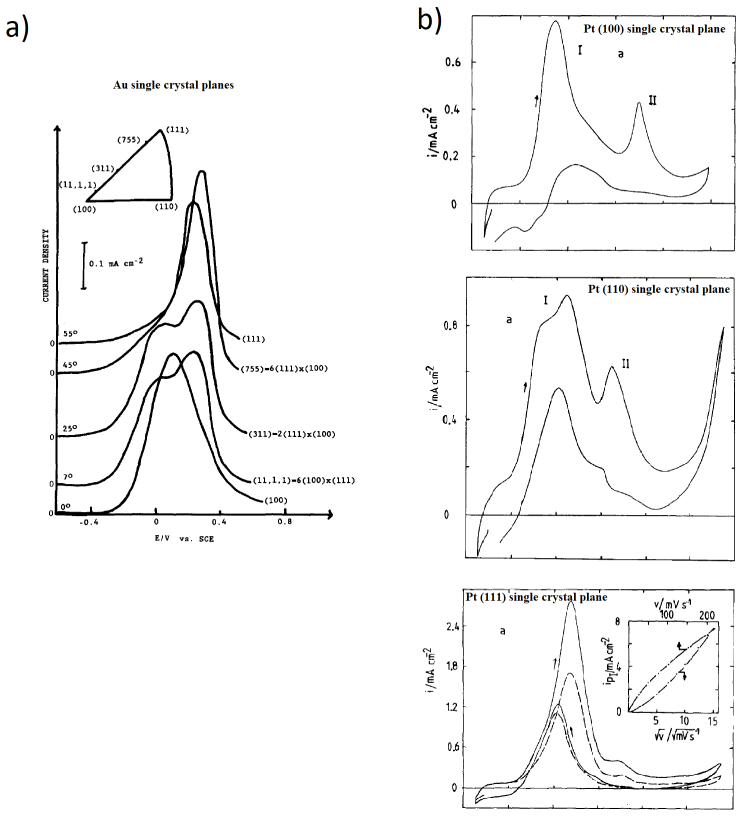

Figure 2.27: Chemisorption of Glucose on a) gold single crystal surfaces of electrode [29] and b)Platinum single crystal surface [30]

2.2.5 Effect of other parameters and multiplexity

Reliability of glucose level measurement in blood, ISF, and other body fluids are also affected by variations of other parameters such as pH, temperature and presence of other ions[28]. Therefore, in order to prepare a platform for future reliable sensing, those factors should be considered in the sensor design. This coupled consideration of different parameters can be done in various ways. One of the possible and promising approaches

to measure different biosignals at the same time is by using multiplexed sensor systems which will be discussed in this section.

2.2.5.1 pH monitoring on glucose sensing

One of the most critical parameters to diagnose different kinds of disease is to analyze the variations in body fluids such as pH. This parameter is also essential factor in interstitial fluid that can shows normal and abnormal health conditions. The pH variation in normal conditions in the range of pH from 7.35 to 7.45.

The pH of body fluids is generally determined by the content of protons (H+). This Proton content is generated from organic acids produced in living cells. A common proton source is a lactic acid (lactate/H+) involved in regulating physiological pH.

To keeping upa steady of body fluid pH, distinctive buffering frameworks are utilized in addition to proton excretion from the cytosol to the extracellular space and eventually exterior of the body. On the rare case that the acidic formation increased or the buffering and excretion frameworks are disabled, body liquid turns acidic, driving to unusual conditions. Also, there is an active link between glucose concentration in blood and pH of the body fluids [108].

Insulin resistance is one of the crucial factors in diabetes variable disorder of carbohydrate metabolism or so-called mellitus. It has been understood that the pH of interstitial fluids is lower in the diabetes mellitus condition compared to the situation in non-diabetic control. This lowered pH is one of the reasons for producing insulin resistance[31]. Therefore pH characterization for interstitial fluid is one of the most important parameters for health monitoring.

Despite the mechanism of interstitial fluid (ISF) extraction, the capability to detect the

pH variations of ISF is the second application we considered for our sensors fabrication. The pH variations in ISF might be different from that in blood. This difference in pH value can result from a mild or severe metabolic disorder that is not detectable from blood. The pH variation in blood and ISF and the binding affinity of insulin to the receptor are shown in Fig.2.28 [31].

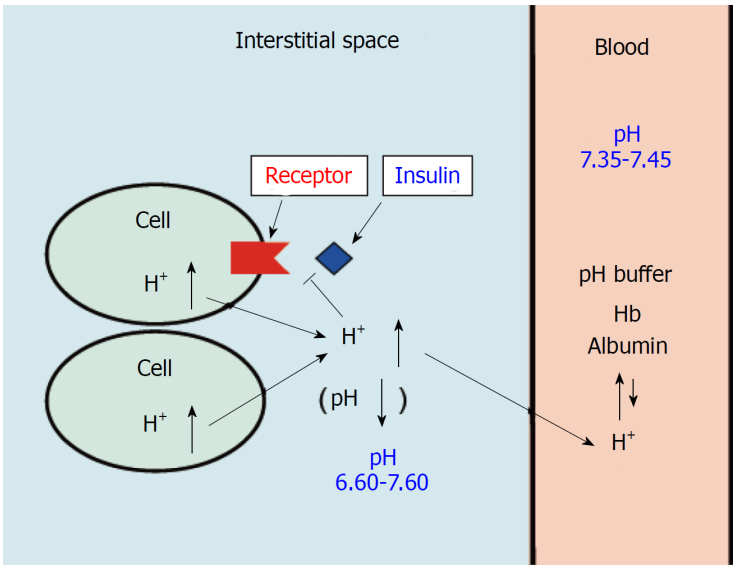

Figure 2.28: pH variations in interstitial fluid (ISF) and blood, and the insulin affinity to the receptor[31]

Unlike the sensor for anastomotic leak detection, which qualitatively detects pH variation in the short term, in the ISF pH monitoring system, the pH measurement in a quantitative way is essential for high sensitivity. This is because the pH in interstitial fluid is generally in the range of 7.35 to 7.45. In the case of abnormality, this pH range might change just slightly. This small variation makes it essential to detect the pH with high sensitivity in this range of pH values. However, the detection of pH using the polyaniline-coated gold electrodes is not highly sensitive.

2.2.5.2 Multiplexed electrochemical sensing

Sensing multiple biological signals for disease diagnosis has recently received a considerable attention due to their importance on clinical decision making. As one of the less complicated type of biosensors, electrochemical devices have become one of the preferred sensing platform[109]. According to the general definition, "Multiplexing is, simultaneous electronic transmission of two or more messages in one or both directions over a single transmission path, with signals separated in time or frequency. In time-division multiplexing, different time intervals are employed for different signals." [110].

Analyzing multiple biomarkers for the health monitoring system is also essential due to the interactive effects of bio-signals on each other and its' importance to have an effective monitoring of health condition. Multiplexing analysis of biomarkers and sensors is one of the best ways to transform data from the sensors to the analyzers. The schematic format of a multiplexed signal transformation and processing system is illustrated in Fig.2.29. The received signal might not be the same as the sensor signals due to noise and constructive or non-constructive signal mixtures. Still, the part of the translated signal can be used to detect the original condition of the received sensor signal.

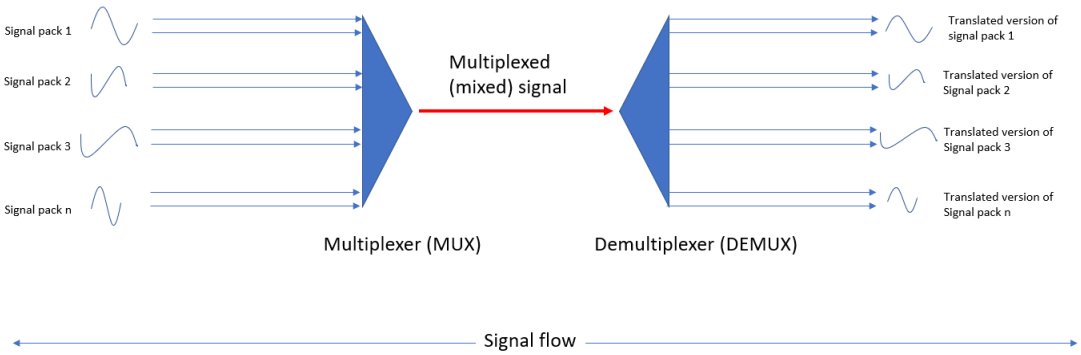

Figure 2.29: General format of multiplexing and demultiplexing signals.

Hwang et al.[111], for example, used multiple microfabrication processes to build electrodes and polymeric microchannels integrated biosensor device that detects matrix metalloproteinases (MMPs) for cancer diagnosis [6]. Photolithography was used to pattern the electrodes after spin coating positive photoresist onto glass wafers. Following that, E-beam evaporation was used to coat Au and Pt, and then wet etching was used to finalize the electrode patterns out of these materials. Photolithography was used for spin-coated negative tone photoresist (SU-8) to fabricate microchannels. Also, a PDMS layer over an SU-8 mould was fabricated as the final top layer. The chip was then connected to this microchannel using oxygen plasma treatment and 100 C temperature baking for an hour.

A similar approach was used by Lee et al [22] to fabricate their device for Multi-Pulmonary Hypertension Biomarker. As illustrated in Fig.2.30, the fabricated device, consists of three PDMS microfluidic layer attached on top of patterned electrode array made of evaporated Au on a glass substrate.

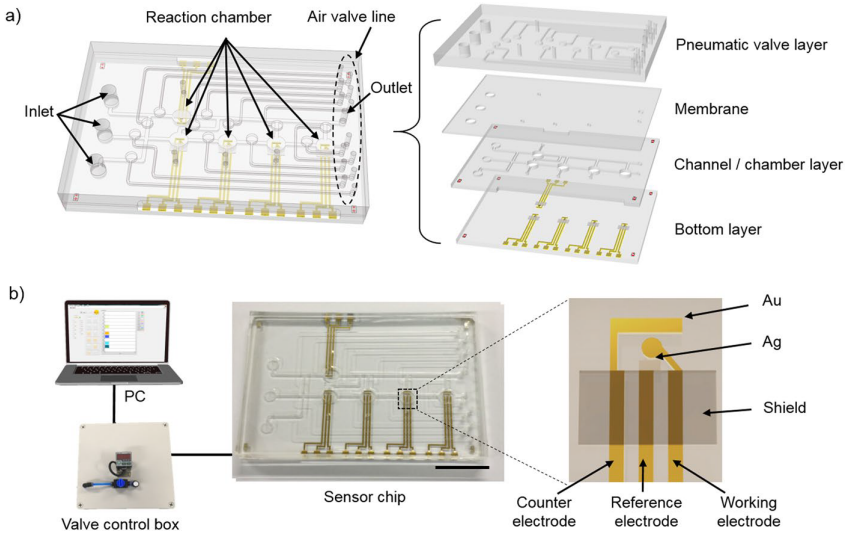

Figure 2.30: Schematic illustration of the microfluidic system for electrochemical analysis composed of a glass bottom layer with electrodes, PDMS channel/chamber layer, PDMS membrane, and PDMS pneumatic valve layer. [22]

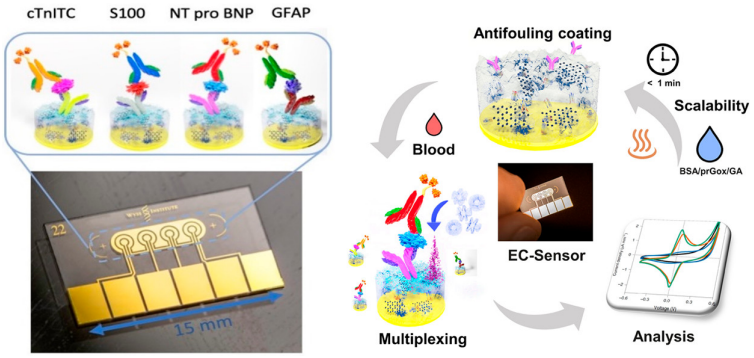

Figure 2.31: Multi-electrode array system for multiplexed electrochemical biosensing with implemented antifouling layer on top of electrodes [32]

In another approach, Timilsina et al. [32] implemented an antifouling layer materials with an embedded gold nanowires on a gold multi-electrode array system fabricated on

glass substrate to improve the ability to use the electrochemical multiplexed sensor system used for longer time without the problem of biofouling on the electrodes as it is shown in Fig.2.31.

Chapter 3

pH sensor, fabrication processes and application-based designs

One of the most crucial fields in biosensing is the point-of-care (POC) system. In this system, the sensing effort is based on point-of-care-testing (POCT), which performs rapid testing by carrying out a diagnostic or prognostic test. This test should be fast and facile performed without the need for expensive or complicated instrumentation [112, 113].

This chapter investigates the fabrication and miniaturization of point-of-care (POC) pH sensors. These sensors will monitor the anastomotic leak in the human body's digestive system. Also, another approach for pH sensing for interstitial fluid (ISF) pH monitoring system will be explored.

3.1 pH monitoring for anastomotic leak detection

As discussed earlier in Chapter 2, anastomotic leakage is one of the most severe complications to patients following colorectal surgery. Conventional methods like CT-Scan, in general, are costly, time-consuming and inefficient. Continuous pH monitoring is one of the possible methods to help surgeons detect these complications in the early stages.

One of the critical points toward the fabrication of practical POC biosensors is the efficiency and cost of fabrication. The pH sensors are fabricated using standard microfabrication techniques to achieve this purpose. Moreover, the possibility of using novel materials as a pH-sensitive transducing layer was investigated. On the other hand, some of these methods might be possible to use as an enhancement method for the sensitivity of ISFETs through gate modification or extended gate field-effect transistor (EGFET).

The practicality of the fabricated sensor, on the other hand, is another essential factor that should be considered. In this research, to achieve such a purpose, the design and fabrication techniques were done based on surgeons' recommendations. Also, the tests administered are based on the Food and Drug Administration (FDA) requirement in Canada.

3.2 Fabrication methodology and design

To reach the most effective bio-sensor for in-vivo applications, first, we need to fabricate a stable, biocompatible electrochemical sensor. Several parameters should be considered

for the most efficient design. Some of these parameters are the method of electrochemical sensing, reference electrode material and types, and working electrode structure.

Method of sensing highly affects the sensor design, materials, and fabrication processes. Based on the application and sensitivity of the materials, one of these methods can be used for biosensing applications.

Furthermore, a suitable reference electrode with maximum efficiency and durability is a dominant factor in the final performance of the biosensing system. This factor might be different based on the estimated capability and durability of the sensor. Therefore, one of the biggest challenges toward miniature pH sensors is the fabrication of suitable reference electrodes with the highest efficiency and durability required for the specific application. In the case of anastomotic leak detection, the maximum durability of the sensor should be one or two weeks after the surgery.

A stable pH-sensitive working electrode with the highest possible sensitivity and efficient, low-cost fabrication is one of the main parameters that should be considered for a practical POC sensor system. The modification of pH sensors toward the highest possible sensitivity using micro- or nano-fabrication methods is one of the practical aspects of efficient miniaturization. In the previous attempts by researchers to increase the sensitivity of the biosensors, they used nanostructured working electrodes or the nanopatterned gate for ion-sensitive field-effect transistors (ISFETS) using some conventional nano-fabrication methods. Some of the investigated materials and designs showed some promising increase in the sensitivity of the sensors depending on the types of sensing. The reported increase in sensitivity is typically in the order of 40mV/pH, and the maximum sensitivity over the Nernstian limit was around 70mV/pH. Only some researchers claimed the huge sensitivity improvements (around 400mV/pH) using the nanostructure gate patterning modification for ISFETs[12].

In the case of anastomotic leak detection, since the change in pH resulting from leakage will be significant in most cases, we focus on the sensor that can detect these variations quickly and, efficiently. Researchers have demonstrated several proposed pH sensors for laboratory use and potential medical applications. However, the pH biosensor used explicitly for this detection is still demanding. In this project, we investigate the possibility of pH sensor fabrication, for this specific application, in the form of a rigid and flexible sensor chip.

The working electrode can be modified using nanostructures to obtain the required sensitivity. For this purpose, several approaches can be taken, including nano-fabrication methods or self-assembly methods. In the case of polysilicon material or amorphous silicon (based on the nano-fabrication techniques), e-beam lithography patterning followed by etching to fabricate a high aspect ratio nano-pillars or even different nanostructures can be patterned. However, the cost of fabrication is one of the critical points that should be considered. The details about the achieved improvement in sensing materials and the effect of their structure will be discussed in Chapter 5.

3.2.1 Materials and Methods

This part will present different approaches used toward the design, modification, and fabrication of miniature pH sensors. Some materials and nanostructure patterning will be discussed later in Ch.5 in a more detailed discussion.

3.2.2 pH sensors, fabrication methods

Depending on the required sensor characterization, two types of fabrication processes have been demonstrated and characterized. These fabrication methods also have been

used for multiplexed sensor fabrication. Rigid sensor fabrication based on silicon and silicon dioxide rigid substrates has been used in some sensor fabrication. Also, polymeric substrate with a high degree of flexibility has been corroborated in this research.

3.2.3 Fabrication of rigid sensors

The rigid pH sensors have been fabricated using 4-inch silicon wafers with thermally grown oxide on top of that as an insulator. Before processing wafers, they were cleaned using standard cleaning, including RCA1 and piranha cleaning procedures (as a standard process to remove the organic compounds on the surface) followed by RCA2 cleaning (to remove any metal residue on the wafer surface). The oxygen plasma cleaning for 60 sec with 20 sccm oxygen flow, 20 mTorr pressure was carried out using Giga to Nano Electronics Laboratory (G2N) reactive ion etching (RIE) equipment for these samples. Some processes were also done in Quantum-Nano Fabrication and Characterization Facility (QNFCF), using oxygen plasma treatment equipment, Yield Engineering Systems (YES)-Ash system.

After cleaning, the wafers are coated with three metal layers. These metal layers and their characteristics are listed in Table3.1. Chromium and titanium can both be used interchangeably in rigid sensor fabrication processes. The first layer (titanium) is used as an adhesion layer. Gold thin film is used as a typical conducting layer and the third layer (here, chromium) as a top layer which needed in the case of dry etching processes. The thickness mentioned in Table 3.1 are the optimal thicknesses based on several experiments.

The coating process was done using e-beam evaporation equipment. The Intlvac Nanochrome™-II e-beam/thermal evaporator system was used for coating electrode materials mentioned earlier. The method used for this coating process was based on 100 rpm rotation of the holder without any substrate heating.

Table 3.1: Metal coatings for pH sensor fabrication

Metals	*Deposition rate*	*Final thickness*	*method used*
Chromium (Cr)	0.5Å /sec	20nm	e-beam evaporation
Gold (Au)	1Å /sec	175nm	e-beam evaporation
Ti (Ti)	1Å /sec	20nm	e-beam evaporation

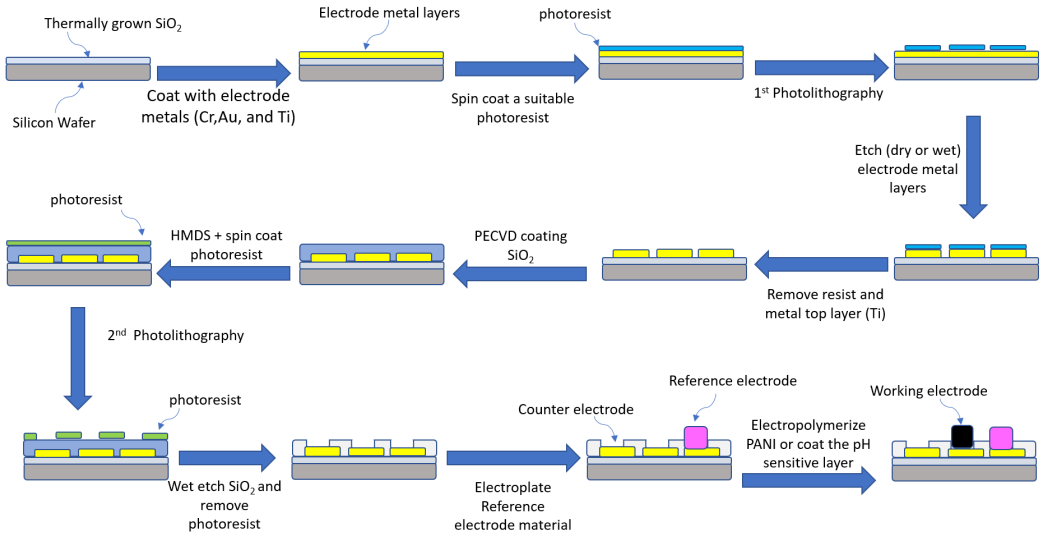

Figure 3.1: Schematic process flow for rigid miniaturized sensors

The lithography process is the next step toward achieving the desired sensor chips' designs. First, the designs for UV-lithography were made using an open-source software tool, KLayout. The designs have been used in two UV-Lithography systems. For the experiment purposes and modification of sensor design, the rapid mask-less aligner (MLA) system of UV-lithography has been used. This MLA system was used to define optimized designs based on the results of later experiments and the requirement proposed by surgeons. The equipment used for MLA lithography was the MLA150 Direct Write UV Lithography

system by Heidelberg Instruments available in QNFCF.

For the first lithography step, the coated thermal silicon dioxide wafers were spin-coated with available positive or negative tone UV-resist. The negative tone Microresist Ma-N 1410 has been tested and parameterized to achieve the desired structure. The spin-coating condition was shown in Fig 3.2. After the spin-coating, based on the recommendation of the manufacturer and the optimal condition defined by the experiments, the spin-coated photoresist was soft-baked using the hotplate with 100 °C for 90 sec.

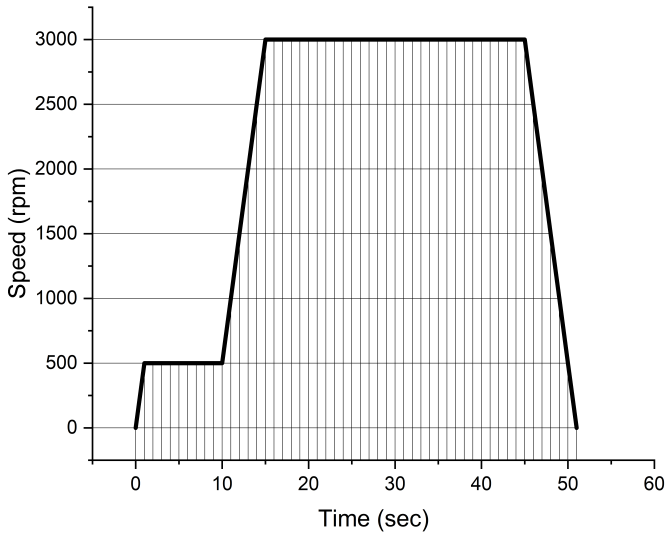

Figure 3.2: Spin-coating profile for MaN-1410 negative tone photoresist

The lithography processes on the spin-coated samples have been done using MLA equipment with 440mJ/cm2 exposure dose. Upon reaching the stable design, the process was done to fabricate UV-lithography masks using commercially available TELIC™ mask blanks covered with 1600Å low reflective (8% @ 450nm) DC Sputtered chromium with

5300Å of AZ1500 photoresist.

The mask blanks were patterned using the MLA lithography system and developed and etched with commercial chromium enchant and cleaned to achieve the desired mask for photolithography systems. The Suss MicroTec MA6 aligner/exposure system was used for the photolithography with the fabricated mask. The exposure dose for the Ma-N 1410 photoresist, was 350 mJ/cm2 using light with 365 nm wavelength, which by close estimation gave 35 sec exposure time for CH1 of MA6 system.

Whether patterned using MLA or Mask aligner system, the exposed samples were developed using MA-D 533s developer for 1 min followed by 1 min DI water rinse and nitrogen gun drying. To ensure no residual photoresist was remaining, the sample was cleaned using 10 sec of oxygen plasma treatment (YES-ash or RIE) to remove any photoresist residue in the trenches.

The photolithography process is followed by wet or dry etching of the samples. In the case of wet-etching, the commercial solutions available for etching films have been used to remove the metal layers from undesired areas as a step-by-step process. For the chromium, gold and titanium etching, Transene chromium etchants 1020, gold etchant TFA, and diluted buffer oxide etchant (BOE) (1:10) have been used. The etch rates for these three wet etching process is listed in Table 3.2.

Table 3.2: Wet etching rate using commercial enchant

Wet etching solution	*etching rate Å /sec*
Transene chromium etchants 1020	40
Gold etchant TFA	28
BOE (1:10) for Ti etch	400

Dry etching using ion milling process is an alternative way to remove unprotected areas

of the coated metal layers on the wafer. Reactive ion etching cannot be used for this purpose due to the gold layer. Instead, the sample was etched using an Ar ion milling tool (AJA ATC-2030-IM) with 400V, 190 mA, and 90-degree angle (normal incident). The ion milling process is an easy, convenient way to remove the metal layers. The etching process for the films mentioned above takes 10min ion milling.

After the etching process, the photoresist was removed by organic solvents or oxygen plasma. In the case of dry etching, removing the resist after the process using solvent needs more effort duo to cross-linking of the resist by plasma. In this case, the combination of solvents and oxygen plasma treatment can remove the resist. The solvents used for this purpose were acetone, Remover PG (Kayaku Advanced Materials,.Inc), or in really harsh condition DuPont™ PlasmaSolv ® EKC265™ Post-Etch Residue Remover.

To prevent the metal lines from participating in electronic exchange during sensing, the samples were coated with a passivation layer. The passivation for the rigid sensors has been done using the plasma-enhanced chemical vapour deposition (PECVD)-coated silicon dioxide. This layer was coated on the sample using Oxford Instruments (System 100) PECVD with deposition condition at 330°C with N_2O/SiH_4 gas mixture. The coated layers on the wafer samples were typically more than 1μm thickness.

Following the passivation layer coating, the layer on the electrode and connection pad areas should be removed. Therefore the second step, lithography, was performed. To achieve good adhesion between the photoresist and the passive oxide layer, the hexamethyl disilizane(HMDS)(C3H9Si) was applied on the surface using YES-310-TA Vapor Prime Oven. Following HMDS treatment, a positive tone photoresist layer, Shipley 1811, was applied on the surface of the wafer using the spin-coating method. The condition of spin-coating is mentioned in Fig 3.3. Based on the standard recommendation of the manufacturer, the coated samples were baked at 115°C for 60 sec.

As we did for the first layer, the second layer lithography was done with an MLA system for rapid optimization of the design. After reaching the optimized design of the sensor, the photomasks were made using MLA to be used for the mask aligner system. The MLA lithography of Shipley 1811 was done with 140 mJ/cm2. In the case where the mask-aligner was used, 125 mJ/cm2 or 3.4 to 5.0 sec were used.

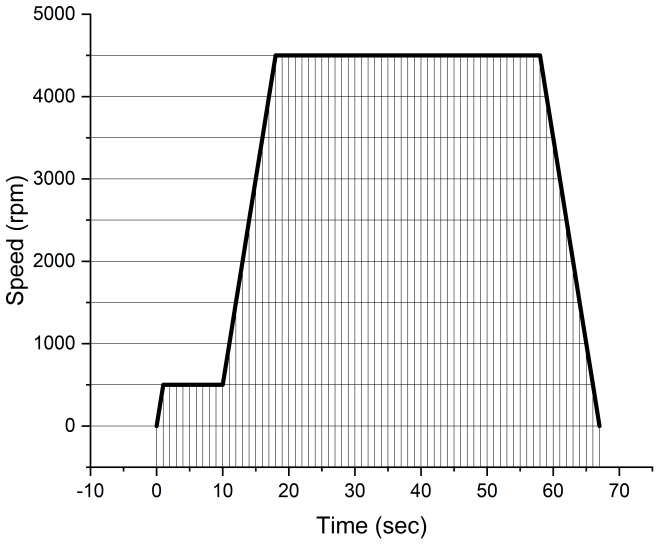

Figure 3.3: Shipley 1811 photoresist spin-coating condition

Whether exposed by MLA or masked photolithography, the exposed wafer was developed by immersing the sample in MF-319 (Microposit) developer solution for 1 min followed by rinsing with DI water and nitrogen gun drying. Some electrodes fabricated based on different designs are illustrated in Fig.3.4

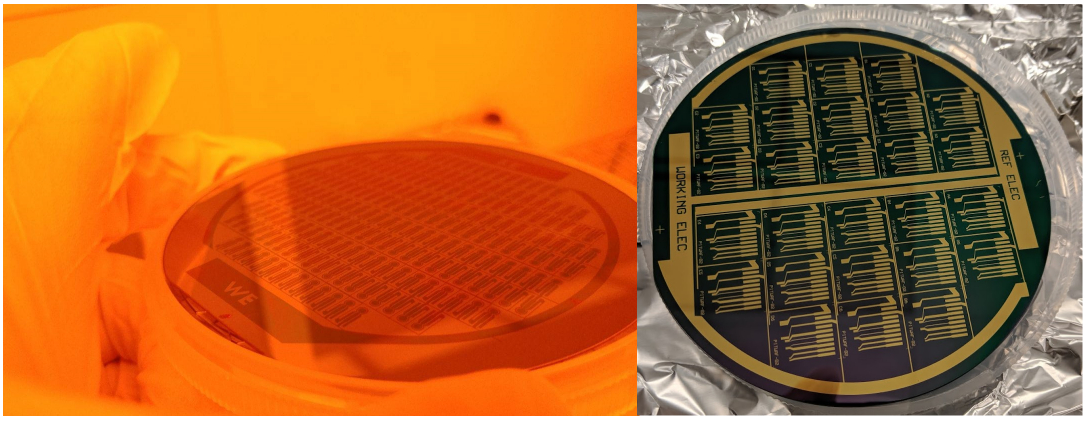

Figure 3.4: Some of fabricated sensor based on electrodes with different designs

The resulting microelectrodes (based on the design) can be used for further electrode material coating process (will be discussed later). The schematic fabrication process flow was illustrated in Fig.3.1.

3.2.4 Fabrication of flexible sensors

Depending on the conditions of performance required for the fabricated sensor, the mechanical stability and degree of flexibility might be a ruling factor. Fabrication of flexible electronic devices has been reported on various polymeric and non-polymeric flexible substrates. Meanwhile, two polymeric substrates are most common for flexible electronics. These two polymeric materials are polyethylene terephthalate (PET) and polyimide (PI). As a biocompatible material with a reasonable degree of flexibility and high stability, polyimide is one of the main options for biosensing applications. To achieve the best mechanical characteristics and fabrication condition, polyimide sheets from DuPont™ Kapton® HPP-ST with different thicknesses, from 100 μm to 500 μm, have been used and tested.

The first step toward the fabrication of flexible devices is the cleaning process. However, since these substrates are polymeric, some solvents can damage them. The cleaning process of polyimide was done by rinsing with acetone, followed by isopropyl alcohol (IPA). The sample was dried using nitrogen gun purging. The dried samples were then treated slightly by oxygen plasma using YES-ash equipment. This oxygen plasma treatment helps slightly roughen the substrate's surface to enhance the adhesion of metal coatings to the polyimide.

The coating process for the flexible samples was almost the same as what we had in rigid sensor fabrication (refer to Table 3.1). However, chromium as an adhesion layer was not perfectly working for polyimide films (when we used chromium as an adhesion layer, the metal film peeled off during the patterning process). Therefore, we used only titanium as an adhesion layer for flexible substrates and chromium as a top layer.

To handle the lithography and etching process, we need to make coated polyimide sheets fixed and attached on a rigid substrate. For this purpose, the coated flexible films were attached to a silicon carrier wafer using photoresist as a bonding layer. The attachment process was done by spin-coating AZ4620 positive tone photoresist, as an attachment glue, on a silicon wafer. Following the spin-coating on a silicon wafer, the backside of the coated PI was placed and pressed firmly and uniformly on top of the photoresist. This process helps us keep the flexible film in a stable position during the lithography processes.

Stable and fixed polyimide film on silicon wafers was used for lithography processing. The lithography procedure is almost identical to what we had for rigid sensor fabrication. For the first step of lithography, a negative tone photoresist, Ma-N1410, has been used. The spin-coating condition and baking condition are the same as done for rigid sensors.

Like rigid sensor fabrication, the process on flexible substrates was done using MLA lithography. The MLA has been used to easily modify designs to reach the optimum

condition we need for the sensors. In the case of the optimum condition, the designs were transferred to quartz photolithography masks used for SUSS mask aligner equipment. Following the exposure, the samples were developed by ma-D 533/S developer (Microresist) for 1 min and rinsed with DI water and dried. The development will follow oxygen plasma discum cleaning to remove photoresist residue in trenches.

As discussed earlier, the metal layers were patterned using a wet or dry etching process for the flexible and rigid sensors fabrication. The wet-etching was done with commercial chromium, gold etchant and BOE for titanium etching. The photoresist used as a mask for first step lithography and etching, was removed using oxygen plasma and acetone.

After the etching process and photoresist removal, the electrodes fabricated in the previous steps should be passivated. The passivation process for flexible sensors is totally different from the rigid sensors. Since the flexibility of materials is the critical factor for this fabrication, SU-8 polymer photoresist was used to replace the silicon dioxide we had for rigid sensors.

SU-8 is a bio-compatible and flexible epoxy-based negative tone photoresist, a great candidate for flexible fabrication and an insulating layer for flexible electronics. Accordingly, the sample was coated with SU8-2002 (Kayaku Advanced Materials, Inc.) with spin coating condition shown in Fig3.5, baked and then patterned with MLA or mask aligner and then developed.

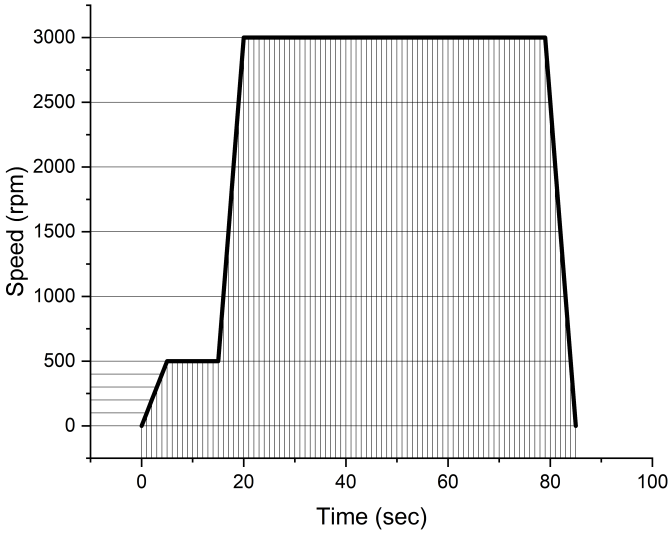

Figure 3.5: SU-8 2002 photoresist spin-coating condition

The SU8 coated samples were baked in two steps, pre-and post-exposure bake. The pre-exposure bake condition used for these samples was 120°C for 2 min using a hot plate. The recommended dose suggested by the manufacturer is 90 - 105mJ/cm2 which should be divided by 1.5 to 2 for highly reflective metal film layers. However, the wavelength used for MLA lithography is 375nm, which is almost entirely transmitted through the SU8 layer. This low absorbance of SU8 for this wavelength (Fig 3.6) increases the required dose to 480mJ/cm2, which is more than four times higher than the standard conditions at 365nm.

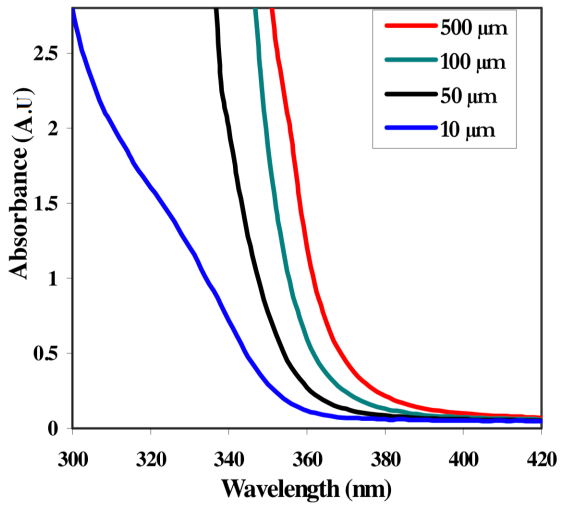

Figure 3.6: SU8 absorbance spectra for different wavelengths and film thickness [33]

After exposure, the samples were baked at 120°C for 8 min. The baked samples were immersed and developed for 1 min in SU-8 developer (propylene glycol methyl ether acetate- PGMEA). Then the samples were rinsed with IPA and dried using nitrogen gun. The samples were finally hard-baked at 150 degrees for 5 min to make sure the photoresist will remain stable during the following processes. Schematic process steps are illustrated in Fig3.7.

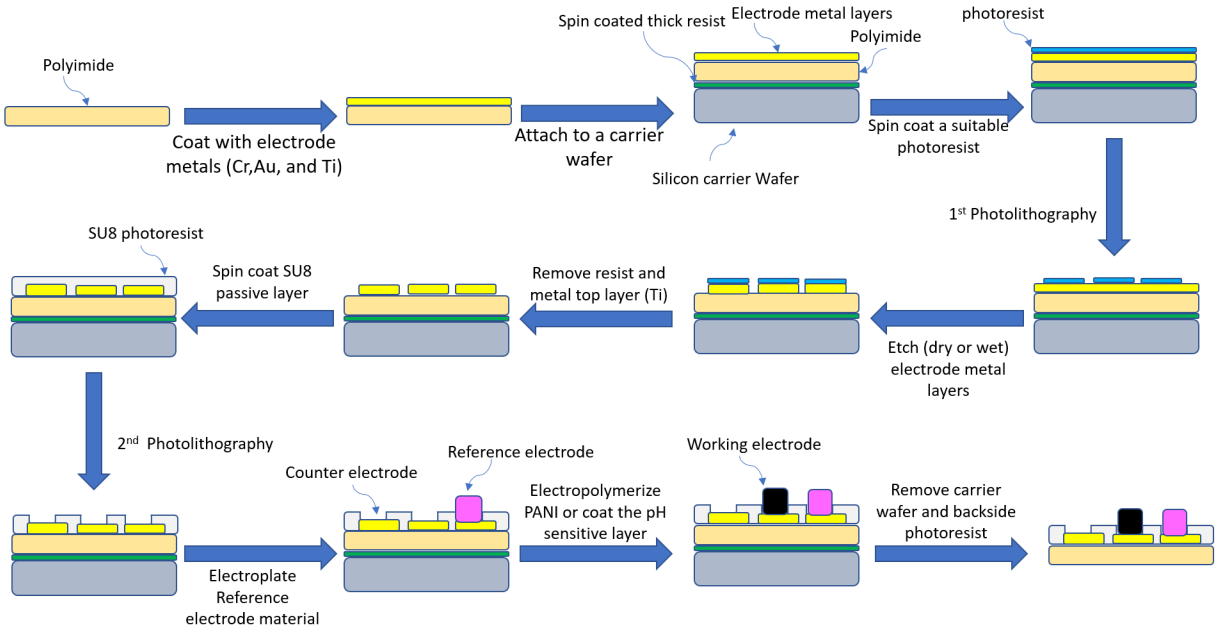

Figure 3.7: Process steps for flexible electrodes fabrication

Some of the flexible sensors fabricated using polyimide substrate with different designs are shown in Fig.3.8. A regular scissor or razor blade can easily separate these arrays of fabricated sensor chips from each other.

3.2.5 Electrode preparation for pH sensing and electrochemical system

Sensitive materials and their preparation are the most critical aspect of sensor fabrication. To achieve a pH sensor, we need to coat pH-sensitive material on the exposed electrode areas. We need suitable reference electrode materials and a sensitive working electrode(s) for two or three electrochemical sensor platforms. The preparation and application of sensing material(s) and the reference electrode highly affect the

sensitivity and applicability. Here we discuss the method used for these electrode materials preparation.

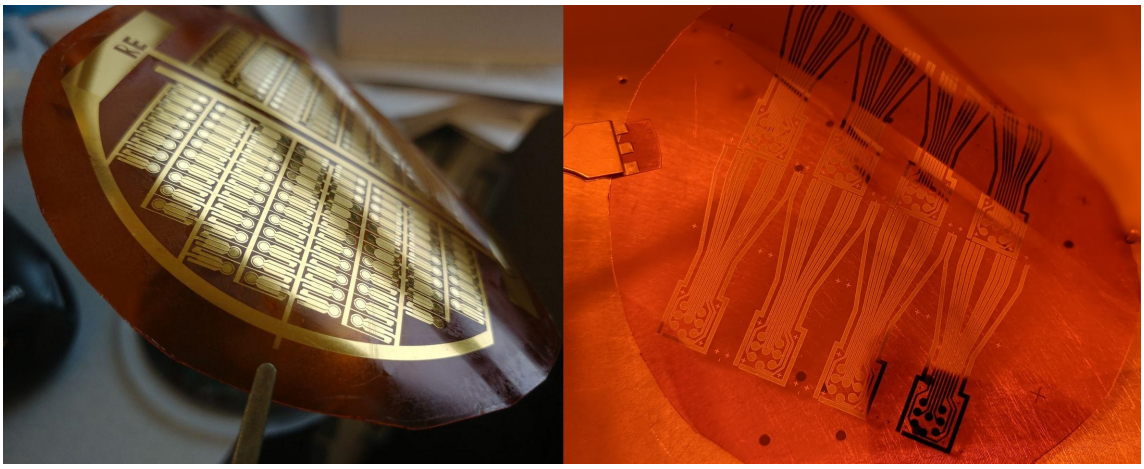

Figure 3.8: Flexible electrodes for pH sensor fabrication

3.2.5.1 Coating reference electrode materials

Since the sensors might be used for days, weeks or months, inside or outside the body, selection of a stable reference electrode are one of the main challenges for fabrication. As a result of biosensor working conditions, a pseudo-reference electrode with specific materials can be used. A combination of silver/silver chloride reference electrode material is one of the best known options.

Silver/silver chloride formation on the surface of a reference electrode can be coated using different methods such as screen printing, Ag/AgCl commercial paste or electroplating of silver followed by chlorination of coated film. Our research used the last option by electroplating Ag material on the surface.

The first step toward this method of fabrication is the electroplating of silver. We used

the commercial cyanide-based silver electroplating solution (this can be replaced with other non-cyanide-based solutions). The solution used in this research was a SILVERSENSE DW®cyanide silver electroplating solution (by Technic Canada Inc.).

The electroplating of silver on the electrode surface was done using different electroplating regimes. First, the electroplating was done based on constant potential on the specific surface area of the electrode that needs to be coated (Fig.3.9-b). However, the process was not easily controllable, and the surface of the silver-coating might be rough (Fig 3.9-a). The uncontrollable process resulted in the dendritic shape formation of electroplated silver. This morphology might not be ideal for the reference electrode. Improving the electroplating condition using a pulse generator helps us improve the uniformity of the morphology of the reference electrode material.

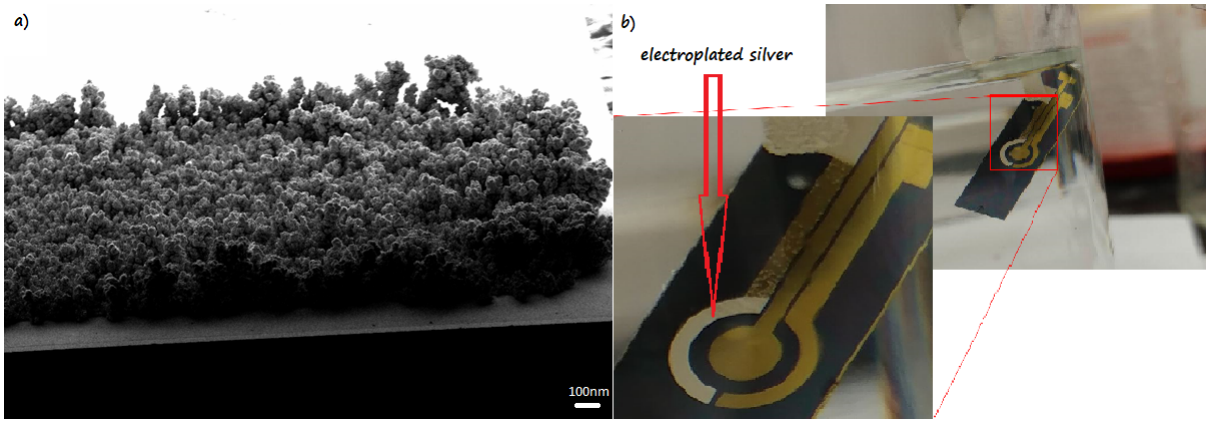

Figure 3.9: Silver electroplating a)Morphology and b)Electrode coating process

Pulse electroplating techniques were used to improve silver coating process. This process was done with an Agilent 33220A waveform generator. The pulse shape used for this process was tested to achieve the optimal state (around 10mA/cm2).

After the electroplating process, some of the coated material is chlorinated to be

transformed into silver chloride. This process was done using the 0.1M $FeCl_3$ solution or 0.1M HCl solution. This process leads to silver-chloride micro-pseudo-reference electrode by apply current of 10 mA/cm-2 for a duration of one minute.

3.2.5.2 Coat pH-sensitive material

The sensing material is the heart of each biosensor device. The quality of sensing material selection highly affects the capabilities of the sensor. Various pH-sensitive materials have been used for sensor fabrication, as discussed in Ch.2.

The pH-sensitive materials are generally in the form of oxides, like Iridium oxide and hafnium dioxide, nitrides like TiN, or polymeric. Among polymeric pH-sensitive materials, polyaniline (PAni) is one of the most popular and reliable materials that shows promising solutions for different types of pH sensing.

The key points that makes polyaniline one of the best selections for pH sensing materials is its ability to be coated using different methods. Electro-polymerization over selective area makes PAni one of the best possible pH sensing materials for electronic fabrication that can be industrialized.

Electropolymerization of polyaniline is a process of selective area polymerization and oxidation of monomer agents on the surface that provides electrons. This process can be done using techniques as simple as constant potential/current or pulsed potential/current or cyclic/potential-sweep method. The method of electropolymerization and the composition of the solution highly affect the morphology and sensing properties of the coated film (Fig3.10).

The cyclic voltammetric electropolymerization method is one of the main methods of coating polyaniline due to its reproducibility, good film adhesion and phase control. The

peaks in cyclic voltammetry define the polymerization steps and the polymer phases coated on the surface. The emeraldine salt (ES) is the only conductive and pH-sensitive polymer structure derived from aniline. Different types of PANI structure molecules are shown in Fig 2.11 in Chapter 2.

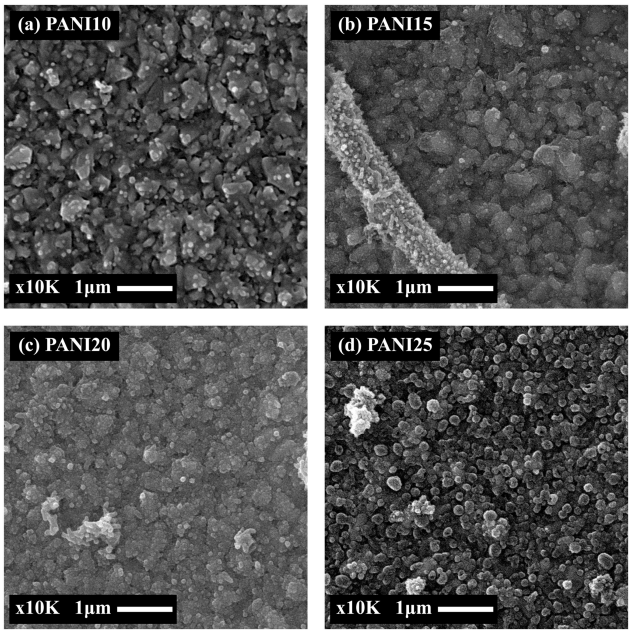

Figure 3.10: Effect of monomoer concentration on morphology of aniline. Numbers show the mM concentration of polyaniline inside the solution [34]

The cyclic voltammetry electropolymerization of PAni on the electrode surfaces was done using the potentiostat/galvanostat equipment (Bio-Logic Science Instruments-SP-50e and PalmSens4 single-channel equipment). The solution prepared for electropolymerization of polyaniline can have different monomer concentrations (aniline) and other oxidizing agents. Aniline used to prepare electropolymerization solution in our research was aniline (ACS reagent, 99.5% From Sigma-Aldrich). A 1ml of Aniline

solution was added to 100ml of Milli-Q water containing 0.5M sulfuric acid. The aniline directly added to water is insoluble due to the presence of oxygen. The solution was de-oxygenized by purging nitrogen inside the solution for 1 hour. This process makes an aniline solution ready for the electropolymerization process.

The electropolymerization process was done using the cyclic voltammetry (CV) technique with the potential sweep from -0.8 up to 0.1V. Commercial Ag/AgCl reference electrodes and platinum wire counter electrode have been used in this setup. The condition used for CV electropolymerization was based on $dE/di = 50mV/s$ scan rate for 30 cycles. The resulted thickness of the coated film depends on the number of cycles and the concentration of monomer inside the solution. A sample potential sweep curve in cyclic voltammetry for electropolymerization of PANI is shown in Fig 3.11

Different peaks in the cyclic voltammetry (CV) graph are related to specific electrochemical reactions. Depending on the conditions used for electropolymerization and the composition of the solution, these peaks might be a little different. In the potential sweep's area we used to do the electropolymerization, the first set of peaks (1 in Fig3.11) appearing between 0.36 and 0.45 V corresponds to the transformation of oxidation leucoemeraldine to leucoemeraldine radical. The second set of peaks typically happened between 0.8 and 1 V (or, in some cases, shift to lower potential) due to the pernigraniline radical cation to pernigranilineis transformation. Naturally, there is a middle peak between these two prominent peaks related to the redox reaction of the emeraldine radical cation to emeraldine[114, 35].

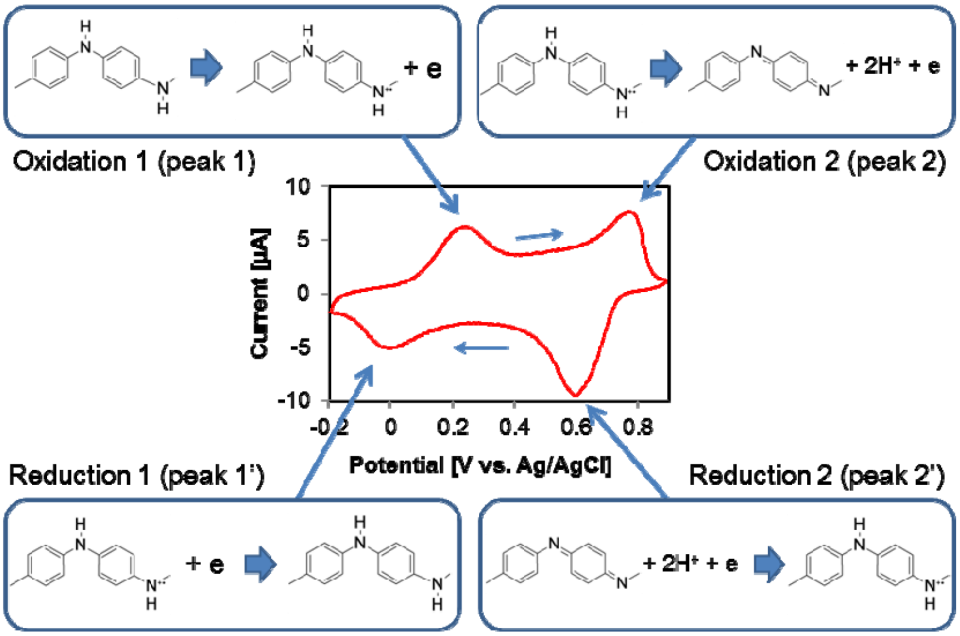

Figure 3.11: Typical peaks in CV electropolymerization of PANI [35]

Therefore, the peaks in the CV curve display polymerization and oxidation-reduction of specific PANI structures. The concentration of oxidizing agent and surface condition highly affect the intensity of the peaks and the potential shifts.

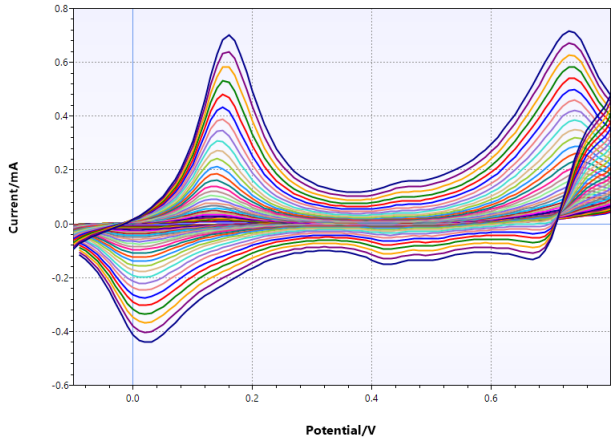

Figure 3.12: PAni electropolymerization cyclic voltammogram, film coated on flexible substrate

3.2.6 Characterization of the miniaturized pH sensor device

This section will discuss the characterization methods and results used for pH sensor devices. This characterization is carried out on both rigid and flexible sensors. Also, the sensitivity and the materials characterization results will be discussed.

3.2.6.1 Scanning electron microscopy (SEM)

Electropolymerization of polyaniline and the preparation of reference electrode as the final process needed toward fabrication of pH sensor is the most critical part of this sensor research and development. The optimal sensor condition will also be affected by design, fabrication processes and parameters that can determine the sensor efficiency. Some of these parameter conditions will be discussed in Chapter 5 in more detail.

The Scanning Electron Microscopic image of the coated sensing materials (electroplating or electropolymerized) or the nanostructure patterns on the electrode has been evaluated and compared to understand the effect of their morphology on the efficiency of sensors. As discussed earlier, the aniline is electropolymerized on the surface of the electrode. This PAni generally forms with nanofibrous morphology, as shown in Fig.3.13.

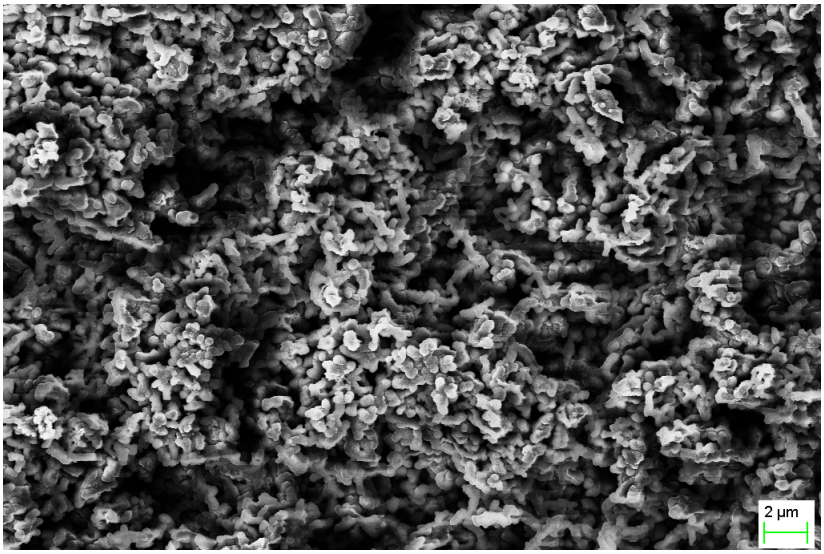

Figure 3.13: PAni electropolymerized using cyclic voltammogram, film-coated on a flexible substrate

Besides the simple morphology characterization through SEM images, other thin film characterization methods have also been used to evaluate the quality of miniaturized pH sensor materials.

3.2.6.2 X-ray diffraction(XRD)

X-ray diffraction (XRD) is a primary characterization tool used to investigate materials. This method can also be carried out for different sensing materials coated on the substrate.

The degree of crystallinity and amorphous phases will be defined using the XRD analysis. This method can be used to analyze the coated materials such as electropolymerized PAni on the working electrode surface based on their crystal structure and preferred orientation.

In the case of polyaniline, these data can also be used to evaluate the compounds in the film, for example, the emeraldine salt (ES) as the desired compound in electropolymerization of PAni[115]. This will help us modify the materials synthesis process condition to achieve the highest possible sensitivity based on the application of sensor materials and performances.

Since polyaniline is a conducting polymer, it can show different local structures and local orders. This order state is highly affected by the synthesis condition and the processing method. The synthesis method, processing procedure, doping type, and concentration factors that dictate the crystallinity orders in these polymers. Polyaniline reaches some structures based on the processing and dopant. Generally, doped PAni shows local order in the form of emeraldine salt (ES). Some of the parameters of the ES structure are described in Table 3.3[2] .

Table 3.3: Typical crystallinity percentage and crystalline coherence length (ξ (Å)) of different polyaniline material types defined in X-ray diffraction. [2]

Materials	*Crystallinity (%)*	$\xi_{\|\|}$ *(Å)*	$\xi^{b}_{\perp}$ *(Å)*	$\xi^{a}_{\perp}$ *(Å)*
$^{i}XPAN - ES^{a}$ (3.5x)	~ 45	73	57	29
$^{h}XPAN - ES^{a}$ (3.5x)	~ 40	64	47	23
$^{h}XPAN - ES^{b}$ (5.5x)	~ 35	57	45	21
$PAN - ES^{b}$ (4x)	~ 30	52	42	23
$^{n}XPAN - ES^{b}$ (1x)	<15		15	

Here have a) means high molecular weight samples; XPAN-ES is the cross-linked PAni ES structure; i, h and n refer to intermediate, high and non-crosslinked samples, respectively; b) means Low molecular weight samples. the coherence length is defined from full-width half maximum of (200), (010), and (002) ES reflections, respectively.

A glancing X-ray diffraction (XRD) analysis of PAni electropolymerized on a gold substrate has been done. The results of this analysis are illustrated in Fig3.14. The first peak corresponds to the emeraldine salt crystal structure of polyaniline. The first peak is a combination of two broad peaks, which corresponds to $(12\overline{1})$ and $(11\overline{3})$ planes. The next peak in $2\theta = 25.5$ deg. belongs to (322) planes[116]. The peaks at higher angles are related to the gold layer underneath the electropolymerized PAni. These peaks show the desired form of the sensing material coated and synthesized during the pH sensor fabrication.

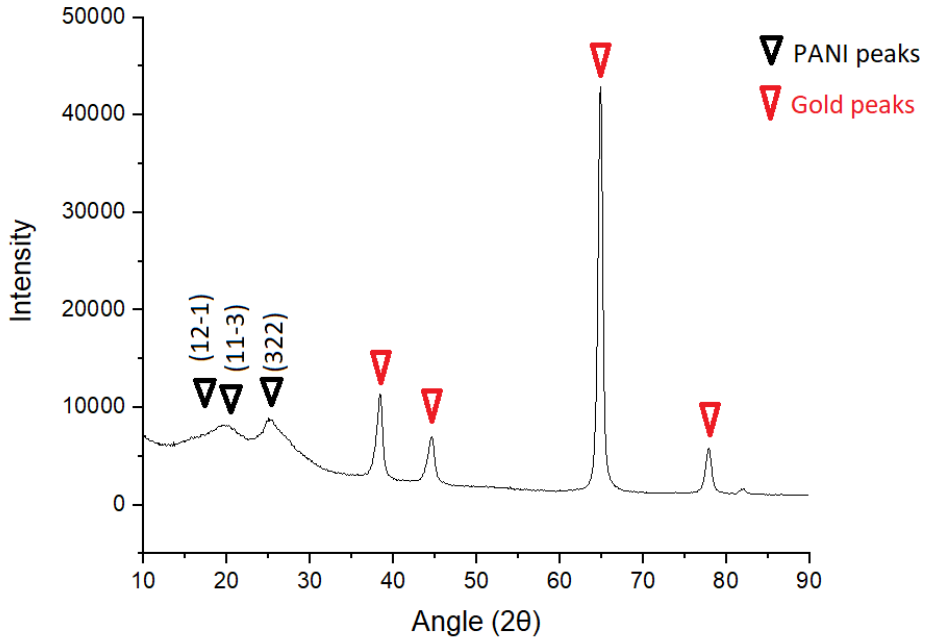

Figure 3.14: Glancing x-ray diffraction (XRD) analysis of PANI film and a gold-coated silicon wafer. The first three peaks show the presence of ES

.

3.2.7 Ultraviolet-visible (UV-Vis), Photoluminescence (PL), and Raman spectroscopy

Researchers have used various analytical techniques to investigate the compounds and the bonding in the polymer-coated as a pH-sensitive material[115, 117]. Photoluminescence (PL) is one of the main methods of characterization, which can give us helpful information about the chemical compound of polymers. The PL spectra for PAni show us the transition

of π^*-π in the benzoic units and de-excitation from the polaron band. The results of the PL test with 380.2nm wavelength excitation laser for electropolymerized PANI film on the gold are illustrated in Fig.3.15. Three prominent peaks in this spectrum with the wavelengths (418nm, 425nm, and 473nm) show the presence of the emeraldine base (EB) and emeraldine salt (ES) but do not perfectly match with the peaks mentioned in the literature[115, 118]. This shift might result from interaction with dopants and their effect on the bonding energies.

Dopants and the synthesis condition affect the results and shift the peaks in PL spectra. Also, substrate materials (in this case, gold) can alter the peaks achieved during the characterization.

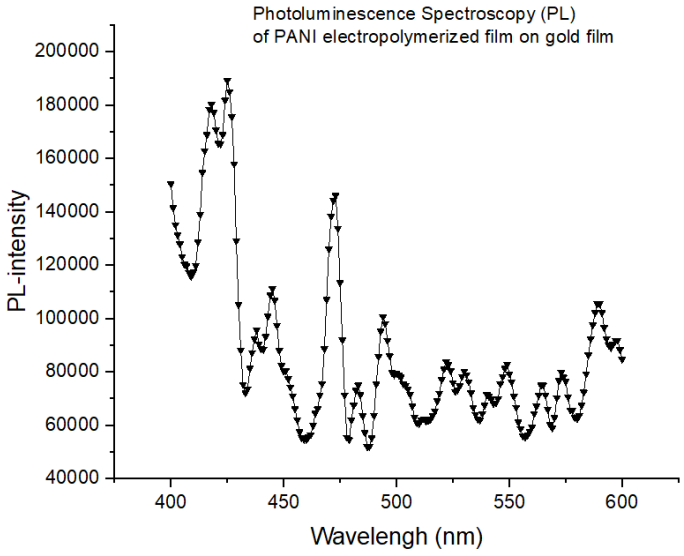

Figure 3.15: Photoluminescence spectroscopy (PL) analysis of PANI film on a gold-coated silicon wafer

Bonding types and energy is another approach to material characterization, specifically polymers. This characterization can be achieved using Raman Spectroscopy. The Reman spectra measured for the PAni film electropolymerized on a gold electrode are below. The resonance peaks shown in Fig.3.16 agree with the resonance data for emeraldine salt reported in the literature[115].

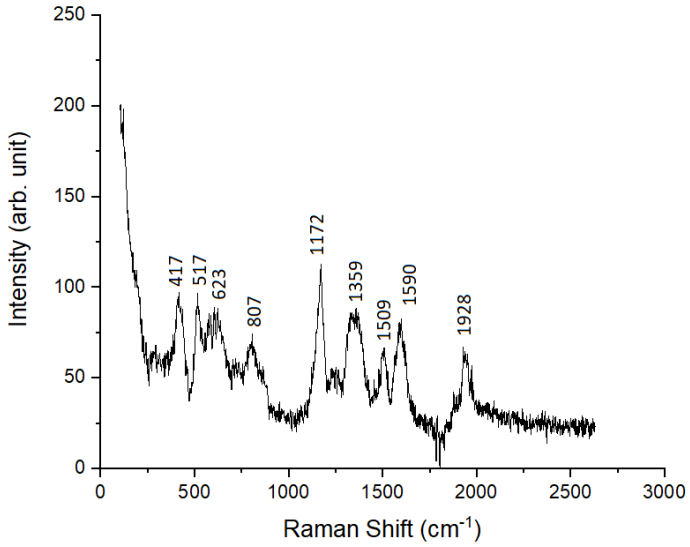

Figure 3.16: Raman spectroscopy analysis of PANI film on a gold-coated silicon wafer

3.2.8 Electrochemical characterization

The primary characterization for any sensing device should be testing its sensing properties. For our case, pH variation and sensitivity is the primary goal of our design and fabrication processes. However, this sensing capability should be based on the final application. Therefore, the pH sensitivity of the materials has been tested over various

test conditions (concentrations and base fluid variations).

Potentiometric open-circuit measurement of pH has been studied using commercial buffer solutions, the potential of the electrode materials vs a commercial reference electrode has been tested. The resulting potential variation of the fabricated microelectrode with PAni as a working electrode and the silver/silver chloride as a pseudo-reference electrode are presented in Fig.3.17.

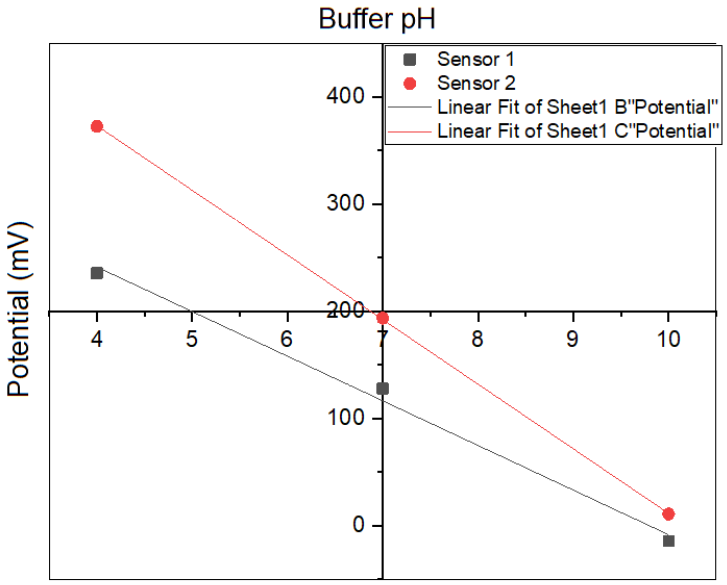

Equation	y=a+b*x	
Plot	Potential	Potential
Weight	No Weighting	
Intercept	408.05±24.62003	614.375±2.66182
Slope	-41.65±3.31976	-60.28833±0.35892
Residual Sum of Squares	198.375	2.31882
Pearson's r	-0.99684	-0.99998
R-Square (COD)	0.99369	0.99996
Adj. R-Square	0.98737	0.99993

Figure 3.17: Sample of the results for pH sensitivity test using the buffer solution

At is visible the response of two electrodes are not exactly the same. The result from the buffer solution gives us the ability to investigate the probable pH sensitivity of the fabricated sensor without any applied current through the electrochemical system. As is shown in Fig.3.17, small unpredictable changes in the PAni coating process (like temperature or small changes in the measured solution) affect the pH sensitivity of the sensor. This graph shows effect of pH change for two fabricated sensors with slightly different PAni electropolymerization conditions. One of the challenges is inevitable minor variations in preparation conditions, resulting in some changes in the pseudo-reference electrode materials or pH sensing materials used for the sensors, making it challenging to monitor pH changes. To overcome this situation, calibration has been carried out for each fabricated sensor.

To study the sensing capabilities of polyaniline, the cyclic voltammetry method is one of the vastly used characterization mechanisms of electrochemical sensors. For this purpose, phosphate-buffered saline (PBS) is one of the most common buffer solutions for biological applications. This PBS solution can be prepared using 137 mM NaCl, 2.7 mM KCl, 8 mM Na_2HPO_4, and 2 mM KH_2PO_4. Also, the commercial solution is available for instant use in different shapes, like pills, powder or solutions. In our case, we used to prepare it by using commercially available powder (for 1 litre PBS solution preparation) with the pH value of 7.4 (by Sigma Aldrich).

The pH of the prepared PBS solution has been varied to achieve different pH variations using droplets of 1M HCl (for lower pH values) or 1M NaOH solution (to reach higher pH values). These solutions with different pH values were analyzed with a commercial desktop pH meter 3 times to ensure accurate final pH values. The solution was later used for cyclic voltammetry characterization using single-channel potentiostat Palmsense 4. The three-electrode system has been used, with both on-chip and external electrodes. Variations

in solution pH were tested on the prepared electrode surface. The resulting graphs are illustrated below in Fig.3.18 It shows the nanofibrous polyaniline's descent sensitivity as a sensing material.

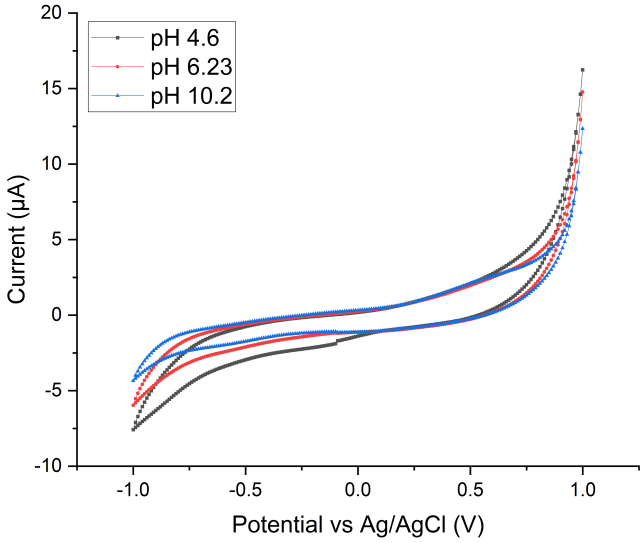

Figure 3.18: Cyclic voltammogram of pH variation in PBS solution detected using on-chip fabricated electrode

Simulating actual conditions is the leading way to emphasize the applicability of the sensor condition. Besides PBS solution, the tests have been done using simulated body fluid. This fluid condition helps us make test conditions closer to a sensor's actual situation on the human body. The chemical composition of this simulated body fluid is listed in Table. 3.4.

Table 3.4: Simulated body fluid-chemical contents

Chemicals	*Quantity*
NaCl	5.585g
$NaHCO_3$	0.965g
Na_2CO_3	1.765g
KCl	0.225g
$K_2HPO_4 \cdot 3H_2O$	0.230g
$MgCl_2 \cdot 6H_2O$	0.217g
HEPES	11.928g
$CaCl_2$	0.191g
Na_2SO_4	0.072g
1.0M NaOH	0.8 mL

3.2.9 Animal Trials for anastomotic leak detection

To simulate the actual condition of the human body, the fabricated sensor for anastomotic leak detection has been tested and characterized for point of care sensing on an approved animal trial. This surgery had been done in the research center of St Micheal's hospital in an approved condition by both the Food and Drug Administration (FDA) and Health Canada and its regulations (FDR) (Fig. 3.19).

An induced small leakage has been used in the animal trial to characterize the abdominal fluid changes. Since these sensors will be used for point of care application, the resulting change in the sensor output shows the possibility of leakage from digestive fluid to the abdominal fluid. However, in the sensor's output, this small change should fade in a couple of seconds since the body-fluid pH does not change as much as a result of a small

change. The sensing result of induced small leakage on the pH on the sensor's output after removing the noise of the system is shown in Fig.3.20. In the case of significant induced leakage, the signal will be broader and last longer as shown in Fig.3.21.

Figure 3.19: Animal trial at St Micheal's hospital, Toronto

In the case where a considerable amount of leakage was induced on the animal being tested, the resulting changes on the sensor output were different, as is shown in Fig.3.21. This change in the output results could help the surgeon investigate the kind of leakage inside the patients' body.

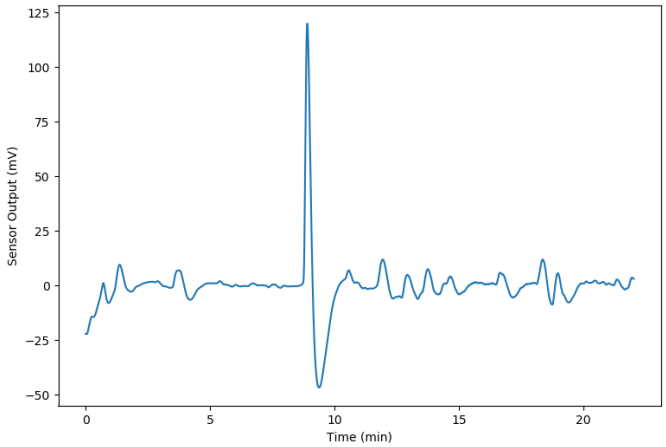

Figure 3.20: Sensor output as a result of small induced leakage in the animal study trial

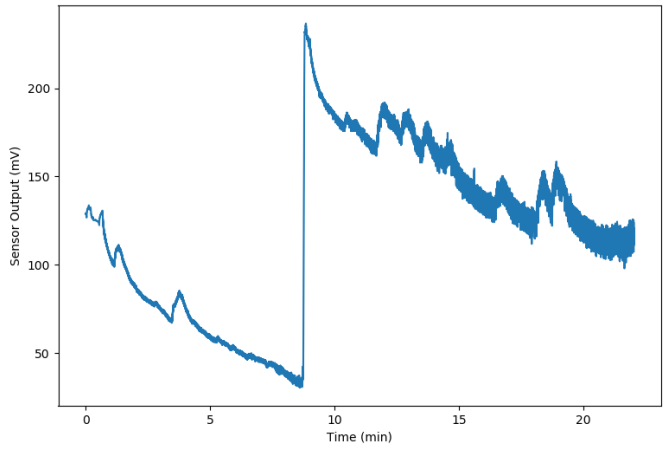

Figure 3.21: Sensor output as a result og large induced leakage in the animal study trial

3.3 The final anastomotic leak detection device

Based on the collaboration with the surgeons and medical doctors who will apply these sensor devices for human application, the system was designed and manufactured based on the additional devices attached to a commonly used surgical drain system, as illustrated in Fig.3.22. These surgical drains are frequently used after the surgical operations for this type of patient to remove the excess body fluid after the surgery. Therefore this drained body fluid can be used to monitor any pH change.

Figure 3.22: Concept design for the first stage pH sensors assembly

3.4 Conclusion

In this chapter, we discussed the various aspects for a sensor device that is able to detect the anastomotic leakage complication that might happen after colorectal surgery. The basic fabrication process of the device using a three-electrode system was shown on both

rigid and flexible substrates. The preparation, coating and characterization of polyaniline as the pH-sensitive material were discussed and presented. The laboratory test results and the animal trial show these sensors' promising capability in different amounts of leakage that resulted in pH variation in body fluid. Since this device is based on the point of care application, and the pH variations due to the leakage are high, the fast response of the fabricated device is the main goal that was achieved. This quick response will be used as a hint for the practitioner to investigate more by taking further necessary actions.

Chapter 4

Glucose sensing, multiplexed sensor characterization

This chapter will discuss the process toward fabrication and characterization of the glucose monitoring system. This sensor fabrication is based on glucose-sensing mechanisms discussed in Chapter 2 of this dissertation. The methodologies will be discussed further, and the characterization mechanisms will be elaborated.

4.1 Glucose senor: fabrication, materials and methods

The glucose monitoring system has attracted considerable attention due to its high priority for health monitoring systems. Continuous monitoring and a reliable system is essential for patients with metabolism disorder and diabetes. There have been several sensing mechanisms developed for continuous glucose monitoring systems. Among those

methods of sensor systems, electrochemical sensing is one of the most reliable and low-cost detection sensing methods.

Sensing material and its morphology is the most crucial factor that should be considered for the fabrication of any sensor. Platinum and black platinum have been extensively used and studied among all the sensing materials developed and introduced for glucose monitoring systems. As discussed in the second chapter, the morphology and condition of this coating have a considerable effect on the sensitivity of these sensors.

4.1.1 Platinum sensing material coating

The coating process of sensing material is one of the most critical steps of sensor fabrication. This process can be done in several ways, depending on the electrode structure or the desired morphology. In our case, platinum as a sensing material has been coated based on controlled electroplating using chronoamperometric or cyclic voltammetry technique. The electroplating baths generally used for this process contain platinum salts such as platinum salt, hexachloroplatinic acid, or sodium hexachloroplatinate. The electroplating solution prepared for our sensor fabrication is based on 1M sodium hexachloroplatinate (Na_2PtCl_6) in Milli-Q water.

The platinum electroplating has been done on different electrodes described earlier, both on rigid and flexible substrates. The cyclic voltammetry of the electroplated platinum solution on the pre-fabricated gold electrode is shown in Fig.4.1.

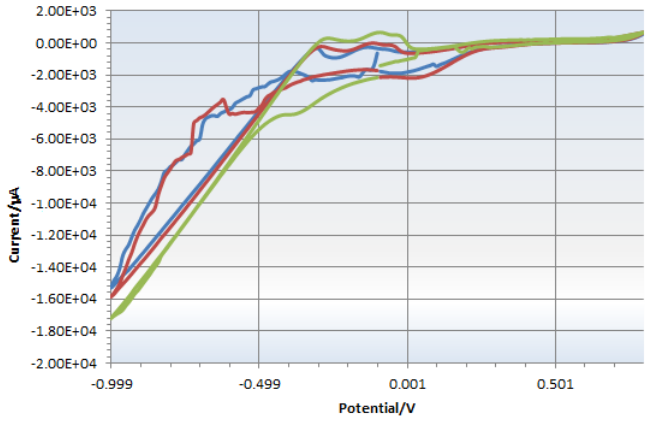

Figure 4.1: Electroplating condition of platinum electrode sensor for glucose sensing using sodium hexachloroplatinate bath.

Nano-grained structure morphology of coated platinum is the desired structure of sensing material which gives us a suitable platform for sensing glucose using the fabricated electrodes. The SEM image of these nano-grains of surface morphology is illustrated in Fig.4.2. These small grain structures generate a rough surface, giving us more sensing potential sites for glucose chemisorption on the surface of the electrode.

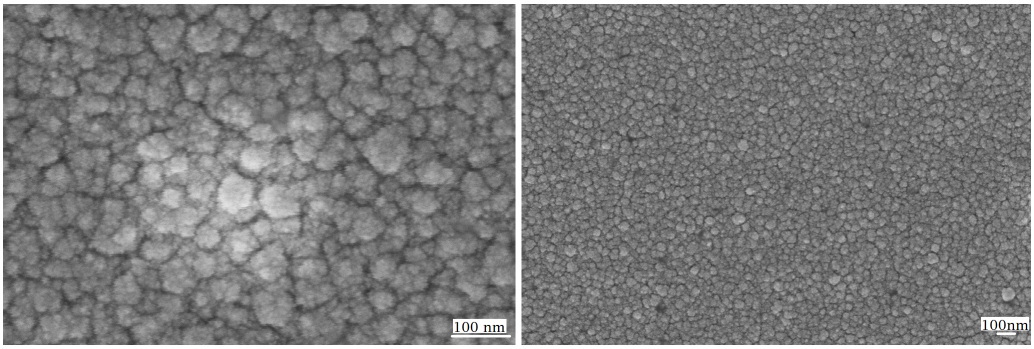

Figure 4.2: Nano-grain structure of platinum electrode coated by electroplating (Colors represent different cycles).

4.1.2 Glucose sensing and methodology of testing

Analyzing the chemisorption of glucose on the platinum surface allows us to detect the concentration of glucose in the surrounding medium. Despite the effect of crystallographic orientation on the chemisorption of glucose molecules on the electrode surface, cyclic voltammetry is one of the potential mechanisms of monitoring glucose adsorption on the surface. As discovered by Mele et al.[119], the general shape of cyclic voltammogram of glucose sensing using platinum is shown in Fig.4.3.

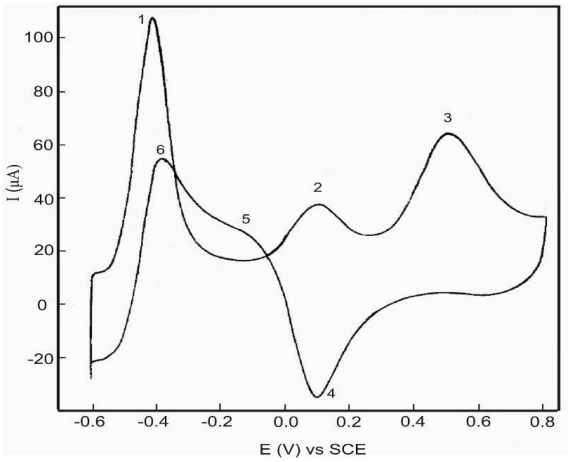

Figure 4.3: Typical shape of Cyclic voltammogram of glucose detection on platinum electrode [1].

Using this description of glucose sensing and reaction with the platinum electrode surface, there will be different regions described by Mele and Toghill [119, 1]. The first three peaks are in the anodic (oxidation) region and the peaks number 4 to 6 are their corresponding cathodic (reduction) peaks. The first peak in this voltammogram is the glucose chemisorption and dehydrogenation in the hydrogen region. In this step, the dehydrogenation of the glucose molecule at the hemiacetalic carbon one atom (C1) and adsorption of the glucose molecule onto the platinum surface occurs, as shown in Fig.4.4 a. In this step, the hydrogen removing process has been considered the rate-determining step.

The second peak is in the double-layer region. In this region, by increasing in anodic potentials, due to fast dissociation of water, the abundance of adsorbed OH species increases, as the rapid dissociation of water reaction shown in Fig.4.4-b(i) and it followed by subsequent adsorption of the hydroxide anion. The resulting hydroxide is catalytic to

the oxidation of the adsorbed glucose, therefore speed-up electro-oxidation as shown in Fig.4.4-b(ii).

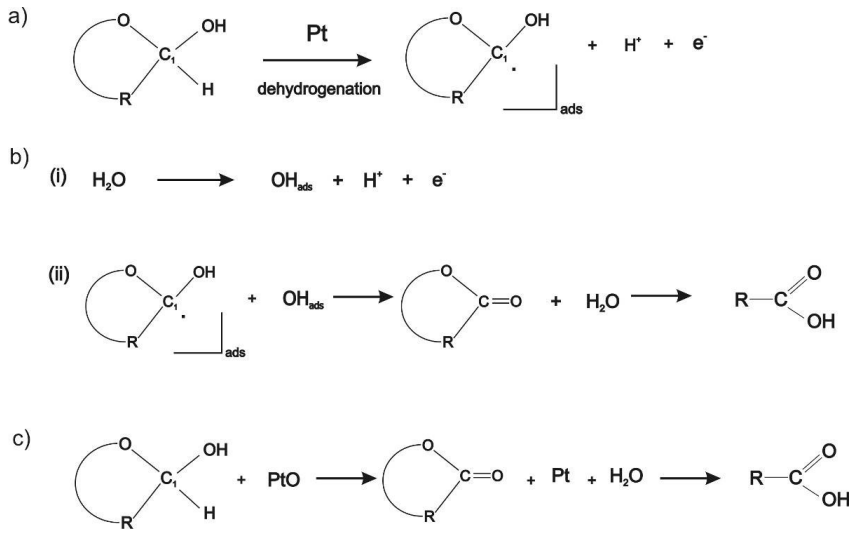

Figure 4.4: The possible theoretical reaction of glucose on the platinum surface a) abstraction of hydrogen and adsorption of glucose molecule on Pt surface; b) (i)dissociation of water, and (ii) oxidation of adsorbed glucose by the adsorbed hydroxide ions; c) oxygen region reaction and oxidation of glucose by platinum oxide [1].

The third peak is in the so-called oxygen region. In this area, the platinum surface will be generally covered by a monolayer of adsorbed oxygen, which at first stops glucose oxidation. The adsorbed OH will be detached from the surface and replaced by adsorbed oxygen. However, when platinum oxide film has formed, glucose solution might get oxidized by the presence of PtO as a direct catalyst, and the kinetics of the reaction becomes diffusion controlled. In this case, the reaction inhibition happened as other oxy-compounds are formed at the platinum surface instead of platinum oxide formation, as shown in Fig.4.4-c [1].

In our experiment, following the coating process, the platinum-coated sensor was tested using PBS solution with different glucose concentrations. The cyclic voltammetry has been used to characterize the glucose-sensing ability of the fabricated electrodes. For this purpose, D-(+)-Glucose ACS reagent (Sigma Aldrich) has been used, and solutions with different molar values have been prepared in PBS solution.

Cyclic voltammogram of sensor device vs on-chip silver/silver chloride in a three-electrode system is shown in Fig.4.5. This graph shows the sensitivity of the platinum-coated electrodes to the glucose variation inside the solution.

Knowing the effect of glucose on the cyclic voltammogram on the surface of platinum, it is visible that the glucose chemisorption on the surface of platinum can be easily distinguished for different concentrations inside the PBS solution (peak 1 described earlier). However, peak 1 in this experiment shows a combination and separation of two peaks in this region, which has not been described in the literature. This double peak separation is more visible in higher glucose concentrations in the solution. Since dehydrogenation of the glucose molecule accrues in this region, followed by the adsorption onto the platinum surface, this double step reaction and its kinetic difference led to the separation of detection on a higher concentration of glucose.

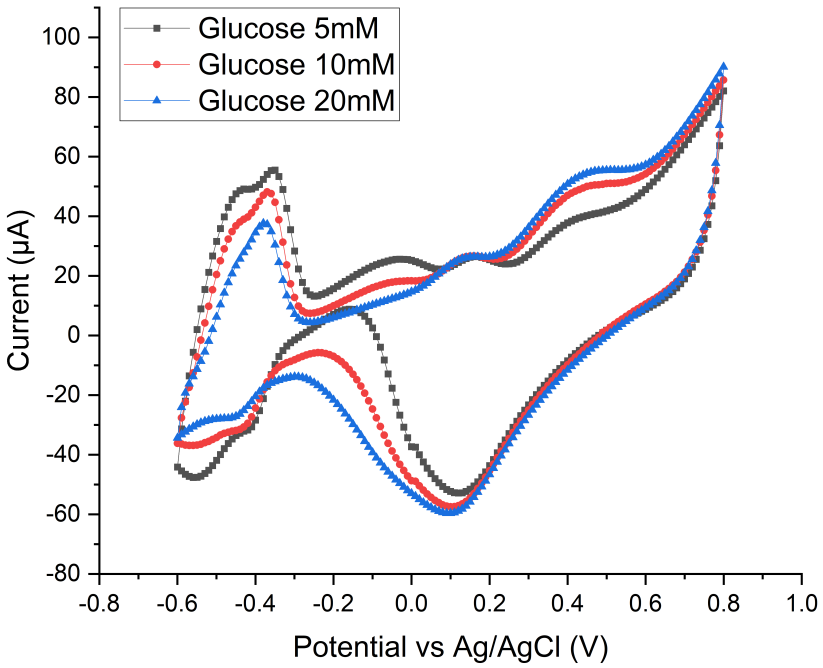

Figure 4.5: Cyclic voltammogram of platinum electroplated electrode for different glucose concentration.

4.1.3 Multiplexing sensor

Regarding our sensor systems, our current consideration is sensing two biomarkers, including pH and glucose, at the same time for interstitial fluid. However, in future processes and platforms, the number of detected biomarkers can increase for other signals. Therefore, we designed a multi-sensor system chip to detect up to eight different signals. Our current focus is on pH and glucose, using working electrode with sensing materials, and two common electrodes as reference and counter electrodes. This electrode

array design is shown in Fig.4.6.

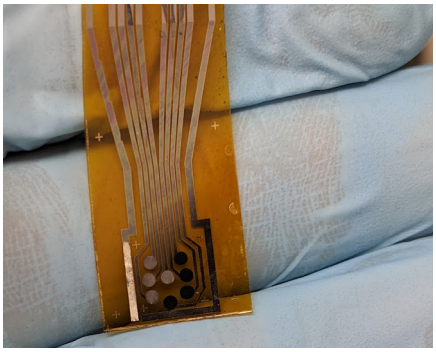

Figure 4.6: Sensor design for multiplexed sensing.

Different sensor materials have been coated on the working electrodes. Each pH and glucose sensing device has four different working electrodes separately (Fig.4.6). These electrodes will then be used for multiplexed sensing. The capability of this design is not limited to glucose and pH only; instead it can be extended to other bio-signals in the future as well.

Using this electrode arrangement, a multiplexed sensor will detect the signals of both pH and glucose variations. Then it will be translated to define the glucose content and pH of the interstitial fluid. The effect of pH on the multiplexed signal is visible, as is shown in Fig.4.7.

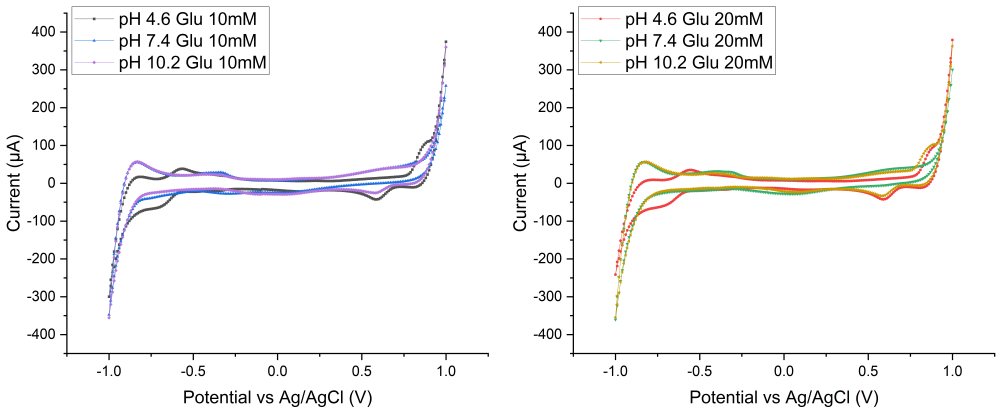

Figure 4.7: The effect of pH variation on multiplexed cyclic voltammogram for 10mM (left) and 20mM (right) constant concentrations of glucose

On the other hand, the effect of the glucose concentration on the multiplexed signals can be slightly different for different pH values, as is shown in Fig.4.8. This effect of pH on glucose-sensing can be described as the effect of acidity on the chemisorption and hydrogen dissociation of glucose molecules, as it was described earlier.

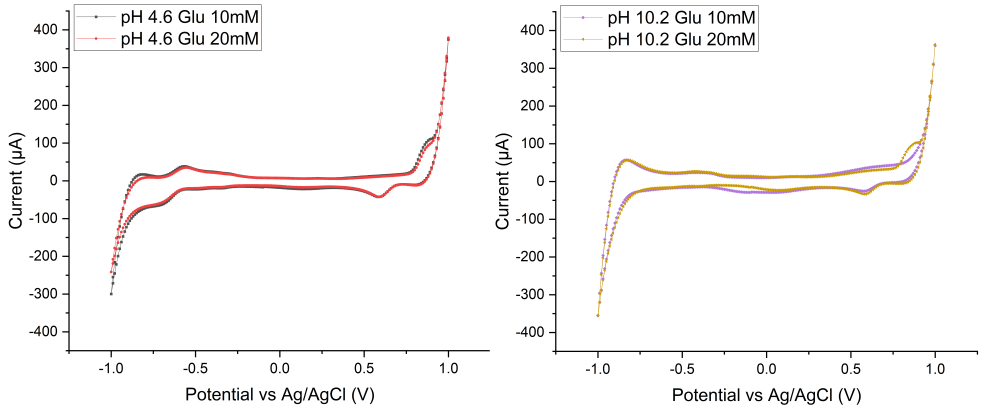

Figure 4.8: The effect of glucose concentration on multiplexed cyclic voltammogram in acidic (left) and basic (right) medium conditions.

4.2 Conclusion

In this chapter, we presented a flexible multiplexed device that can be used as a platform for monitoring glucose and other biological signals. Besides, as one of the most critical biological signals that also has a considerable effect on glucose sensing, the pH of interstitial fluid was also used in this multiplexed sensing mechanism. The glucose sensor with the ability to sense a few mM glucose concentration was fabricated based on the non-enzymatic method of glucose sensing using the electroplated black-platinum electrodes. Besides that, the polyaniline electrode (as discussed in the previous chapter for pH sensing) was used for this platform as the second electrode of this multiplexed sensing. In the last part of this chapter, the co-effect of pH and glucose on each other was shown and analyzed using cyclic voltammetry. This flexible device has demonstrated the ability to detect these two biomarkers, with the potential to be used for simultaneous detection of several other biomarker.

Chapter 5

Nanostructures, materials and microneedles

Sensitivity enhancement for sensors and biosensors has attracted considerable attention recently. Several processes have been developed and introduced toward signal enhancement, sensitivity improvement in point of care detection depending on the sensor types and applications. This chapter will discuss some of the possible approaches we introduced to improve sensitivity and materials morphology for sensor application.

5.1 Fabrication of nanostructures for signal enhancement

There are several ways to improve the sensitivity of the sensors. The two main approaches are sensing materials selection and their morphology improvement. Materials selection toward progress on the sensitivity depends highly on the method of sensing (we will discuss

later in this chapter), which makes electrical, chemical, magnetic or optical properties vastly important. On the other hand, the morphological aspects of coated materials or substrates might enhance the sensitivity of the sensor. Nanostructured sensors, in specific, improve the interaction of sensors with the surrounding medium. The nanostructures can change the properties of materials used for sensing and enhance the surface area and, therefore, the signal received from the device. Many methods have been used to fabricate these types of nanostructures.

The structures used for sensing enhancement can be fabricated based on two approaches. One way is to make micro- or nano-patterned electrode designs. For example, as Kuo et al.[10] proposed, the electrodes' lateral micro/nano zigzag design improves the sensitivity due to larger electrode area and sharp edges, which affect the current distribution. Another possible approach is to make micro and nanopatterns like nanopillars, nanowires, or nanorods on the surface of the electrode vertically. For this purpose, nanofabrication techniques or self-assembly might be used.

The suitability of biosensors for general applications is highly affected by the design and cost of fabrication. Therefore, the fabrication method for the later electrode modification should be done with the lowest possible prices. This section will discuss the technique that can be used for sensitivity enhancement based on the electrode modification that can be used for the electrochemical sensor from potentiometric to even gate change of ISFET based devices.

The nanostructured morphology of the sensing material can be done by coating on top of the nanostructures on the substrate. Depending on the substrates being used, this can be done for silicon (rigid substrate) or Polyimide (flexible substrate). As an example, this method has been used by Yoon et al. [11] on PET substrate using nanopillar arrays. These nanopillar arrays were coated later with the sensing material (in this case, the polyaniline

for pH sensor).

To reduce the cost of fabrication for each of the sensors, we mostly worked on the self-assembly methods of fabrication. These methods can make the fabrication process easier for making the final device. A verity of self-assembly techniques have been developed recently, such as block copolymer self-assembly or self-assembly based on coating mechanisms.

The self-assembly using bock copolymers like PS-b-PDMS can structure the materials on the surface of electrodes (on electrochemical sensors or ISFET based sensors). Block-copolymer self-assembly, compared to conventional nanofabrication techniques, such as e-beam lithography (EBL), can decrease the fabrication costs and improve the simplicity of the fabrication. However, methods such as EBL can still be used in a research-based approach to distinguish the effect of structure shape, size, and distributions on sensing properties.

On the other hand, coating methods can be manipulated to make nanostructures on the surface of the electrode. Modifying the pH-sensitive materials or glucose sensing materials by making nanostructures using the deposition method is one possible way to enhance the sensitivity. These mechanisms will be discussed in detail in this section.

5.1.1 Self-assembly method of nanostructures

Nanostructures formation on the electrode surface can be done using self-assembly methods. These methods, as mentioned earlier, can be classified into various processes. This method aims to make nano-dimension structured materials on the surface of electrodes, whether as a sensing material or the mask that can be used further for etching processes. Here we will discuss the general background and the processes we developed and tested.

5.1.2 Self-assembly by nano-islands growth

Nanostructures on sensor surfaces can be prepared by growing metal nanoisland film as a mask for the etching process or on sensing material. The first and most straightforward approach to making these nanostructures is to apply the basic physical phenomena of the angle coating process (wafer tilted during deposition). This process can lead to the formation of nanoisland film.

The physical phenomena behind this nanoisland growth can be described based on the original theories of thin-film coatings[36, 120]. Based on the theory of thin films growth mechanisms, there will be three typical growth modes (Fig.5.1), namely:

(i) Frank-van der Merve (FVdM)

(ii) Staranski-Krastanov (SK)

(iii) Volmer-Weber (VW)

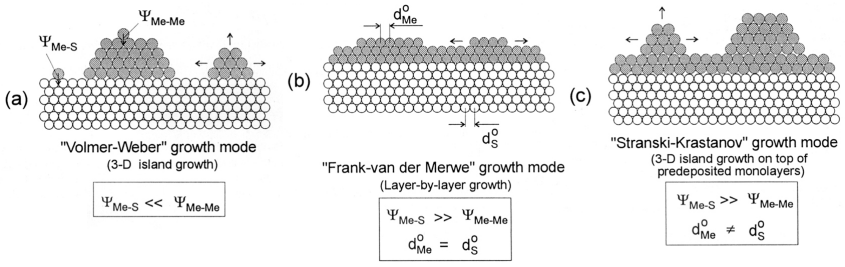

Figure 5.1: Schematic representation of various growth models[36]

According to the Volmer-Weber model, the initial stage of the nucleation happened in a kind of 3D mode, also called island growth, on the surface of the substrate. However,

by increasing the nucleation sites and the deposition time, the nuclei on the surface start to grow and get connected[120]. Suppose the first stage of the growth will be considered as a Volmer-Weber mode. In that case, the nucleus can be used as an initial platform for angle deposition by EBPVD (electron beam evaporation/physical vapor deposition). The effect of shadowing, typically known as an oblique angle deposition method, is applicable (Fig.5.2(b))[121, 37]. By applying this method, the nanostructure island growth of the metals could be achieved. This morphology will be used later for different nanofabrication approaches.

As one of the test methods toward the nanopillars formation on rigid substrates, we tested the LPCVD (low-pressure chemical vapour deposition) coated polysilicon on a standard silicon wafer. The sample was further coated with materials using angle deposition with an e-beam evaporator (or EBPVD). For this purpose, the 80°angle deposition was set using the angle stage. The samples were attached to the stage, and the standard profile without rotation was set with a low deposition rate (0.1A/sec). This situation was used for aluminum, chromium and silver coating using the ®Intelvac e-beam/thermal evaporator.

The schematic representation of this process is illustrated in Fig 5.2-part (a). The size of the island and the distance between them is theoretically directly proportional to the deposition angle.

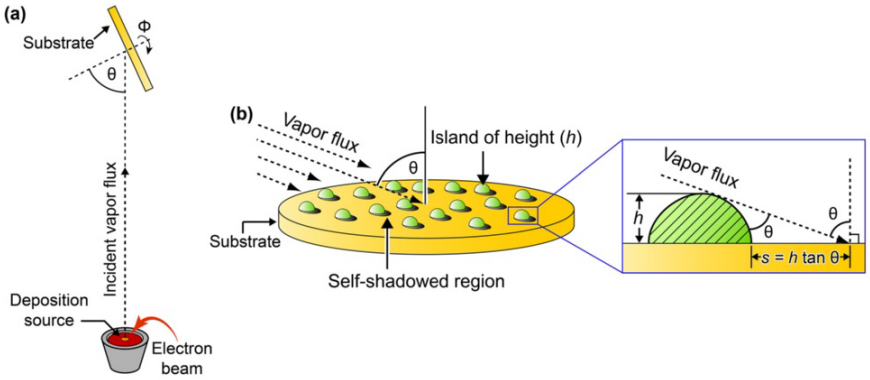

Figure 5.2: Schematic of a) angle deposition and b) the island size dependency to the deposition angle [37]

The island formation is not only limited to angle deposition, but for some of the materials such as gold and silver, it is easier to reach nanoisland growth morphology in very thin film or by dewetting mechanisms for gold and silver. These methods are not only applicable for metal masking for dry etching, but they can be used for other processes and applications such as silver or gold nanoisland for Surface Enhanced Raman Spectroscopy (SERS) as we did for silver on the TiO2 layer shown in Fig.5.3.

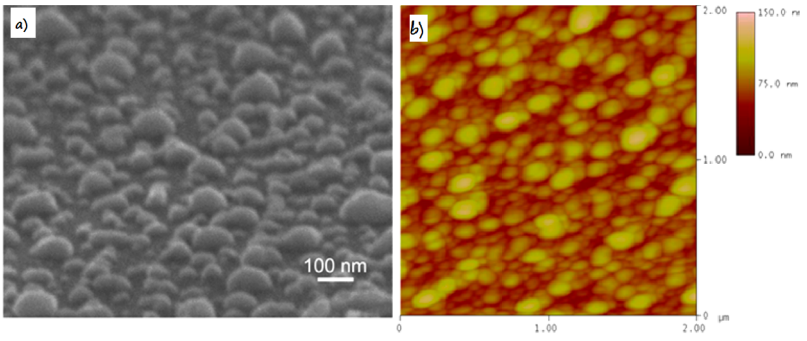

Figure 5.3: Nano-island growth of silver coated on TiO2 layer for SERS based sensor a)SEM image and b) Atomic Force Microscopy (AFM) analysis [38]

This type of nanoisland formation also happens when the substrate temperature becomes high and local melting happens for the thin metal layer. It is a well-known process named "dewetting," generally used for metals such as gold and silver. This nanoisland can also be used as a catalytic etching for the metal-assisted chemical etching (MACE) process, which can be used for several materials such as silicon, GaAs, AlGaAs, InP[3, 122, 123].

5.1.3 Island film growth using surface energy modification

Promoting metals nanoisland growth by modifying the surface energy is one of the well-known mechanisms for nanoisland formation. This process happens due to a change in the mechanism of the coating process from SVdM to VW, as mentioned in the previous section. In this approach, some surface modification has been used to decrease the surface energy and the bonding energy between the atoms of the coating materials and the substrate atoms. For this purpose, the silane surface treatment method is proposed. It has been used to investigate the possibility of island growth formation of metal masks on the surface of the gate materials.

As mentioned in the second chapter, silane treatment is one of the well-known mechanisms for reducing the surface energy of silicon substrate. Using this mechanism, silane in a vapour phase will be coated on the silicon surface with the help of chlorosilane droplet vaporized and condensed on the material's surface. Following the silane treatment, the excess silane coated on the surface was removed through rinsing with isopropyl alcohol (IPA).

Using the silane mono-layer self-assembly makes the island formation on the surface easier due to the surface energy reduction. Due to nucleation and growth theory, coating samples at the normal angle with e-beam evaporation with a very thin metal deposition

should generate the desired metal nanoisland film.

5.1.4 Etching process

The self-masking etching process has been used for several optical antireflective surface modifications [39]. In this process, the materials used for plasma etching and the redeposited materials from the chamber can generate nano-masks on the surface of the silicon wafer. These nano-masks generate a rough morphology during etching process on the surface of silicon or fused silica wafer. This self-induced phenomena is not favourable in most of the device etching processes. However, this process is also used to make antireflective surface or biological surface modification. Surface modification can be done on fused silica substrate (as shown in Fig5.4) or silicon surfaces.

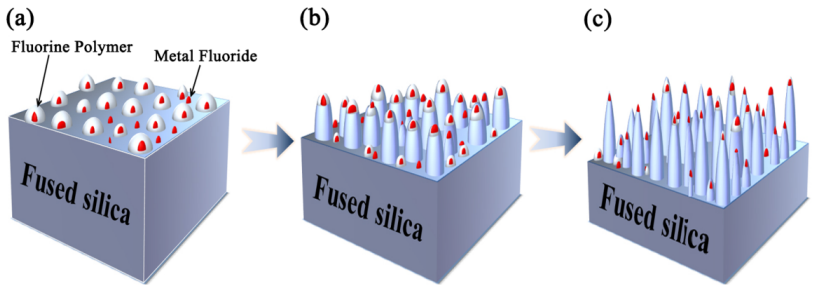

Figure 5.4: Theoritical mechanism of micro- or nano-masking with single step dry etching process [39]

In our case, we combined the possibility of using nano-masking and nanoisland masking on the samples coated with oblique angle deposited aluminum. For this purpose the samples were coated using ebeam evaporation with 80 degree tilted stage with 10 nm of Aluminum. Then the sample where used for 30 and 60 sec etching by 40sccm C_4F_8/ 20sccm SF_6 gas

mixture was used. The resulted nanopillar on LPCVD polysilicon sample is shown in Fig.5.5

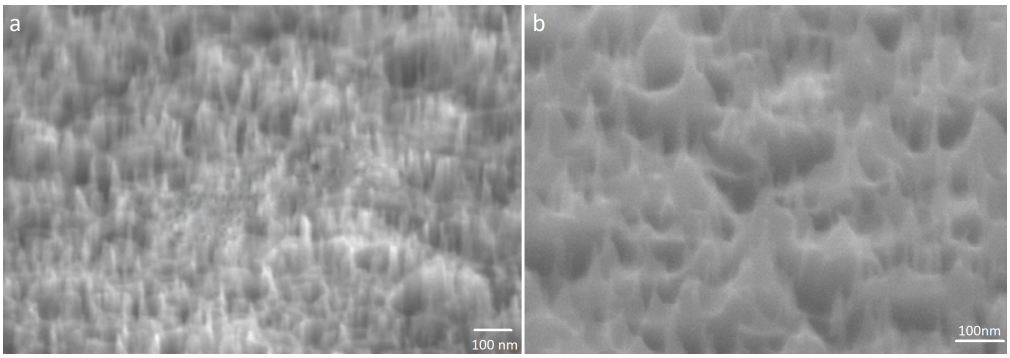

Figure 5.5: Etched sample with C_4F_8/SF_6 for 30 sec with aluminum nano-island film as mask.

This process can give us the ability to make highly rough nanopillar arrays on the sample's surface. However, the process is not readily suitable for flexible devices fabrication.

5.1.5 Self-assembly metal oxide growth

Metal oxides are among the novel materials used in sensing, electronics and photonics industries. Some of these materials, like zinc oxide and their doped semiconducting/conducting materials like indium doped tin oxide (ITO) and aluminum-doped zinc oxide (AZO), are well known for solar-cell, display and sensing industries. These materials' fascinating electrical and optical properties make them one of the best materials for electronic and optoelectronic industries.

Sensing capabilities are the most exciting properties of these materials. The sensitivity to different species in various conditions that affect the film's electrical or optical properties

makes these materials suitable for a variety of sensor applications. For materials such as copper oxide, tungsten oxide, vanadium oxide, rhodium oxide, titanium oxide, iridium oxide, etc. depending on the type of sensing and the surrounded medium, their electrical bandgap energy profile and interaction with the other presented materials in the sensor or the medium around the film affect the sensing properties. The morphology and structure of the metal oxide semiconductors also affect its' sensing properties.

5.1.5.1 Conventional synthesis of metal oxide nanostructured surfaces

Metal oxide semiconductors can generate nonstructural surfaces depending on their coating or fabrication process. Various of nanostructuring methods have been proposed by the researchers, from the costly way like EBL and etching to highly economical techniques such as the self-assembly method of fabrication. The most well-known approach of self-assembly for nanostructuring metal oxides is the vapour-liquid-solid (VLS or CVD-VLS) method. This process is widely used for the nanowire growth of silicon, metal oxides, nitrides, and sulphides[124]. The VLS method of nanowire growth typically happens as a catalytic process. Regarding the silicon nanowire growth, this catalytic behaviour happens due to eutectic assisted growth in the presence of gold nanoislands (Fig5.6) [40].

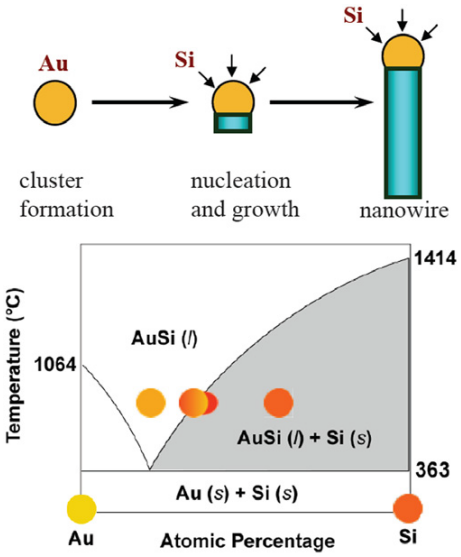

Figure 5.6: Silicon nanowire growth above eutectic temperature with the presence of gold nanoisland [40]

Metal oxide nanowire growth self-assembly has been widely processed using different methods. VLS methods can be done using different metal catalysts, including gold, as we have for silicon nanowire self-assembly or copper (Fig 5.7) [41]. The process' incompatibility with the CMOS fabrication industry is one of the primary concerns. However, the general high temperature of processing (around 450°C) makes this process unsuitable for mass production.

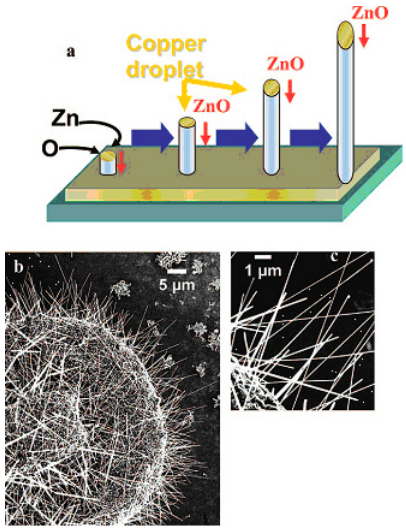

Figure 5.7: ZnO nanowire growth mechanism using cCu as catalyst (a) and SEM images (b) using VLS method on copper substrate [41]

5.1.5.2 Metal oxide nanowire growth mechanism by thermal oxidation

High-temperature thermal oxidation of metals is another processing condition used for some metal oxides nanowire growth. This method has been used for cupric oxide (CuO) nanowire formation through thermal oxidation of copper films or foils (Fig.5.8).

Metal oxide nanowire formation during the process of coating might seem undesirable. However, this nanowire formation can allow us to reduce the cost of post-processing steps and the cost of fabrication for some specific applications like sensors and solar cells. As a widely used conductive transparent film, indium doped tin oxide (ITO) generally is a smooth with high conductivity and transparency. This material coating can be done with different methods, including sol-gel, sputtering and evaporation. Due to the high conductivity of this film, it can be used for optoelectronic applications.

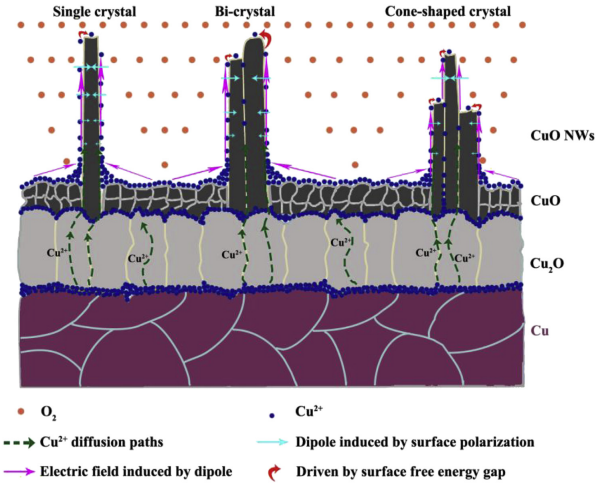

Figure 5.8: CuO nanowire formation with thermal oxidation method[42]

5.1.5.3 Direct nanowire synthesis by magnetron sputtering

One of the most common methods of coating ITO is the magnetron sputtering technique, with direct current (DC) or radio frequency (RF) mode of sputtering. The condition of the coating process highly affects the properties of the film being coated, specifically in the RF sputtering technique. The process condition such as gas pressures, power and substrate temperature can alter the morphology of coated film on the substrate. In some specific situations, this alteration can cause a substantially different coating morphology and formation of nanorods or nanowire. This typically happens in higher sputtering power and higher substrate temperature.

The formation of nanorods and nanowire branches is a catalytic growth. However, in this case, the ITO film seed layer can also act as a self-catalyst for the development of nanostructures, as shown in Fig.5.9. The theoretical proposed mechanism for the formation of In-Sn alloy on the surface of the substrate is linked to the depletion of Sn on the surface

of the sputtering target. This depletion results in a higher than normal amount of indium sputtered on the substrate's surface, leading to the formation of In-Sn alloy nanoislands and the formation of catalytic base area for nanorod or nanowire growth. [43].

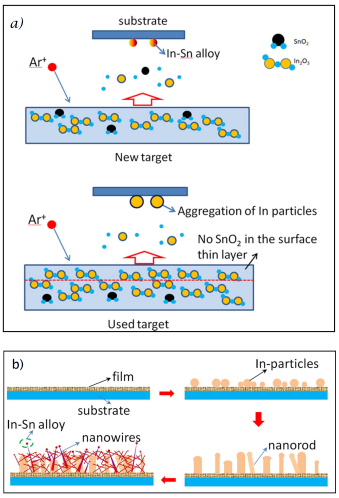

Figure 5.9: ITO nanowire growth by self-catalytic RF magnetron sputtering due to Sn depletion on the target surface (a), and the formation of nanorods and nanowires on the substrate surface (b) [43]

In our research, we used this phenomenological opportunity to coat ITO nanowire and nanorod as the base system to improve the morphology of the sensing electrodes and materials. The process was done with AJA sputtering system with RF magnetron sputtering with the power of 75 W. The substrate temperature was 300°C with 27 sccm of argon flow and deposition pressure of 3mTorr. The resulting film on the sample with 100nm thickness showed the nanorod formation on the fused silica wafer's surface and on polyimide substrate, as shown in Fig.5.10 and 5.11.

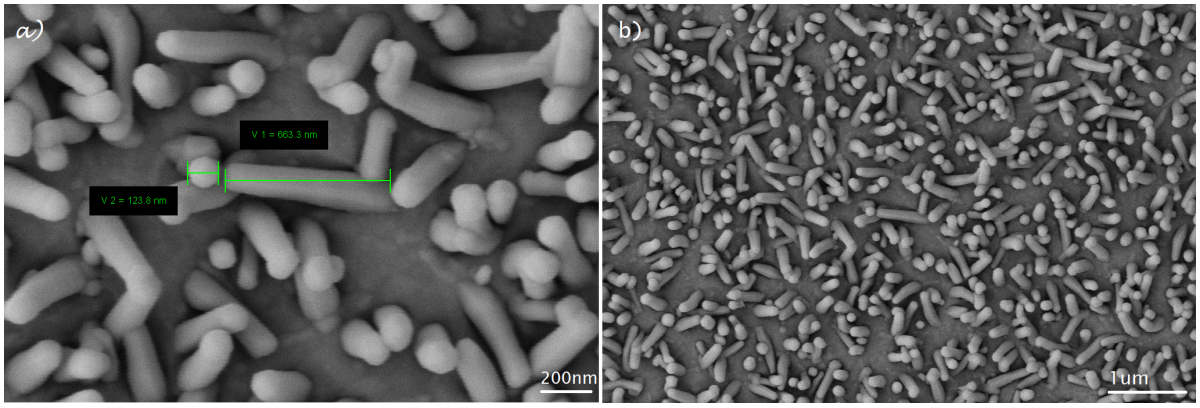

Figure 5.10: SEM images of ITO nanorod growth self-assembly by RF magnetron sputtering on fused silica substrate on 300°C without the seed layer with two different magnification

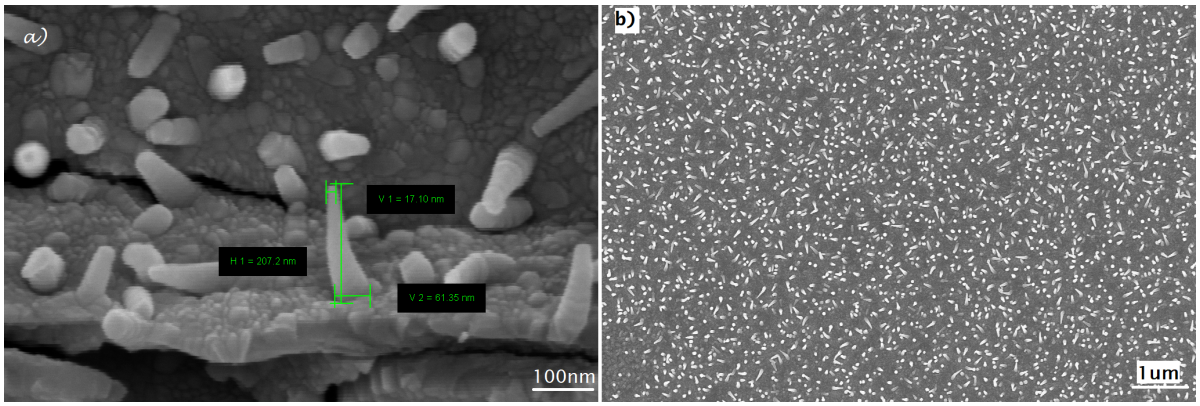

Figure 5.11: SEM images of ITO nanorod growth self-assembly by RF magnetron sputtering on polyimide sheet on 300°C without the seed layer with two different magnifications

The substrate type has a significant effect on the morphology, density, and growth mechanisms of these nanostructures. As shown in the images, the nanostructures on

fused silica substrate has cylindrical shape, as compared to cone shape on the polyimide surface. This can be due to the nucleation and growth mechanism of these nanostructure films.

On polyimide surfaces, the nucleation sites are smaller due to the trapping of sputtered material in the surface of the polymer or the roughness generated on the polymer surface with pre-processing of cleaning and oxygen plasma. This nucleation makes the nanostructures smaller compared to fused silica. Also, The cone shape structure usually happens when lateral growth speed is lower than the longitudinal growth rate. The high speed of nanostructure growth on the length generates a cone shape of pillars. This seems not the case for fused silica surfaces likely due to the large area of growth (large nucleation). Moreover, the size of pillars without any seed layer is also smaller on inflexible substrate which can be due to the more challenging formation of nucleation sites on these materials.

5.1.5.4 Effect of seed layer dewetting on ITO nanowire nucleation

Improving the nanostructure formation on the surfaces was also tested with the presence of different seed layer coating. Nanoisland formation of gold using the dewetting method mentioned earlier has been used to generate the nano structured island as a catalyst for nanowire growth initiation. The dewetting of gold has been done by coating a thin layer of gold on a substrate using an e-beam evaporation system. The high temperature of the process during the further sputtering process (300deg) generates nanoislands on the surface of the substrate.

The gold and indium can generate a solid solution. The phase diagram of indium-gold (Fig.5.12) and their application used for the wafer bonding process shows us some

similarities between this method and the formation of the gold-silicon catalytic process for silicon nanowire formation. The advantages of solid solution over dewetting of pure gold are the lower melting point and higher possibility of nucleation site formation.

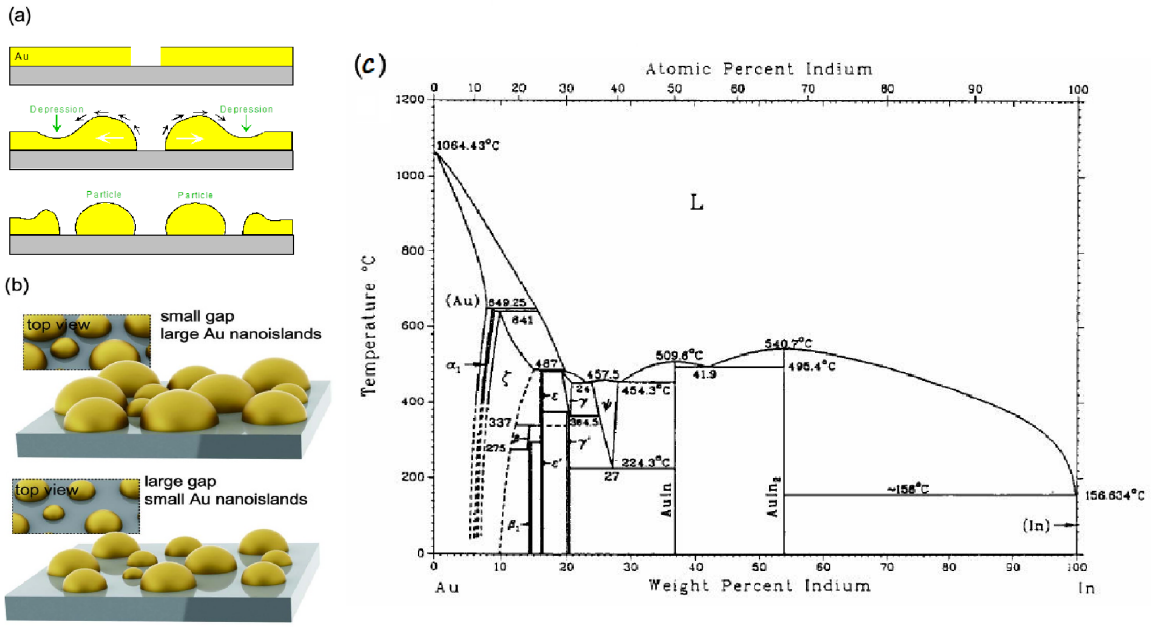

Figure 5.12: Dewetting mechanism of gold thin film (a) [44], The nucleation site effect on size and distance between nanoislands (b) [45], and gold-indium phase diagram (c) [46]

In situ dewetting of gold thin film and formation of nanoisland on the samples was done by coating 10nm gold layer using e-beam evaporation. The pieces were placed in the sputtering chamber and processed at 300°C substrate temperature and the same process conditions as mentioned earlier.

The temperature used for sputtering is higher than the dewetting temperature of gold which formed nanoislands. Analyzing the results with SEM shows a promoted nanowire formation using this method (Fig.5.13). The nanocap on the tip of cone shape nanowires

shows the effect of nanostructure growth assisted by the catalytic process.

Despite the advantages of this process, the effect of surface conditions on nucleation of gold nanoislands and, therefore, their size and distribution makes this nanowire initiation growth sites not equally and uniformly distributed all over the surface. This might be improved using the nano-patterned rough surface, which can help proper island distribution.

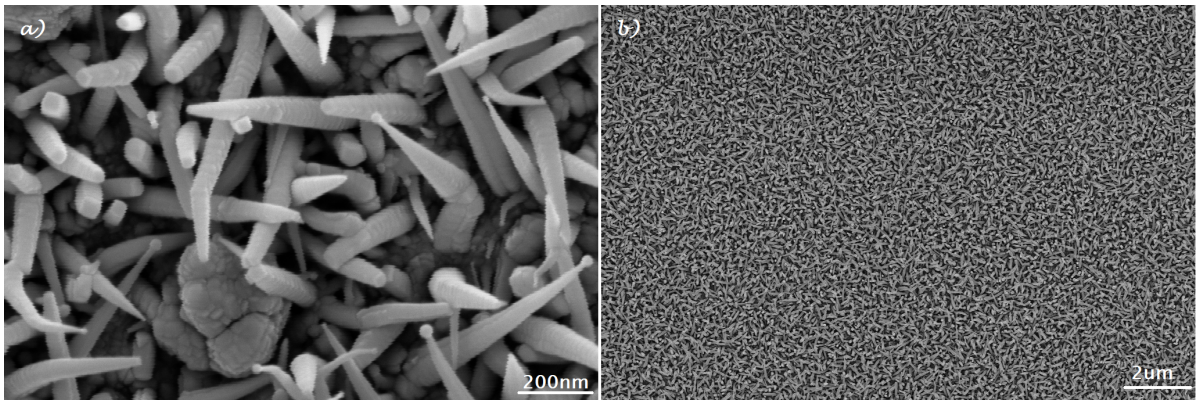

Figure 5.13: ITO nanowires growth using gold dewetted seed layer

An excess amount of indium can promote nucleation and growth of nanowires during the sputtering process. Some researchers used an excess indium sputtering befor ITO sputtering to enhance the nanowire nucleation and growth [125]. Indium is a well-known material that can be easily coated on desired surfaces using electroplating. For this purpose, we initially coat a thin layer of ITO as a conductive film, followed by electroplating indium for 5 sec using commercial indium electroplating solution and pulsed electroplating source with 500mV to zero potential and a frequency of 1kHz. The resulting thin films were used as a seed layer for ITO high-temperature magnetron sputtering system.

The indium can quickly melt and generate indium-tin alloy nanoislands on the sample's

surface. These nanoislands promote the nucleation and growth of nanowires, as shown in Fig.5.14. This method gives us more uniformity of nanowire growth. However, the higher thickness of indium on some areas generates a huge indium micro-sphere (Fig.5.15) which is not desirable for our case. This might be improved if we used e-beam evaporation of indium as a promoting seed layer.

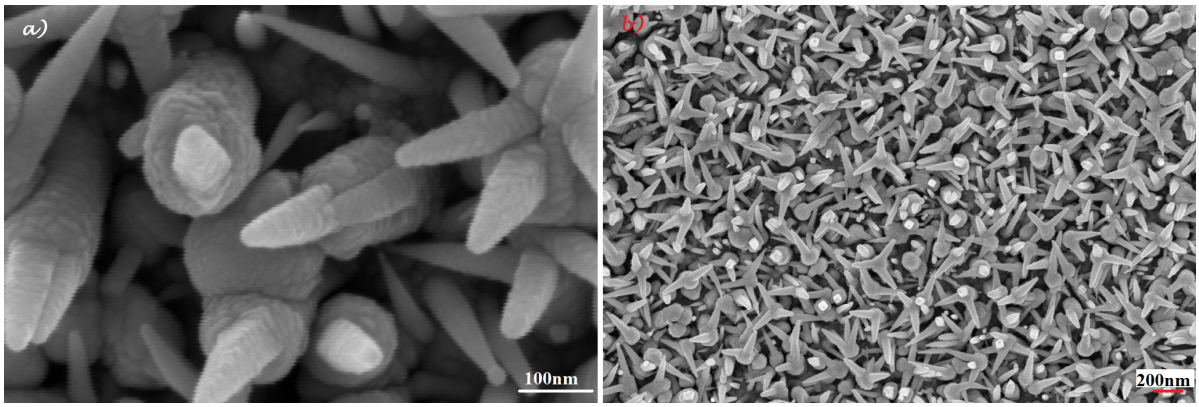

Figure 5.14: ITO nanowires growth using ITO and electroplated indium seed layer

Branched nanowires are the main visible difference between the two methods of seed layer preparation. The indium seed layer increases the density of nanorods, and some nanowires branch out from the tip of the rod in different directions. This is the same as the theory we discussed earlier for the formation of nanostructures during the self-catalyzed growth using RF magnetron sputtering.

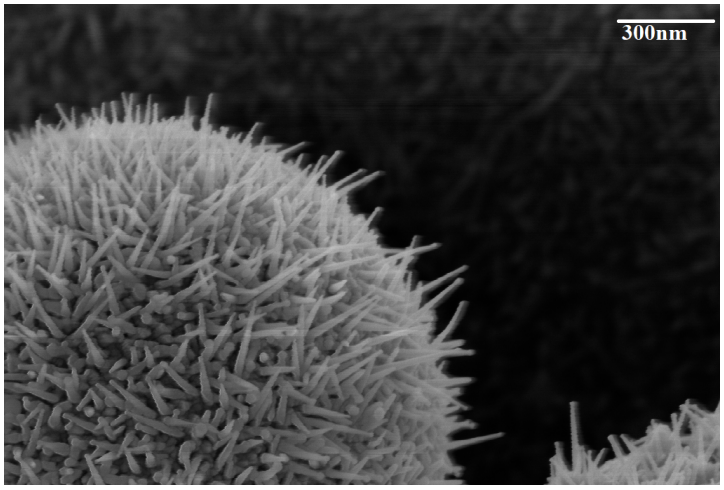

Figure 5.15: ITO nanowires growth on a nanosphere of indium

The nanostructured and modified electrode material using ITO can be used to fabricate high sensitivity devices. The implementation of these nanostructured surfaces will be discussed in the following sections.

5.2 Implement of ITO nanostructured electrode for sensors fabrication

As we discussed in previous sections, the nanostructured surface of the electrode material can have a significant effect on the fabrication of the sensors. In this part, we will use this nanostructured electrode and investigate its impact on sensing materials' morphology and their sensing properties.

5.2.1 Effect of the nanostructured electrode on pH sensor

Coating pH-sensitive materials on nanostructured ITO electrode allow us to investigate more about the formation of this electrode material. Aniline is a pH-sensitive material that has been coated by electropolymerization, as mentioned in CH2. Conductive ITO nanorods and nanowires affect the distribution of charge transfer through the electrode and solution interface.

The non-uniformity of charge transfer from the electrode interface highly affects polyaniline's polymerization and morphology. The process of PAni electropolymerization was done using 0.5M aniline solution prepared as mentioned in Chapter 2 with the presence of 1M sulfuric acid as an oxidizing agent for polymerization.

Analytical investigation of the morphology of electropolymerized aniline on the surface of the electrode showed a significant reduction in the size of PAni polymer fibres, as is illustrated in Fig.5.16.

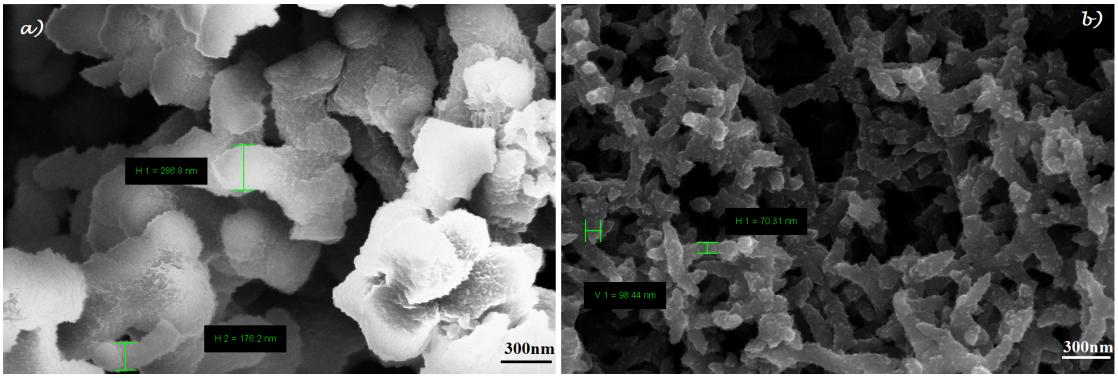

Figure 5.16: SEM image of polyaniline nanofibers electroplated on a) Gold electrode, and b) Nanostructured ITO electrode

Fibre size reduction on the surface of nanostructured ITO film can be due to more

initiation sites available on the surface of electrode and the density of these nucleation sites. This is simply understandable based on the step-by-step SEM images taken to analyze nanofibers' growth (Fig.5.17). The polyaniline nanofibers start with the size and shape of the ITO nanorods on the surface as the first stage. After that, the branching of fibres starts to happen and connect the neighbouring growth sites. And finally, these branches begin to grow in different directions and form a porous and nano-fibrous morphology of polyaniline film on the surface, as is illustrated in Fig5.17 and Fig.5.16.

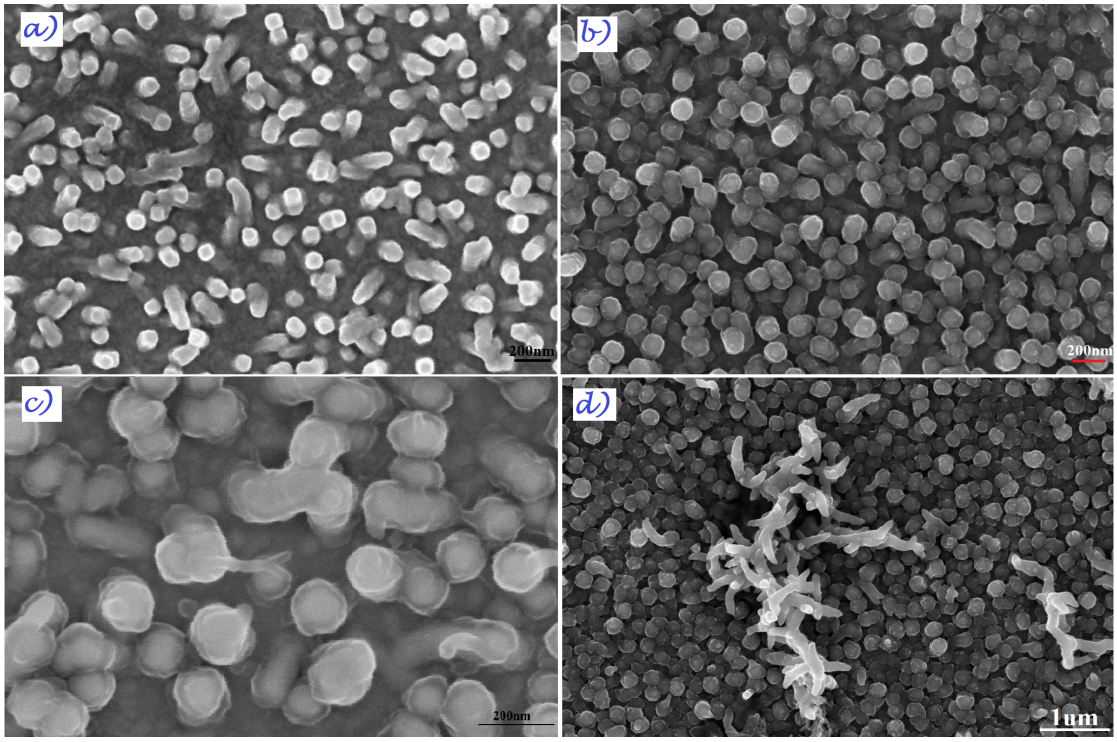

Figure 5.17: SEM image of polyaniline nanofibers growth on nanostructured ITO a) nucleation sites and nanorod shape growth, b) increase in density of nanorod shape PAni, c) branching and connections, and d) dendritic growth of branches.

The nano-fibrous polymerization of polyaniline on the nanostructured ITO, compared

to the larger fibre-shaped PAni on a gold electrode, shows a promising way to increase the sensitive material surface area and the possibility of miniaturization.

We used this method to investigate the sensitivity of the PAni coated ITO film to pH changes. For this purpose, the solution test was done using phosphate-buffered saline (PBS) solution (Sigma-Aldrich) in Milli-Q water. The 1M HCl acid solution has been used to manipulate the pH toward a more acidic region, and the 1M NaOH solution has been used to change the pH toward more basic pH ranges. The pH variation not only changed the signal received in cyclic voltammetry, but it is also affected the colour of polyaniline coated on the ITO film, as is visible in Fig.5.18. This colour change shows the possibility of using this combination of materials for optical pH sensing.

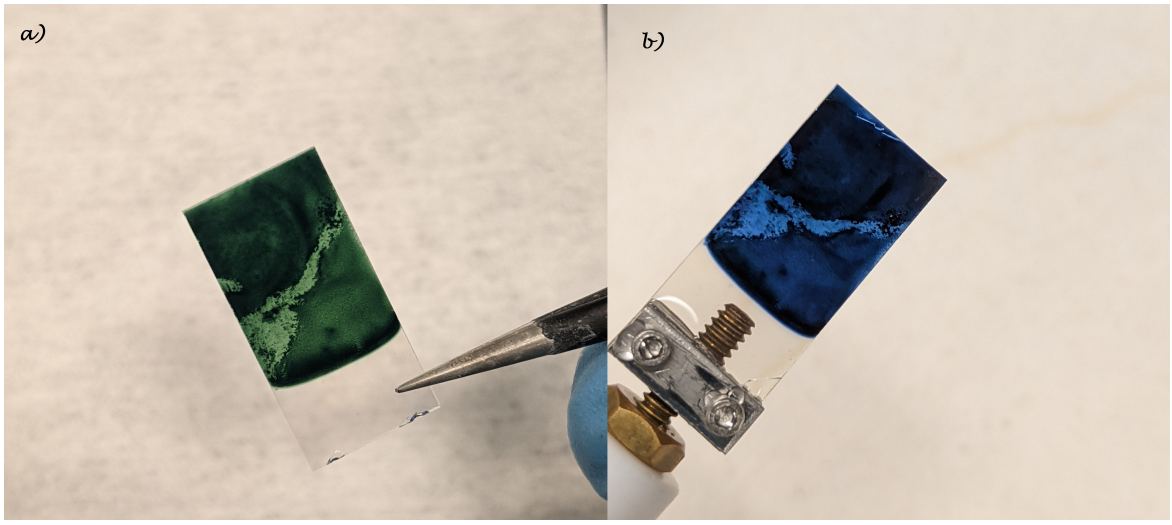

Figure 5.18: Polyaniline coated on ITO a) As deposited or in neutral pH range and b) In acidic medium

.

The effect of nanostructured morphology on sensing was investigated using the cyclic

voltammetry (CV) for pH sensing. As seen in Fig.5.19, the effect of the new materials and their morphology to small pH change is apparent. This high sensitivity allows us to use this process for pH sensing in interstitial fluid (ISF). If we consider the shift as a parameter for pH sensing, the sensitivity of the potential shift in the peak based on pH variation is 1.07V/pH.

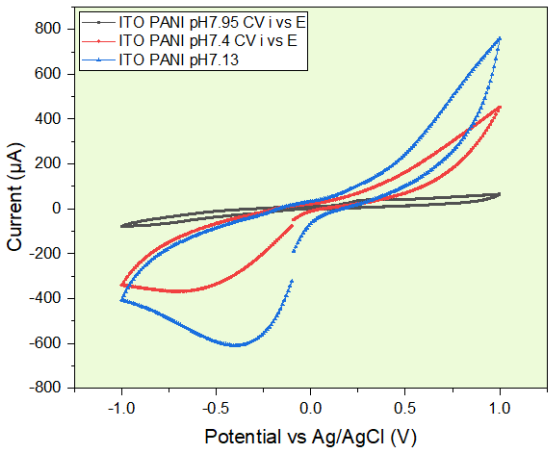

Figure 5.19: CV measurment of nanostructured ITO-polyaniline in small pH variation.

5.2.2 Effect of the nanostructured electrode on glucose sensor

Improving the sensitivity to glucose is essential to achieve the best required POC monitoring device. Failure to precisely measure the glucose level in blood in continuous monitoring systems is threatening, especially diabetic patients. Improving the morphology of the sensing material is one of the best options to promote the sensitivity in glucose sensors.

Nonstructured morphology in the electrochemical sensing of glucose molecule gives us the

ability to enhance the received signal due to the increase in adsorption and electroactive sites. This change in morphology of the electrodes can generate new electroactive sites that can act as chemisorption reaction points on the surface of the electrode and enhance participating locations that can transfer electrons to or from the electrolyte.

As the primary material used for glucose sensing in this project, the typical performance of platinum, coated on flexible gold electrodes using electroplating, has been investigated in the last chapter. Here we will discuss the effect of changing electrode surface morphology by nanostructured ITO as the base electrode material (beyond gold); and a new means of sensing using cupric oxide will also be studied.

As described in the previous section, for pH sensing, using PAni nanoribbons can greatly affect the sensing property. Likewise the morphology of sensing materials can also play a significant role for glucose sensing. In this case, the self-assembled nanowires and nanorods of ITO can be used as a template for coating glucose sensing materials.

That is, coating platinum on the surface of nanostructured ITO film could be a promising approach toward improving the morphology of Pt sensing material on the electrode and boosting the sensitivity. Glucose sensing is related to the morphology of the platinum surface and chemisorption of glucose on the surface of platinum. In the previous attempt, the platinum sensing material was coated on a flat gold surface using electroplating of platinum. This platinum electroplating gives us some nano grain size morphology of coated material. Using the nanostructured ITO, the existing nanorod and nanowire will act as a template for the platinum deposition. Besides electroplating, the nanostructured ITO has also been used as a template for coating very thin (10 nm) platinum using the e-beam evaporation.

After coating, the characterization has been done using cyclic voltammetry in order to

examine the impact of these nanostructured morphologies and the coating process on its sensing capability. For this purpose, the detection signal for a specific amount of glucose has been compared for three different electrode processing, including electroplated and evaporated Pt on nanostructured ITO and the conventional electroplated platinum on gold electrodes. The resulting cyclic voltammogram of these different electrodes for 25mM glucose in PBS solution is shown in Fig.5.20.

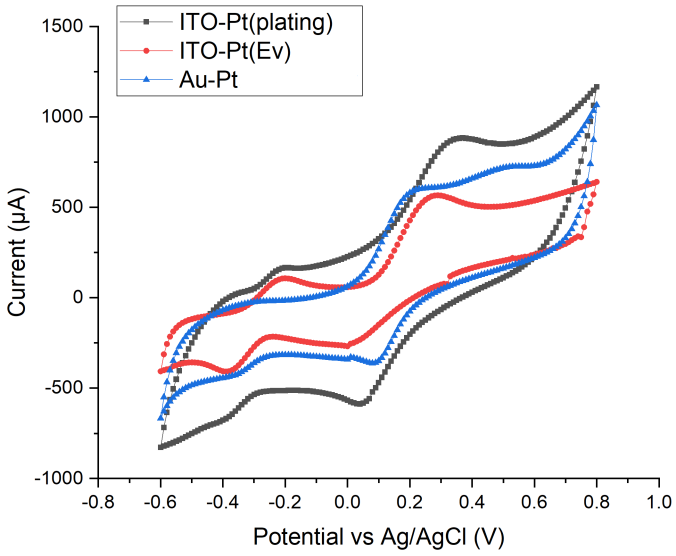

Figure 5.20: CV measurement for specific amount of glucose detection using electroplated and evaporated platinum, both on nanostructured ITO template, and electroplated platinum on gold electrode surface.

Clear contrast of signals in the adsorption region and the double-layer region in platinum coated on nanostructured ITO (evaporated or electroplated), as compared to signals on conventional platinum coated on gold electrodes, are clearly visible. The difference between

the evaporated and electroplated electrodes might result from the very different thickness and morphology of these two films. The 10nm evaporated platinum on nanostructured ITO electrodes gave less electrochemical capacity but distinctive signal peaks in these regions.

Besides Pt, other materials, such as some semiconducting materials, also attracted considerable attention due to their ability to detect biological biomarkers for different applications. Copper oxides as one of these semiconducting materials have been investigated recently by various researchers based on their suitability to be used as a chemical or biological sensor. Copper oxides' ability to nonenzymatically sense glucose has been studied and approved for CuO and CU_2O.

The extraordinary potential of copper oxide as a sensing material is due to its ability to generate self-assembled nanostructures during oxidation. These nanostructures can be formed by either wet oxidation or dry oxidation using regular high-temperature oven based thermal oxidation. The latter approach is the simplest way to generate CuO nanowires that are highly sensitive to glucose.

The nanowire formation is highly dependent on the coating process of copper. The growth of CuO nanowires generally needs specific film stress conditions, which can be more easily formed for copper foils or sputtered copper films. Oxidation of copper first grows CU_2O oxide which is not in the form of a nanowire but is still a potential sensitive material for glucose monitoring.

Using nanostructured ITO film as a templated substrate for copper coating might enhance the formation of copper oxide during the oxidation process. For this purpose, the ITO nanowire structured electrode film on flexible and rigid substrates was coated with copper. These copper-coated samples were then placed inside a thermal oxidation oven to convert the copper on the surface of ITO to some form of copper oxide.

Different oxidation temperatures have been tested to determine the possibility of CuO nanowires formation on top of the ITO nanostructures. However, as mentioned earlier, the formation of CuO nanowires is highly dependent on the coating condition and film intrinsic stress. The processes we used for CuO nanowire formation didn't successfully reach the desired CuO nanowire morphology. However, the growth of copper oxide film on nanostructured ITO still gave us the ability to enhance the sensitivity shown in Fig.5.21 compared to conventional gold electrode film.

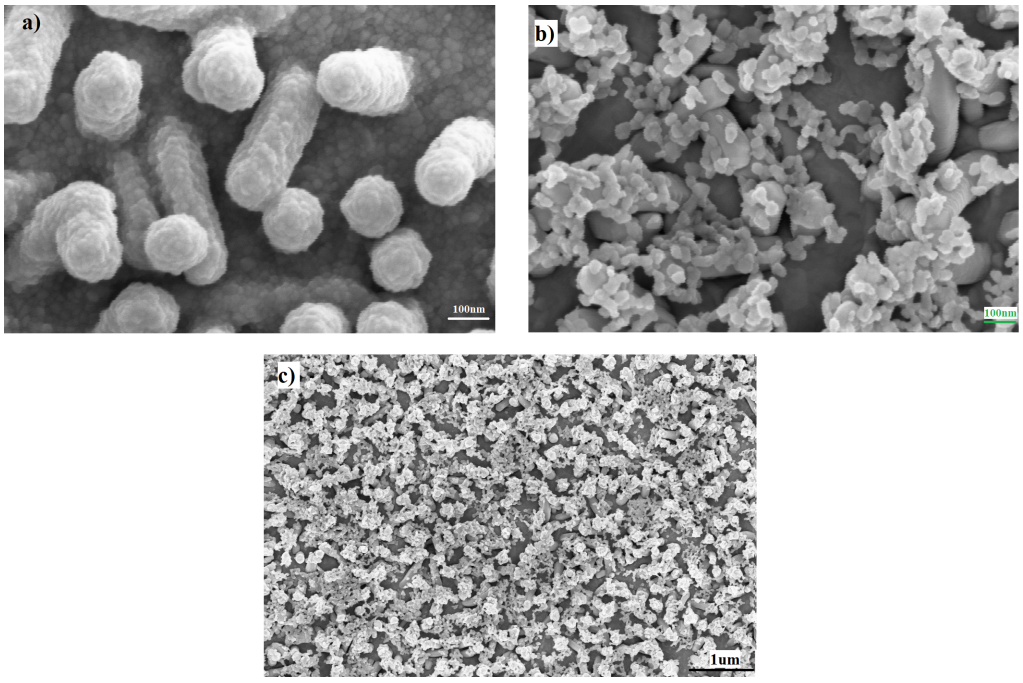

Figure 5.21: Morphology of copper oxide film formed on ITO nanostructures using thermal oxidation process. a) Common film morphology on the surface; b) Some nanowire growth of CuO on nanostructured ITO surface and c) 450°C for 2hr.

The effect thermal copper oxide film on top of nanostructured ITO electrode has been investigated using cyclic voltammetry. This new material and morphology, as compared

to the gold-platinum sensor or platinum coated on nanostructured ITO has apparent improvement for glucose monitoring for a specific amount of 20 mM glucose as shown in Fig.5.22. However, the reproducibility of the sensor signal remain a challenge.

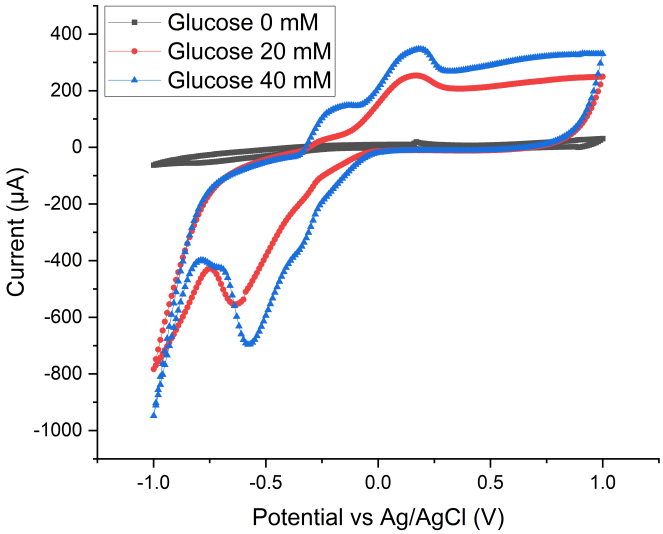

Figure 5.22: Cyclic voltammetry of ITO(NW)-CuO/Cu_2O for different concentration of glucose

5.3 Implementation of microneedles, multiplexed sensing of biomarkers in ISF

Multiplexed sensing of bio-analyte from ISF (interstitial fluid) is one of the best methods of continuous monitoring of health conditions. To achieve the sensing capability, the senor might be placed under the skin, which is not practical; or the ISF is extracted and brought to the electrode's surface. Several ISF extraction method have been

proposed and investigated by researchers. Among them, microneedle is one of the most practical approaches to extract ISF.

Materials used for the fabrication of microneedles can be diverse from metal to silicon or polymer. Polymeric microneedles have attracted considerable attention due to their easy fabrication method. The most popular material used for polymeric microneedles is methacrylated hyaluronic acid (MeHA). The fabrication method for these sharp polymeric structures is generally carried out by molding using polydimethylsiloxane (PDMS) molds.

One way for ISF extraction for analysis is swelling the polymer microneedles that, due to reverse osmosis pressure, extracts the ISF as shown in Fig. 5.23. Generally, the swelled microneedle is then placed inside a solution to transfer the ISF to the solution, and the resulting solution can be analyzed to detect the biomarkers.

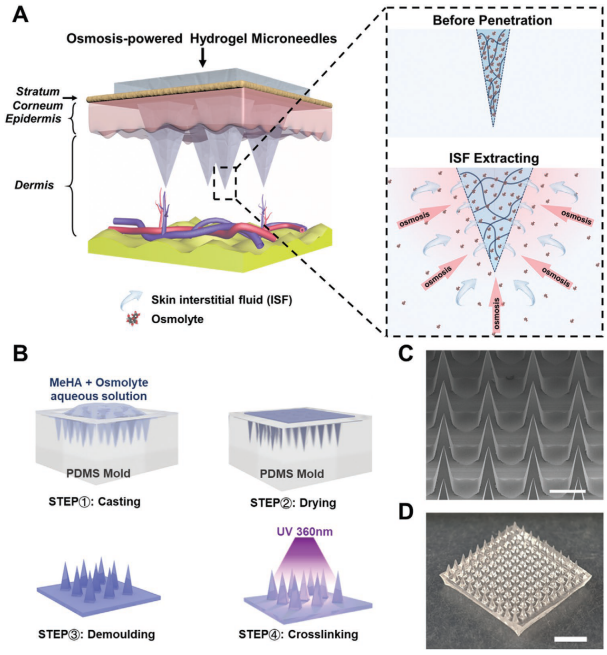

Figure 5.23: Hydrogel microneedle preparation and ISF extraction mechanism [47].

This non-continuous analysis of ISF can be modified to continuously analyze ISF by attaching the sensing electrode to the backside of hydrogel microneedles as described by Zheng et al.[47] in their proposed enzymatic glucose-sensing mechanism. In our research, using similar approach, the hydrogel microneedle has been fabricated using PDMS mold. However, instead of methacrylate hyaluronic acid (MeHA), our research used a novel dopamine-conjugated dialdehydeHA (DAHA) hydrogel as a microneedle base polymer material. This hydrogel system showed remarkable tissue adhesion performance [126]. Microneedle arrays fabricated using this hydrogel are shown in Fig. 5.24. These fabricated microneedles were later attached to a multiplexed sensor fabricated and discussed earlier.

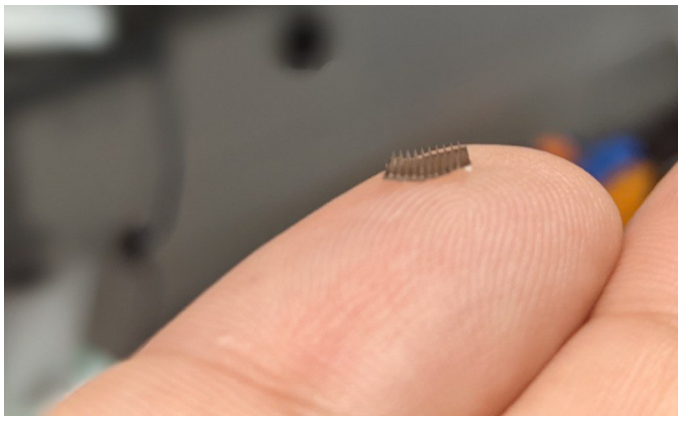

Figure 5.24: DAHA hydrogel microneedle arrays.

The fabricated multiplexed electrodes were attached to the backside of microneedle patch arrays. We did not use any glue for the attachment since the glue may generate chemicals that might affect the sensor performance. Therefore, the multiplexed sensor is just simply placed on the backside of microneedle arrays (without using any glue), as shown in Fig.5.25.

Analyzing the effect of microneedles on the sensing capability of the sensor was done

by simulating the actual condition. These in-vitro tests have been demonstrated using hydrogels (to simulate ISF environment) prepared with different pH values and glucose concentrations. A stretched and extremely thin para-film had been used to cover the hydrogel to act as an artificial skin. This parafilm (a semi-transparent, flexible film composed of a blend of waxes and polyolefins) will help us evaluate microneedles' ability to penetrate through the skin. This microneedle is attached to the surface of the electrode, as shown in Fig. 5.25.

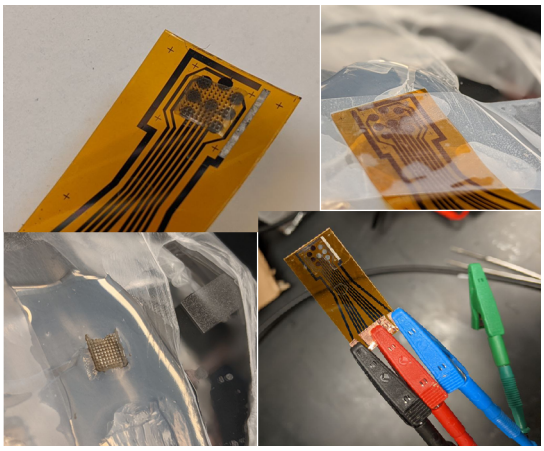

Figure 5.25: In-vitro test using hydrogel with different concentrations of glucose and pH values covered with extremely thin parafilm to simulate the skin condition

Without the penetration of microneedles into the para-film, it is almost impossible to use the multiplexed sensor. The extraction of fluid and bringing it to the surface of the electrode using microneedles enhanced the sensing signal greatly. As shown in Fig.,5.26, the effect of microneedle on sensing is apparent, as compared to the sensor electrode placed directly on the surface of hydrogel (even without para-film).

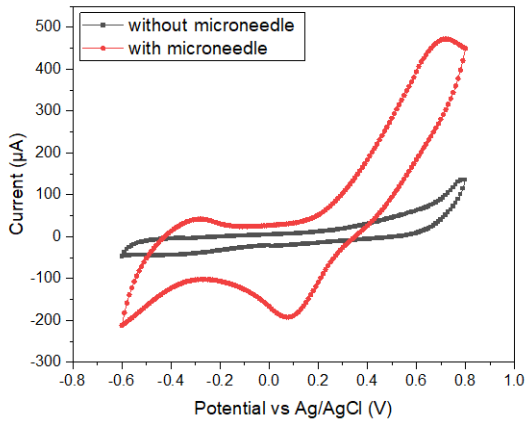

Figure 5.26: Cyclic voltammogram of microneedle assisted sensing compared to sensing without microneedles using 20mM glucose concentration.

As it is clear in the cyclic voltammogram, the signal for the sensor with the microneedles attached was very close to what we had for glucose sensing inside the solution. This apparent difference shows that the multiplexed sensing platform with microneedle attachment is a promising continuous monitoring method.

5.4 Conclusion

In this chapter, a novel approach for self-assembly of nanostructures was investigated. The most promising method that is practical for biosensor device fabrication using self-assembly of ITO (as one of the essential conductive oxides) nanostructures was developed using a simple magnetron sputtering technique. This nanostructure formation improves the morphology of sensing materials discussed for pH (polyaniline) and glucose (platinum) sensing. The results show the effect of substrate morphology, ITO nanostructured vs flat gold electrode, on the device's sensitivity. This change in

sensitivity can be due to the higher active surface area and the different surface activity of these nanostructured materials. Besides platinum, the oxidation of copper on top of these nanostructured ITO substrates was investigated as a new platform of glucose sensing. However, the problem with the reproducibility of glucose sensing using copper oxide is still challenging. In the end, the fabricated device was analyzed by implementing polymeric microneedle on top of the electrode for a more accessible and practical extraction of interstitial fluid. The resulted in-vitro tests show the improvement in the sensing capability for the case of microneedle implementation. This combination of the multiplexed sensors with microneedles is a promising biosensor platform that can be used for other biological elements characterization besides glucose and pH.

Chapter 6

Conclusion and future directions

A sensing system that can monitor biomarkers with low fabrication cost and high reliability is demanding. The ability of the device to sense multiple biomarkers is very critical. This kind of sensors can generate and analyze various health-related signals from the human body to understand the mechanism of biological interactions and their effect on a complicated human health system. The considerable improvement in electronics and analytical tools and the possibility to fabricate and analyze nanostructured devices make a significant impact on health monitoring systems. However, these improvements are still on the way to maturity.

As one of the most precise sensing systems, electrochemical monitoring devices are still benefiting from the considerable advancement in fabrication processes and synthesis of novel materials. In our research, we try to investigate the effect of novel sensing materials and their morphology on the sensing capabilities of biosensors. Two different sensors were fabricated to monitor anastomotic leakage after surgery and biomarkers in interstitial fluid.

The first type of sensor is based on the detection of pH variations within a short time to

prevent dreadend complications as a result of anastomotic leakage after the surgery. This device was fabricated using rigid and flexible electrodes. Polyaniline has been synthesized using electro-polymerization, and utilized as a pH-sensitive material. The second type of sensor is a multiplexed sensor for simultaneous monitoring of pH and glucose. These flexible multiplexed sensors have been designed for monitoring blood glucose levels through interstitial fluid analysis. The pH sensing was based on nanofibrous polyaniline, and the glucose monitoring was based on electroplated platinum having rough surface morphology.

To enhance the sensitivity for pH and glucose sensing, a novel method of self-assembled nanostructuring has been investigated. The self-assembled indium tin oxide material using magnetron sputtering has been developed, and the effect of the seed layer was investigated. Pre-preparation of the substrate and the seed layer selection highly affect the growth of the ITO nanowires.

These ITO nanorod and nanowire structures have been used as a template for synthesis of nanostructured sensing materials. This approach improves the sensing properties of the device by reducing the size of nanostructured island film and enhancing the electrode analyte interactions. Combining this nanostructured ITO with sensing materials, such as polyaniline, platinum and copper oxides, allows us to improve the morphology-assisted sensing.

The continuous monitoring of ISF needs a system that can extract the ISF from under the skin and bring it to the surface of the sensing electrodes. This desired system has been achieved by integrating sensor devices and polymeric microneedles. The effect of this integration was investigated, which shows the applicability and high sensitivity of the device. For multiplexed sensing, we improved the design of multiple sensor electrodes and analyzed the resulted signal to detect the biomarkers. This system may be trained and improved by analyzing the received signal with a machine learning platform to enhance

detection and monitoring.

This electrochemical sensor can also be used for other biomarker monitoring. This will help analyze the connection among these parameters and their complicated interaction inside the body. In addition, the extracted data from the health monitoring system, combined with an artificial intelligence system, can help us understand the sensing capabilities of the device. The simple electrochemical sensing platform can also be replaced by a transistor based electrochemical sensing system (ISFET, Ion sensitive field effect transistor). The transistor system, integrated into a flexible system, can improve the ability to miniaturize the sensor design and reproducibility of the analyzing system.

The investigated monitoring device with the nanostructured material shed light on a long journey toward a more accurate and reliable sensor for future biosensors. Hopefully, this research will be part of the development of new biosensor systems for future health monitoring.

References

[1] Kathryn E. Toghill and Richard G. Compton. Electrochemical non-enzymatic glucose sensors: A perspective and an evaluation. *International Journal of Electrochemical Science*, 5(9):1246–1301, 2010.

[2] James E. Mark. *Physical Properties of Polymers Handbook*, volume 158. Springer New York, New York, NY, 2007.

[3] Jayoung Kim, Alan S. Campbell, Berta Esteban Fernández de Ávila, and Joseph Wang. Wearable biosensors for healthcare monitoring. *Nature Biotechnology*, 37(4):389–406, 2019.

[4] Mark Gray, Jamie R.K. Marland, Alan F. Murray, David J. Argyle, and Mark A. Potter. Predictive and diagnostic biomarkers of anastomotic leakage: A precision medicine approach for colorectal cancer patients. *Journal of Personalized Medicine*, 11(6), 2021.

[5] Healthcare associates. What Is the Difference Between My A1c and the Numbers on My Glucometer?, 2018.

[6] Yan Li, Hang Zhang, Ruifeng Yang, Yohan Laffitte, Ulises Schmill, Wenhan Hu, Moufeed Kaddoura, Eric J.M. Blondeel, and Bo Cui. Fabrication of sharp

silicon hollow microneedles by deep-reactive ion etching towards minimally invasive diagnostics. *Microsystems and Nanoengineering*, 5(1), 2019.

[7] Khanh T.M. Tran, Tyler D. Gavitt, Nicholas J. Farrell, Eli J. Curry, Arlind B. Mara, Avi Patel, Lindsey Brown, Shawn Kilpatrick, Roxana Piotrowska, Neha Mishra, Steven M. Szczepanek, and Thanh D. Nguyen. Transdermal microneedles for the programmable burst release of multiple vaccine payloads. *Nature Biomedical Engineering*, 5(9):998–1007, 2021.

[8] John G. Webster and Halit Eren. *Measurement, Instrumentation, and Sensors Handbook*. CRC Press, dec 2017.

[9] Gang Yan Zhou, Ai Wei Lee, Jia Yaw Chang, Chi Hsien Huang, and Jem Kun Chen. Fabrication of metamaterial absorber using polymer brush-gold nanoassemblies for visualizing the reversible pH-responsiveness. *Journal of Materials Chemistry C*, 2(39):8226–8234, 2014.

[10] Yi Ching Kuo, Chih Kung Lee, and Chih Ting Lin. Improving sensitivity of a miniaturized label-free electrochemical biosensor using zigzag electrodes. *Biosensors and Bioelectronics*, 103(1):130–137, 2018.

[11] Jo Hee Yoon, Seok Bok Hong, Seok Oh Yun, Seok Jae Lee, Tae Jae Lee, Kyoung G. Lee, and Bong Gill Choi. High performance flexible pH sensor based on polyaniline nanopillar array electrode. *Journal of Colloid and Interface Science*, 490:53–58, 2017.

[12] M. Hajmirzaheydarali, M. Sadeghipari, M. Akbari, A. Shahsafi, and S. Mohajerzadeh. Nano-textured high sensitivity ion sensitive field effect transistors. *Journal of Applied Physics*, 119(5), 2016.

[13] Chenhao Ge, Neal R. Armstrong, and S. Scott Saavedra. pH-sensing properties of poly(aniline) ultrathin films self-assembled on indium-tin oxide. *Analytical Chemistry*, 79(4):1401–1410, 2007.

[14] Tarek M. Abdolkader and Abdurrahman G. Alahdal. Performance optimization of single-layer and double-layer high-k gate nanoscale ion-sensitive field-effect transistors. *Sensors and Actuators, B: Chemical*, 259:36–43, 2018.

[15] Korbua Chaisiwamongkhol, Christopher Batchelor-Mcauley, and Richard G. Compton. Optimising amperometric pH sensing in blood samples: An iridium oxide electrode for blood pH sensing. *Analyst*, 144(4):1386–1393, 2019.

[16] Libu Manjakkal, Katarina Cvejin, Jan Kulawik, Krzysztof Zaraska, Robert P. Socha, and Dorota Szwagierczak. X-ray photoelectron spectroscopic and electrochemical impedance spectroscopic analysis of RuO2-Ta2O5 thick film pH sensors. *Analytica Chimica Acta*, 931:47–56, 2016.

[17] Joseph Wang. Electrochemical glucose biosensors. *Electrochemical Sensors, Biosensors and their Biomedical Applications*, pages 57–69, 2008.

[18] Jamie Hu. The evolution of commercialized glucose sensors in China. *Biosensors and Bioelectronics*, 24(5):1083–1089, 2009.

[19] Homehealth-uk. 8 Parameter Urine Dipstick Test Strips Ketone Glucose pH 100 Tests — Home Health UK, 2020.

[20] N. S. Oliver, C. Toumazou, A. E.G. Cass, and D. G. Johnston. Glucose sensors: A review of current and emerging technology. *Diabetic Medicine*, 26(3):197–210, 2009.

[21] Lanjie Lei, Chao Zhao, Xiaofei Zhu, Shuai Yuan, Xing Dong, Yinxiu Zuo, and Hong Liu. Nonenzymatic Electrochemical Sensor for Wearable Interstitial Fluid Glucose Monitoring. *Electroanalysis*, pages 1–9, 2021.

[22] Hyunjae Lee, Changyeong Song, Yong Seok Hong, Min Sung Kim, Hye Rim Cho, Taegyu Kang, Kwangsoo Shin, Seung Hong Choi, Taeghwan Hyeon, and Dae Hyeong Kim. Wearable/disposable sweat-based glucose monitoring device with multistage transdermal drug delivery module. *Science Advances*, 3(3):1–9, 2017.

[23] Vuslat B. Juska and Martyn E. Pemble. A critical review of electrochemical glucose sensing: Evolution of biosensor platforms based on advanced nanosystems. *Sensors (Switzerland)*, 20(21):1–28, 2020.

[24] Mitsuhiro Ebara. *Biomaterials Nanoarchitectonics*. 2016.

[25] Stefano Ferri, Katsuhiro Kojima, and Koji Sode. Review of glucose oxidases and glucose dehydrogenases: A bird's eye view of glucose sensing enzymes. *Journal of Diabetes Science and Technology*, 5(5):1068–1076, 2011.

[26] Hiroyuki Kudo, Tamon Yagi, Ming Xing Chu, Hirokazu Saito, Nobuyuki Morimoto, Yasuhiko Iwasaki, Kazunari Akiyoshi, and Kohji Mitsubayashi. Glucose sensor using a phospholipid polymer-based enzyme immobilization method. *Analytical and Bioanalytical Chemistry*, 391(4):1269–1274, 2008.

[27] Muhammad Adeel, Kanwal Asif, Md Mahbubur Rahman, Salvatore Daniele, Vincenzo Canzonieri, and Flavio Rizzolio. Glucose Detection Devices and Methods Based on MetalOrganic Frameworks and Related Materials. *Advanced Functional Materials*, 2106023:1–28, 2021.

[28] Dae Woong Hwang, Saram Lee, Minjee Seo, and Taek Dong Chung. Recent advances in electrochemical non-enzymatic glucose sensors A review. *Analytica Chimica Acta*, 1033:1–34, 2018.

[29] R. R. Adzic, M. W. Hsiao, and E. B. Yeager. Electrochemical oxidation of glucose on single crystal gold surfaces. *Journal of Electroanalytical Chemistry*, 260(2):475–485, 1989.

[30] G. Kokkindis, J. M. Leger, and C. Lamy. Structural effects in electrocatalysis. Oxidation of D-glucose on pt (100), (110) and (111) single crystal electrodes and the effect of upd adlayers of Pb, Tl and Bi. *Journal of Electroanalytical Chemistry*, 242(1-2):221–242, 1988.

[31] Yoshinori Marunaka. Roles of interstitial fluid pH in diabetes mellitus: Glycolysis and mitochondrial function. *World Journal of Diabetes*, 6(1):125, 2015.

[32] Sanjay S. Timilsina, Pawan Jolly, Nolan Durr, Mohamed Yafia, and Donald E. Ingber. Enabling Multiplexed Electrochemical Detection of Biomarkers with High Sensitivity in Complex Biological Samples. *Accounts of Chemical Research*, 54(18):3529–3539, 2021.

[33] SU-8 2-25 Permanent Negative Epoxy Photoresist. Technical report.

[34] Hugo José Nogueira Pedroza Dias Mello and Marcelo Mulato. Effect of aniline monomer concentration on PANI electropolymerization process and its influence for applications in chemical sensors. *Synthetic Metals*, 239(January):66–70, 2018.

[35] Edward Song and Jin-Woo Choi. Conducting Polyaniline Nanowire and Its Applications in Chemiresistive Sensing. *Nanomaterials*, 3(3):498–523, 2013.

[36] W. J. Lorenz and G. Staikov. 2D and 3D thin film formation and growth mechanisms in metal electrocrystallization - an atomistic view by in situ STM. *Surface Science*, 335(C):32–43, 1995.

[37] Hyunah Kwon, Seung Hee Lee, and Jong Kyu Kim. Three-Dimensional Metal-Oxide Nanohelix Arrays Fabricated by Oblique Angle Deposition: Fabrication, Properties, and Applications. *Nanoscale Research Letters*, 10(1), 2015.

[38] Xiaolei Zhang, Yaoze Liu, Mohammad Soltani, Peng Li, Bing Zhao, and Bo Cui. Probing the Interfacial Charge-Transfer Process of Uniform ALD Semiconductor-Molecule-Metal Models: A SERS Study. *Journal of Physical Chemistry C*, 121(48):26939–26948, 2017.

[39] Jingjun Wu, Xin Ye, Laixi Sun, Jin Huang, Jibin Wen, Feng Geng, Yong Zeng, Qingzhi Li, Zao Yi, Xiaodong Jiang, and Kuibao Zhang. Growth mechanism of one-step self-masking reactive-ion-etching (RIE) broadband antireflective and superhydrophilic structures induced by metal nanodots on fused silica. *Optics Express*, 26(2):1361, 2018.

[40] Wei Lu and Charles M. Lieber. Semiconductor nanowires. *Journal of Physics D: Applied Physics*, 39(21), 2006.

[41] Babak Nikoobakht. Analysis of Copper Incorporation Into Zinc Oxide Nanowires.

[42] Juan Shi, Liang Qiao, Yi Zhao, Zhonggui Sun, Wangjun Feng, Zhiya Zhang, Jun Wang, and Xuehu Men. Synergistic effects on thermal growth of CuO nanowires. *Journal of Alloys and Compounds*, 815:152355, 2020.

[43] Qiang Li, Yuantao Zhang, Lungang Feng, Zuming Wang, Tao Wang, and Feng Yun. Investigation of the influence of growth parameters on self-catalyzed ITO nanowires by high RF-power sputtering. *Nanotechnology*, 29(16), 2018.

[44] Eugen Rabkin. Solid state dewetting of thin metal films, 2021.

[45] Minhee Kang, Sang Gil Park, and Ki Hun Jeong. Repeated Solid-state Dewetting of Thin Gold Films for Nanogap-rich Plasmonic Nanoislands. *Scientific Reports*, 5:1–7, 2015.

[46] Yoon Chul Sohn, Qian Wang, Suk Jin Ham, Byung Gil Jeong, Kyu Dong Jung, Min Seog Choi, Woon Bae Kim, and Chang Youl Moon. Wafer-level low temperature bonding with Au-In system. *Proceedings - Electronic Components and Technology Conference*, pages 633–637, 2007.

[47] Mengjia Zheng, Zifeng Wang, Hao Chang, Lulu Wang, Sharon W.T. Chew, Daniel Chin Shiuan Lio, Mingyue Cui, Linbo Liu, Benjamin C.K. Tee, and Chenjie Xu. Osmosis-Powered Hydrogel Microneedles for Microliters of Skin Interstitial Fluid Extraction within Minutes. *Advanced Healthcare Materials*, 9(10), 2020.

[48] Parikha Mehrotra. Biosensors and their applications - A review. *Journal of Oral Biology and Craniofacial Research*, 6(2):153–159, 2016.

[49] Daniel Geißler, Loïc J. Charbonnière, Raymond F. Ziessel, Nathaniel G. Butlin, Hans Gerd Löhmannsröben, and Niko Hildebrandt. Quantum dot biosensors for ultrasensitive multiplexed diagnostic. *Angewandte Chemie - International Edition*, 49(8):1396–1401, 2010.

[50] Edoardo Fabini, Barbara Zambelli, Luca Mazzei, Stefano Ciurli, and Carlo Bertucci. Surface plasmon resonance and isothermal titration calorimetry to monitor the

Ni(II)-dependent binding of Helicobacter pylori NikR to DNA. *Analytical and Bioanalytical Chemistry*, 408(28):7971–7980, 2016.

[51] Ajit Sadana and Neeti Sadana. *Handbook of Biosensors and Biosensor Kinetics*. Elsevier, 2011.

[52] G. A. Nicksa, R. V. Dring, K. H. Johnson, W. V. Sardella, P. V. Vignati, and J. L. Cohen. Anastomotic Leaks: What is the Best Diagnostic Imaging Study? *Diseases of the Colon & Rectum*, 50(2):197–203, feb 2007.

[53] World health Organization. Diabetes, 2021.

[54] Sherry Calder. Diabetes Canada, 2019.

[55] Ligia Maria Moretto and Kurt Kalcher, editors. *Environmental Analysis by Electrochemical Sensors and Biosensors*. Nanostructure Science and Technology. Springer New York, New York, NY, 2015.

[56] A. K. Convington, R. G. Bates, and R. A. Durst. International union of pure and applied chemistry. Definition of ph scales , standard reference values , measurement of ph and related terminology. *Pure & Appl. Chem.*, 57(3):531–542, 1985.

[57] Halit Eren. *Measurement, Instrumentation, and Sensors Handbook, Second Edition*. CRC Press, second edition, jan 2017.

[58] P Bergveld. Development of an Ion-Sensitive Solid-State Device for Neurophysiological Measurements. *IEEE Transactions on Biomedical Engineering*, BME-17(1):70–71, jan 1970.

[59] Rodrigo Wrege, Marcio Cherem Schneider, Janaina Gonçalves Guimarães, and Carlos Galup-Montoro. ISFETs: Theory, modeling and chip for characterization. *2019*

IEEE 10th Latin American Symposium on Circuits and Systems, LASCAS 2019 - Proceedings, 900:109–112, 2019.

[60] Ahmed M. Dinar, AS Mohd Zain, F. Salehuddin, Mothana L. Attiah, M.K. Abdulhameed, and Mowafak k. Mohsen. Modeling and simulation of electrolyte pH change in conventional ISFET using commercial Silvaco TCAD. *IOP Conference Series: Materials Science and Engineering*, 518:042020, 2019.

[61] Uda Hashim, Mohd Khairuddin Md Arshad, and Chin Seng Fatt. Silicon nitride gate ISFET fabrication based on four mask layers using standard MOSFET technology. *IEEE International Conference on Semiconductor Electronics, Proceedings, ICSE*, pages 626–628, 2008.

[62] El Grour Tarek, Najari Montassar, Mehdi Akermi, and El Mir Lassad. Graphene field-effect transistor for pH sensing application: Compact modelling and simulation study. *AIP Conference Proceedings*, 1976(September), 2018.

[63] Oleksandr O Soldatkin, Margaryta K Shelyakina, Valentyna N Arkhypova, Esin Soy, Salih Kaan Kirdeciler, Berna Ozansoy Kasap, Florence Lagarde, Nicole Jaffrezic-renault, Burcu Akata Kurç, Alexei P Soldatkin, and Sergei V Dzyadevych. Nano- and microsized zeolites as a perspective material for potentiometric biosensors creation. 2015.

[64] A S Poghossian. The super-Nernstian pH sensitivity of Ta2O3 -gate ISFETs. *Sensors and Actuators B*, 7:367–370, 1992.

[65] A. K. Covington, R. G. Bates, and R. A. Durst. Definition of pH scales, standard reference values, measurement of pH and related terminology (Recommendations 1984). *Pure and Applied Chemistry*, 57(3):531–542, jan 1985.

[66] Guang Zhong Yang. *Implantable sensors and systems: From theory to practice*. 2018.

[67] Xueji Zhang, Huangxian Ju, and Joseph Wang. *Electrochemical Sensors, Biosensors And Their Biomedical Applications*. Elsevier, 2008.

[68] Di Wei, Marc J.A. Bailey, Piers Andrew, and Tapani Ryhänen. Electrochemical biosensors at the nanoscale. *Lab on a Chip*, 9(15):2123–2131, 2009.

[69] Quan Cheng and Anna Brajter-Toth. Permselectivity, Sensitivity, and Amperometric pH Sensing at Thioctic Acid Monolayer Microelectrodes. *Analytical Chemistry*, 68(23):4180–4185, 1996.

[70] Kay L. Robinson and Nathan S. Lawrence. Redox-sensitive copolymer: A single-component pH sensor. *Analytical Chemistry*, 78(7):2450–2455, 2006.

[71] Wei Gao and Junfeng Song. Polyaniline film based amperometric pH sensor using a novel electrochemical measurement system. *Electroanalysis*, 21(8):973–978, 2009.

[72] Xuewu Liu, Zhaohui Aleck Wang, Robert H. Byrne, Eric A. Kaltenbacher, and Renate E. Bernstein. Spectrophotometric Measurements of pH in-Situ: Laboratory and Field Evaluations of Instrumental Performance. *Environmental Science & Technology*, 40(16):5036–5044, aug 2006.

[73] T. S. Moerland and S. Egginton. Intracellular pH of muscle and temperature: Insight from in vivo 31P NMR measurements in a stenothermal antarctic teleost (Harpagifer antarcticus). *Journal of Thermal Biology*, 23(5):275–282, oct 1998.

[74] Satyendra K. Mishra and Banshi D. Gupta. Surface plasmon resonance based fiber optic pH sensor utilizing Ag/ITO/Al/hydrogel layers. *Analyst*, 138(9):2640–2646, 2013.

[75] Vivek Semwal and Banshi D. Gupta. Highly sensitive surface plasmon resonance based fiber optic pH sensor utilizing rGO-Pani nanocomposite prepared by in situ method. *Sensors and Actuators, B: Chemical*, 283(May 2018):632–642, 2019.

[76] Ying Lian, Wei Zhang, Longjiang Ding, Xiaoai Zhang, Yinglu Zhang, and Xudong Wang. Nanomaterials for Intracellular pH Sensing and Imaging. In *Novel Nanomaterials for Biomedical, Environmental and Energy Applications*, chapter 8, pages 241–273. Elsevier, 2019.

[77] Madou J. Marc. *Fundamentals of Microfabrication; the science of minaturization*. CRC Press, second edi edition, 2010.

[78] Marc Madou. *Fundamentals of Microbabrication: The Science of Miniaturization*. Second edi edition, 2002.

[79] G. Urban, G. Jobst, F. Keplinger, E. Aschauer, A. Jachimowicz, and F. Kohl. Miniaturized Biosensors for Integration on Flexible Polymer Carriers for in Vivo Applications. *Biosensors '92 Proceedings*, 7:467–471, 2014.

[80] U. Oesch, D. Ammann, and W. Simon. Ion-selective membrane electrodes for clinical use. *Clinical Chemistry*, 32(8):1448–1459, 1986.

[81] Chun Lung Lien and Chiun Jye Yuan. The development of CMOS amperometric sensing chip with a novel 3-dimensional TiN nano-electrode array. *Sensors (Switzerland)*, 19(5), 2019.

[82] Arif Ul Alam, Yiheng Qin, Shruti Nambiar, John T.W. Yeow, Matiar M.R. Howlader, Nan Xing Hu, and M. Jamal Deen. Polymers and organic materials-based pH sensors for healthcare applications. *Progress in Materials Science*, 96(January):174–216, 2018.

[83] Tung Ming Pan, Chih Wei Wang, Somnath Mondal, and See Tong Pang. Super-Nernstian sensitivity in microfabricated electrochemical pH sensor based on CeTixOy film for biofluid monitoring. *Electrochimica Acta*, 261:482–490, 2018.

[84] M. Hajmirzaheydarali, M. Akbari, A. Shahsafi, S. Soleimani-Amiri, M. Sadeghipari, S. Mohajerzadeh, A. Samaeian, and M. A. Malboobi. Ultrahigh Sensitivity DNA Detection Using Nanorods Incorporated ISFETs. *IEEE Electron Device Letters*, 37(5):663–666, 2016.

[85] Linghao He, Bingbing Cui, Jiameng Liu, Yingpan Song, Minghua Wang, Donglai Peng, and Zhihong Zhang. Novel electrochemical biosensor based on core-shell nanostructured composite of hollow carbon spheres and polyaniline for sensitively detecting malathion. *Sensors and Actuators, B: Chemical*, 258:813–821, 2018.

[86] Elisa Scarpa, Enrico Domenico Lemma, Roberto Fiammengo, Maria Pia Cipolla, Ferruccio Pisanello, Francesco Rizzi, and Massimo De Vittorio. Microfabrication of pH-responsive 3D hydrogel structures via two-photon polymerization of high-molecular-weight poly(ethylene glycol) diacrylates. *Sensors and Actuators, B: Chemical*, 279(May 2018):418–426, 2019.

[87] Myer Kutz, editor. *Handbook of Materials Selection*. John Wiley & Sons, Inc., New York, jul 2007.

[88] Agner Fog and Richard P. Buck. Electronic semiconducting oxides as pH sensors. *Sensors and Actuators*, 5(2):137–146, 1984.

[89] G. Kocak, C. Tuncer, and V. Bütün. PH-Responsive polymers. *Polymer Chemistry*, 8(1):144–176, 2017.

[90] Luís F. Marchesi, Sheila C. Jacumasso, Ronaldo C. Quintanilha, Herbert Winnischofer, and Marcio Vidotti. The electrochemical impedance spectroscopy behavior of poly(aniline) nanocomposite electrodes modified by Layer-by-Layer deposition. *Electrochimica Acta*, 174:864–870, 2015.

[91] Libu Manjakkal, Katarina Cvejin, Branimir Bajac, Jan Kulawik, Krzysztof Zaraska, and Dorota Szwagierczak. Microstructural, Impedance Spectroscopic and Potentiometric Analysis of Ta2O5 Electrochemical Thick Film pH Sensors. *Electroanalysis*, 27(3):770–781, 2015.

[92] J. Huo. Applications of Electrochemical Impedance Spectroscopy in pH Sensor Characterization and Failure Analysis. *ECS Transactions*, 75(16):291–302, sep 2016.

[93] Libu Manjakkal, Elvira Djurdjic, Katarina Cvejin, Jan Kulawik, Krzysztof Zaraska, and Dorota Szwagierczak. Electrochemical Impedance Spectroscopic Analysis of RuO<inf>2</inf> Based Thick Film pH Sensors. *Electrochimica Acta*, 168:246–255, 2015.

[94] National Health Service UK. Diabetes insipidus., 2019.

[95] Somasekhar R. Chinnadayyala and Sungbo Cho. Porous platinum black-coated minimally invasive microneedles for non-enzymatic continuous glucose monitoring in interstitial fluid. *Nanomaterials*, 11(1):1–15, 2021.

[96] Tuuli A. Hakala, Alejandro García Pérez, Melissa Wardale, Ida A. Ruuth, Risto T. Vänskä, Teemu A. Nurminen, Emily Kemp, Zhanna A. Boeva, Juha Matti Alakoskela, Kim Pettersson-Fernholm, Edward Hæggström, and Johan Bobacka. Sampling of fluid through skin with magnetohydrodynamics for noninvasive glucose monitoring. *Scientific Reports*, 11(1):1–9, 2021.

[97] Youngeun Kim and Mark R. Prausnitz. Sensitive sensing of biomarkers in interstitial fluid. *Nature Biomedical Engineering*, 5(1):3–5, 2021.

[98] Vladimir L. Alexeev, Sasmita Das, David N. Finegold, and Sanford A. Asher. Photonic crystal glucose-sensing material for noninvasive monitoring of glucose in tear fluid. *Clinical Chemistry*, 50(12):2353–2360, 2004.

[99] Pinak Chakraborty, Nitumoni Deka, Dulal Chandra Patra, Kamalesh Debnath, and Suvra Prakash Mondal. Salivary glucose sensing using highly sensitive and selective non-enzymatic porous NiO nanostructured electrodes. *Surfaces and Interfaces*, 26(July):101324, 2021.

[100] Takahiro Arakawa, Yusuke Kuroki, Hiroki Nitta, Prem Chouhan, Koji Toma, Shin ichi Sawada, Shuhei Takeuchi, Toshiaki Sekita, Kazunari Akiyoshi, Shunsuke Minakuchi, and Kohji Mitsubayashi. Mouthguard biosensor with telemetry system for monitoring of saliva glucose: A novel cavitas sensor. *Biosensors and Bioelectronics*, 84:106–111, 2016.

[101] Jiangqi Zhao, Yuanjing Lin, Jingbo Wu, Hnin Yin Yin Nyein, Mallika Bariya, Li Chia Tai, Minghan Chao, Wenbo Ji, George Zhang, Zhiyong Fan, and Ali Javey. A Fully Integrated and Self-Powered Smartwatch for Continuous Sweat Glucose Monitoring. *ACS Sensors*, 4(7):1925–1933, 2019.

[102] Stella Quinones Shokrekhodaei, Maryamsadat. Review of Non-Invasive Glucose Sensing Techniques :. *Sensors (Switzerland)*, page 1251, 2020.

[103] T Togawa and F A Spelman. *Sensors in Medicine and Health Care*, volume 3. 2004.

[104] Chao Chen, Qingji Xie, Dawei Yang, Hualing Xiao, Yingchun Fu, Yueming Tan, and Shouzhuo Yao. Recent advances in electrochemical glucose biosensors: A review. *RSC Advances*, 3(14):4473–4491, 2013.

[105] Andrew G. McDonald, Sinéad Boyce, and Keith F. Tipton. ExplorEnz: The primary source of the IUBMB enzyme list. *Nucleic Acids Research*, 37(SUPPL. 1):593–597, 2009.

[106] Jody L. House, Ellen M. Anderson, and W. Kenneth Ward. Immobilization techniques to avoid enzyme loss from oxidase-based biosensors: A one-year study. *Journal of Diabetes Science and Technology*, 1(1):18–27, 2007.

[107] Christian Wolf. *Dynamic Stereochemistry of Chiral Compounds*. Royal Society of Chemistry, Cambridge, 2007.

[108] Wataru Aoi and Yoshinori Marunaka. Importance of pH Homeostasis in Metabolic Health and Diseases: Crucial Role of Membrane Proton Transport. *BioMed Research International*, 2014(Figure 1), 2014.

[109] Arunima Ghosh and Sajjad Ahmed. *Modern Techniques in Biosensors*, volume 327 of *Studies in Systems, Decision and Control*. Springer Singapore, Singapore, 2021.

[110] The Editors of Encyclopaedia. Multiplexing, 2007.

[111] Seung Yong Hwang, In Jae Seo, Seung Yong Lee, and Yoomin Ahn. Microfluidic multiplex biochip based on a point-of-care electrochemical detection system for matrix metalloproteinases. *Journal of Electroanalytical Chemistry*, 756:118–123, 2015.

[112] Roger J. Narayan. *Medical Biosensors for Point of Care (POC) Applications*. 2016.

[113] Paul Yager, Gonzalo J. Domingo, and John Gerdes. Point-of-care diagnostics for global health. *Annual Review of Biomedical Engineering*, 10:107–144, 2008.

[114] Gertrude Fomo, Tesfaye T. Waryo, Priscilla Baker, and Emmanuel I. Iwuoha. Electrochemical deposition and properties of polyaniline films on carbon and precious metal surfaces in perchloric acid/ acetonitrile. *International Journal of Electrochemical Science*, 11(12):10347–10361, 2016.

[115] Ashwini B. Rohom, Priyanka U. Londhe, S. K. Mahapatra, S. K. Kulkarni, and N. B. Chaure. Electropolymerization of polyaniline thin films. *High Performance Polymers*, 26(6):641–646, 2014.

[116] Sambhu Bhadra and Dipak Khastgir. Determination of crystal structure of polyaniline and substituted polyanilines through powder X-ray diffraction analysis. *Polymer Testing*, 27(7):851–857, 2008.

[117] S. Padmapriya, S. Harinipriya, K. Jaidev, V. Sudha, Deepak Kumar, and Samanwita Pal. Storage and evolution of hydrogen in acidic medium by polyaniline. *International Journal of Energy Research*, 42(3):1196–1209, 2018.

[118] Ashwini B Rohom, Priynka U Londhe, and N B Chaure. Enhancement of Optical Absorption by Incorporation of Plasmonic Nanoparticles in PANI Films. *Nanoscience and Nanotechnology*, 6(1A):83–87, 2016.

[119] M. F. L. de Mele, H. A. Videla, and A. J. Arvía. Potentiodynamic Study of Glucose ElectroOxidation at Bright Platinum Electrodes. *Journal of The Electrochemical Society*, 129(10):2207–2213, 1982.

[120] Osamu Nakatsuka and Shigeaki Zaima. Heteroepitaxial Growth of Si, Si1-xGex-, and Ge-Based Alloy. *Handbook of Crystal Growth: Thin Films and Epitaxy: Second Edition*, 3:1301–1318, 2014.

[121] Ashok K. Sood, Roger E. Welser, Yash R. Puri, Martin F. Schubert, David J. Poxson, Jong Kyu Kim, E. Fred Schubert, Dennis L. Polla, and Martin B. Soprano. Design and development of nanostructure based antireflection coatings for EO/IR sensor applications. *Infrared Systems and Photoelectronic Technology IV*, 7419(August):74190U, 2009.

[122] Lingyu Kong, Yunshan Zhao, Binayak Dasgupta, Yi Ren, Kedar Hippalgaonkar, Xiuling Li, Wai Kin Chim, and Sing Yang Chiam. Minimizing Isolate Catalyst Motion in Metal-Assisted Chemical Etching for Deep Trenching of Silicon Nanohole Array. *ACS Applied Materials and Interfaces*, 9(24):20981–20990, 2017.

[123] Munho Kim, Hsien Chih Huang, Jeong Dong Kim, Kelson D. Chabak, Akhil Raj Kumar Kalapala, Weidong Zhou, and Xiuling Li. Nanoscale groove textured β-Ga2O3 by room temperature inverse metal-assisted chemical etching and photodiodes with enhanced responsivity. *Applied Physics Letters*, 113(22):1–6, 2018.

[124] Chuancheng Jia, Zhaoyang Lin, Yu Huang, and Xiangfeng Duan. Nanowire Electronics: From Nanoscale to Macroscale. *Chemical Reviews*, 119(15):9074–9135, 2019.

[125] Grazielle O. Setti, Mónica B. Mamián-López, Priscila R. Pessoa, Ronei J. Poppi, Ednan Joanni, and Dosil P. Jesus. Sputtered gold-coated ITO nanowires by alternating depositions from Indium and ITO targets for application in surface-enhanced Raman scattering. *Applied Surface Science*, 347:17–22, 2015.

[126] Ding Zhou, Shangzhi Li, Minjie Pei, Hongjun Yang, Shaojin Gu, Yongzhen Tao, Dezhan Ye, Yingshan Zhou, Weilin Xu, and Pu Xiao. Dopamine-Modified Hyaluronic Acid Hydrogel Adhesives with Fast-Forming and High Tissue Adhesion. *ACS Applied Materials and Interfaces*, 12(16):18225–18234, 2020.